

Shape Memory Alloy Actuators
for
Upper Limb Prostheses

Alcimar Barbosa Soares

Degree of Doctor of Philosophy

University of Edinburgh

1997



Declaration

This thesis has been composed by me and the work described in it is my own.

To the one who always looks upon me,
to the one who gave me everything I have,
to the one who guides me through the night,
to God.

To you Taninha,

My support and main pillar throughout all these years,
for being with me even when I didn't deserve so.

To my parents Norozira and José Leal
and to my brothers Adeilson and Alcenir,
so far away... yet so close.

Acknowledgements

I cannot possibly list here all those friends who were with me during these years, helping me in many different ways... you will be always remembered. However, I would like to express my gratitude to some of you who had direct contact with this particular work.

To Harry and David, my supervisors and friends. Thank you for your continuous support, advice, encouragement and “patience” throughout this project. I will be always indebted to you.

To Norman (Prof.). For your unconditional support and advice whenever I was in need of. For those great days at Fribush and everywhere else. A great friend above all.

To Rab (O’Donnell). You have been around for no more than two months, but it was enough to show us that your abilities are second to none. Another friend I was lucky to find.

To Tom, Carmel, Derek, Kumar, Fauzia, Ian, Irene and Catriona. Always there in one way or another... helping me or just being friends.

To Bill (Hello computer!). Very few times in my life I found such a great friend, I learned a lot with you.

To my friends and fellow Ph.D. students of the Department of Medical Physics and Medical Engineering. Particularly Shao and Ali who were with me in the very beginning, supporting me and helping me whenever I needed.

To my Brazilian friends Edgard and Eugênia (“Homi rapaiz!”). You’ve been around long before we started this journey and I know you will always be there.

To my great friend Edilberto (“... always in blue pyjamas ...”). I shall never forget your support throughout these years.

I am also indebted to the Departamento de Engenharia Elétrica (Universidade Federal de Uberlândia - Brasil). Everybody over there had “something to do with this”, and I thank you all.

My special thanks to my sponsor (CAPES - Brazilian government) for the all-important financial support. In particular I would like to thank Mrs. Vanda Lucena for the help she always gave me since the very beginning.

And finally I would like to thank those who provided me with obstacles and difficulties. It is also by overcoming barriers that we grow stronger and wiser.

Contents

Chapter 1

Introduction.....	1
1.1 - The Artificial Limb: A Problem Waiting for a Solution	1
1.2 - The Perfect Actuator.....	2
1.3 - Parallels between Shape Memory Alloys and Skeletal Muscles	3
1.4 - Aims of this Work	10
1.5 - Layout of Thesis	10

Chapter 2

Prosthetics.....	12
2.1 - Introduction	12
2.2 - Background on Prostheses.....	14
2.2.1 - <i>The Main Parts of a Standard Prosthesis</i>	15
2.2.2 - <i>Classification of Prosthetic Devices</i>	17
2.3 - State of the Art of Prosthetics.....	19
2.3.1 - <i>Strategies for Control</i>	19
2.3.1.1 - <i>Harnessing</i>	20
2.3.1.2 - <i>Cineplasty</i>	21
2.3.1.3 - <i>Myoelectric Control</i>	22
2.3.1.4 - <i>Neuroelectric Control</i>	25
2.3.1.5 - <i>Sensory Feedback</i>	26
2.3.2 - <i>Design of Prostheses</i>	28
2.3.2.1 - <i>Passive Prostheses</i>	28

2.3.2.2 - <i>Body-Powered Prostheses</i>	29
2.3.2.3 - <i>Externally Powered Prostheses</i>	30
2.3.3 - <i>Acceptance and Usage of Prostheses</i>	33
2.4 - <i>Problems to be Overcome</i>	35
2.4.1 - <i>Actuators</i>	35
2.4.2 - <i>Power Supply</i>	36
2.4.3 - <i>Adaptation of New Techniques for Clinical Use</i>	36
2.4.4 - <i>User's Control and Feedback</i>	37
2.4.5 - <i>Natural Behaviour</i>	37
2.5 - <i>Benefits and Possible Applications of Shape Memory Alloys in Prosthetics</i> ...	38
2.6 - <i>Conclusion</i>	41

Chapter 3

Shape Memory Alloys and Actuators	42
3.1 - <i>Introduction</i>	42
3.2 - <i>Background</i>	42
3.2.1 - <i>The Shape Memory Effect</i>	44
3.2.1.1 - <i>Microscopic Analysis</i>	44
3.2.1.2 - <i>Macroscopic Analysis</i>	46
3.2.1.3 - <i>The Rhombohedral Phase</i>	46
3.2.1.4 - <i>The Two Way Effect</i>	48
3.2.1.5 - <i>Superelasticity</i>	49
3.2.2 - <i>Measuring the Transformation Temperature</i>	49
3.2.3 - <i>General Applications</i>	51
3.2.4 - <i>Considerations on Using SMAs</i>	54
3.2.4.1 - <i>Heat Treatment</i>	54
3.2.4.2 - <i>Training</i>	55
3.2.4.3 - <i>Joining to Mountings</i>	55
3.2.4.4 - <i>Operational Temperature</i>	56
3.2.4.5 - <i>Environment</i>	56

3.2.4.6 - <i>Fatigue and Degradation</i>	56
3.2.4.7 - <i>Young's Modulus</i>	57
3.2.4.8 - <i>Stress</i>	57
3.2.4.9 - <i>Strain</i>	58
3.2.4.10 - <i>Deformation Force</i>	58
3.2.4.11 - <i>Bend Radius</i>	59
3.3 - Basic Considerations on Using SMA as the Driving Element for Actuators	60
3.3.1 - <i>Advantages</i>	60
3.3.2 - <i>Disadvantages</i>	61
3.3.3 - <i>Typical Shapes for the SMA Elements</i>	62
3.4 - Conclusion	63

Chapter 4

The Design of an Artificial Hand Powered by SMA Actuators for Young Children	64
4.1 - Introduction	64
4.2 - Initial Considerations	64
4.3 - Specification and Design of the Artificial Hand	67
4.3.1 - <i>The Hand Mechanism</i>	69
4.3.2 - <i>Simulation of the Hand Mechanism</i>	71
4.3.2.1 - <i>Motion</i>	71
4.3.2.2 - <i>Forces</i>	74
4.3.2.3 - <i>Software</i>	83
4.3.3 - <i>Using the Simulator in the Design of the Device</i>	85
4.4 - Conclusion	96

Chapter 5

The Design and Construction of the SMA Actuator	97
--------------------------------------------------------------	-----------

5.1 - Introduction	97
5.2 - Specifications of the Actuator	97
5.3 - Selecting the Actuator Configuration	98
5.4 - Selecting the SMA Elements.....	100
5.4.1 - <i>Material Selection</i>	100
5.4.2 - <i>Choice of the Shape and Dimensions of the SMA Elements</i>	101
5.4.2.1 - <i>Transformation Temperature</i>	102
5.4.2.2 - <i>Choice of the SMA Wires</i>	102
5.4.2.3 - <i>Length and Maximum Strain of the SMA Wires</i>	114
5.5 - Mechanical and Electrical Arrangement of the SMA Elements.....	115
5.6 - Position Feedback.....	115
5.7 - Required Protections	117
5.7.1 - <i>Protection Against Overstrain</i>	117
5.7.2 - <i>Protection Against Overload</i>	117
5.7.3 - <i>Protection Against Overheating</i>	119
5.8 - Development of the Final Actuator	120
5.8.1 - <i>The First Prototype</i>	120
5.8.2 - <i>The Second Prototype</i>	123
5.9 - Conclusion.....	129

Chapter 6

A Control System for the SMA Actuator	130
6.1 - Introduction	130
6.2 The Requirements for the Operation of the Hand Mechanism	132
6.3 - The Control System.....	133
6.3.1 - <i>Timer</i>	134
6.3.2 - <i>Compensator</i>	134
6.3.3 - <i>Pulse Width Modulator</i>	135
6.3.4 - <i>Power Driver</i>	138
6.4 - Experiments.....	139

6.4.1 - Follow-up Response for Triangular and Sine Wave Inputs	140
6.4.2 - Step Response	141
6.5 - Conclusion.....	142

Chapter 7

Construction and Evaluation of the Prototype..... 144

7.1 - Introduction	144
7.2 - The Hand Mechanism.....	144
7.3 - Assembly of Prototype	145
7.4 - Laboratory Experiments	147
7.5 - Evaluation of the Prototype	151
7.6 - Conclusion.....	152

Chapter 8

General Conclusions and The Way Ahead..... 154

8.1 - Introduction	154
8.2 - Summary and General Conclusions	155
8.3 - Future Work.....	158

Appendix A

Main Code of the Computer Program to Simulate the Operation of the Hand Mechanism 160

Appendix B

**The Steeper Scamp Hand and The VV Series Electric Hands from
Variety Ability Systems Inc. 177**

Appendix C

Publications..... 182

Appendix D

**Practical Aspects of Working with Shape Memory Alloys Based on
Experience During the Development of the Hand Actuator 189**

References..... 194

ABSTRACT

Despite the technological advances of the twentieth century, we are not yet able to produce artificial limbs which “mimic” perfectly their natural counterparts. In general, artificial limbs are not as dextrous as human limbs, the control is unnatural and there is no proper feedback by which the user can assess the status of the prosthesis.

In this thesis the problems related to upper limb prostheses are considered. The use of a special material known as Shape Memory Alloy (SMA) is investigated towards producing improved joint actuators for small artificial prostheses such as those required by young children.

SMA actuators can be very lightweight, their motion is silent and smooth and yet they are capable of delivering considerable power per unit of weight. The Shape Memory phenomenon and the many challenges involved in its application are discussed.

The detailed design of a SMA joint actuator for a hand mechanism in an above-elbow prosthesis for young children is given. To assist the design and construction of both the artificial hand and the actuator, a mathematical model was developed and incorporated in a computer program simulating the forces and movements within the hand. The model was used to optimise the hand mechanism and specify the required joint actuator. Suitable SMA elements were identified through laboratory tests. The hand mechanism was constructed and the actuator, control systems and power source were attached to it. Tests were performed to investigate the characteristics of the complete device. The results show that, although SMA actuators must be designed and used with great care, they do offer a viable alternative to conventional actuators such as pneumatic devices and electric motors in certain applications.

Chapter 1

Introduction

1.1 - The Artificial Limb: A Problem Waiting for a Solution

The human body is often regarded as the perfect machine. All parts work in perfect harmony with each other resulting in a very complex and intricate system. Nevertheless, most of us are able to control this “machine” with minimal or no effort at all. We just take it for granted. It is so perfect that we do not appreciate it until that perfect harmony is somehow disturbed by illness or a physical aggression resulting in the loss of some of the functionality of the body.

The absence of a limb caused by trauma or congenital disorders can severely affect our lives. Simple tasks such as walking and dressing may no longer be possible or may be very difficult to achieve. It is accepted that the best solution to a missing limb is the development of some kind of genetic manipulation that stimulates the regeneration of the limb. However, while this is not possible, the best that can be done is to work towards artificial replacements. Throughout the history of mankind there are numerous examples of artificial devices designed to replace some functionality of a lost limb. Many of those first devices can still be found in museums around the world.

The twentieth century (particularly after the Second World War) has produced an enormous technological advance. This, reflected into prosthetics, allowed the

development of very sophisticated artificial devices. However, they have not evolved enough, as yet, to produce artificial limbs capable of perfectly “mimicking” the natural ones. In general, artificial limbs are not as dexterous as their natural counterparts, the control is not natural and often requires a great deal of mental effort and there is no proper feedback so that the user can assess the status of the artificial limb in a natural fashion. Also the interface between the body and the device is often achieved by means of sockets and harnesses, which are normally uncomfortable and not very reliable.

All those problems, and others to be discussed later in this work, lead to the general “feeling” that there is yet a lot to be done in order to provide a more “natural” way of replacing a lost limb.

1.2 - The Perfect Actuator

Most of the latest researches have been towards the development of prostheses relying upon electric motors powered by battery cells to provide motion of artificial joints. This is particularly evident in the development of upper limb prostheses. Those motors are the substitutes for the skeletal muscles in the artificial system. However, there is not much in common between DC motors and muscles. It is not intended here to imply that the human body is the best of all models (one could always argue that if we thought so the human race would never have invented the wheel to help locomotion). However, it is “natural” to think that when replacing a lost limb, the more human-like a prosthesis is, the better. Human muscles, although not the most efficient of all actuators, are fast, quiet, are found in a variety of sizes and shapes and are very strong. The combination of those characteristics with a “specially designed” skeleton results in very powerful and flexible limbs, sometimes capable of manipulating loads many times as heavy as their own weight.

1.3 - Parallels between Shape Memory Alloys and Skeletal Muscles

After studying the behaviour of a special type of metal known as Shape Memory Alloy (SMA), it is not surprising that one starts to recognise some similarities between those alloys and a general skeletal muscle. Those similarities are sometimes so remarkable that they inspired companies such as the Japanese Toki Corporation to give the trade name of *Biometal* to the Ni-Ti alloys which they sell commercially. Roger G. Gilbertson wrote a book on SMA entitled *Muscle Wires* (Gilbertson (1992)). It is not intended here to propose that SMA can work exactly as a human muscle but it is acceptable to think that, if there are similarities in behaviour, those alloys may provide a viable option for the design of prosthetic devices. A brief description of the mechanism involving the contraction of skeletal muscles will be given, followed by the discussion on how a SMA actuator can be designed so that it replicates some of the characteristics of those muscles.

The Skeletal Muscle

The skeletal muscles are made of numerous fibres ranging between 10 and 80 μ m in diameter. Each of those fibres in turn is made of successively smaller sub-units as illustrated in figure 1.1.

The general mechanism of muscle contraction described in Guyton (1991) is given below (the subsequent paragraphs are also based on the same reference).

The initiation and execution of muscle contraction occurs in the following sequential steps:

1. An action potential travels along a motor nerve to its endings on muscle fibres.

Skeletal muscle

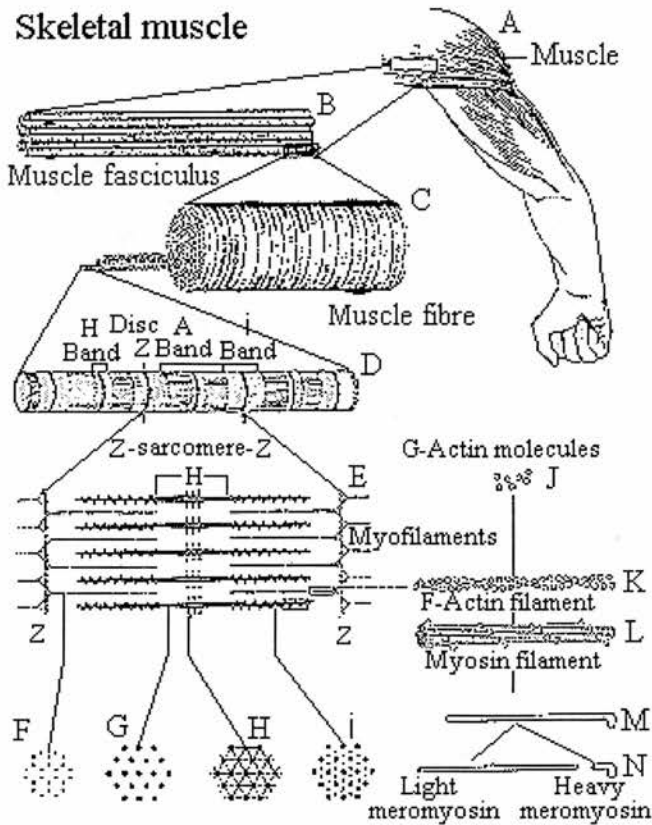


Figure 1.1: Organisation of a skeletal muscle, from the gross to molecular level. F, G, H and I are cross sections of the levels indicated (extracted from Guyton (1991)).

depolarises the muscle fibre membrane and also travels deeply within the muscle fibre. Here it causes the sarcoplasmic reticulum¹ to release into the myofibrils large quantities of calcium ions that have been stored within the reticulum.

6. The calcium ions initiate attractive forces between the actin and myosin filaments, causing them to slide together (see figure 1.2), which is the contractile process.

2. At each ending, the nerve secretes a small amount of the neurotransmitter substance called "acetylcholine".

3. The acetylcholine acts on a local area of the muscle fibre membrane to open multiple acetylcholine-gated protein channels in the muscle fibre membrane.

4. Opening of the acetylcholine channels allows large quantities of sodium ions to flow to the interior of the muscle fibre membrane at the point of the nerve terminal. This initiates an action potential that travels along the muscle fibre membrane.

5. The action potential

¹ The myofibrils are suspended inside the muscle fibre in a matrix called *sarcoplasm*, which is composed of usual intracellular constituents. Also in the sarcoplasm is an extensive endoplasmic reticulum, which in the muscle fibre is called sarcoplasmic reticulum. Those reticulum surround all the myofibrils within the fibre and play an important role in the control of muscle contraction.

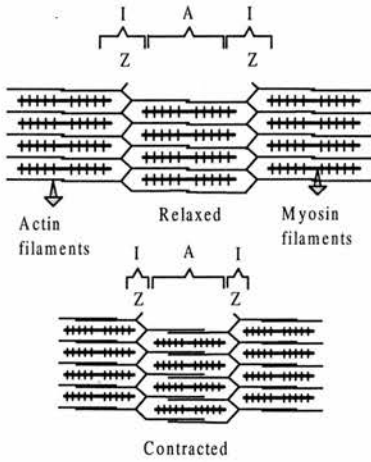


Figure 1.2: The relaxed and contracted states of a myofibril.

7. After a fraction of a second, the calcium ions are pumped back into the sarcoplasmic reticulum, where they remain stored until a new muscle action potential comes along. Muscle contraction ceases.

Each *motor neuron*² that leaves the spinal cord innervates many different muscle fibres. All the muscle fibres innervated by a single *motor nerve* fibre are called a *motor unit*. The muscle fibres in each motor unit are spread out in the muscle in microbundles of three to fifteen fibres and lie among similar microbundles of other motor units.

This interdigitation allows the separate motor units to contract in support of each other rather than entirely as individual segments. The intensity of the overall muscle contraction can be increased by adding together the individual twitch contractions (*multiple fibre summation*) and/or by increasing the frequency of stimulation (*frequency summation or tetanization*). In multiple fibre summation when the Central Nervous System (CNS) sends a weak signal to contract a muscle, the motor units in the muscle that contain the smallest and fewest muscle fibres are stimulated first. Then, as the strength of the signal increases, larger and larger motor units begin to be excited as well. In this process the different motor neurons are driven asynchronously by the spinal cord, so that contraction alternates among motor units one after another, thus providing smooth contractions even at low frequencies of nerve signals. In the process of frequency summation individual twitch muscle contractions occur individually one after another at a low frequency of stimulation. Then, as the frequency increases, there comes a point when each new contraction occurs before the preceding one is completed. As a result, the second contraction is added partially to the first, so that the total strength of the contraction rises progressively with

² Located in the spinal cord motor neurons are 50 to 100 per cent larger than most neurons and give rise to the motor nerve fibres that leave the cord and innervate the skeletal muscle fibres.

increasing frequency. When the frequency reaches a certain critical level, the successively contractions are so rapid that they fuse together and the contraction appears to be completely smooth and continuous (*tetanzation*). At still higher frequency, the strength of contraction reaches its maximum and, an increase in frequency beyond that point will have no further effect in increasing contractile force.

As described earlier, when an action potential travels along the muscle fibre membrane, large quantities of calcium ions are released into the sarcoplasm surrounding the myofibrils. These calcium ions in turn activate the forces between the filaments, and contraction begins, but energy is also needed for the contractile process to proceed. This energy is derived from the high-energy bonds of Adenosine Triphosphate (ATP), which is degraded to Adenosine Diphosphate (ADP) to liberate the energy required. Although some theories have been suggested, it is still not known exactly how ATP is used to provide the energy for contraction. We shall concentrate on the fact that, when a muscle contracts against a load, work is performed and therefore energy is required. However, the concentration of ATP in the muscle fibre is sufficient to maintain full contraction for only one to two seconds at most. Fortunately, after ATP is split into ADP, the ADP is rephosphorylated to form new ATP within a fraction of a second. There are several sources of energy for this rephosphorylation, such as substances called *phosphocreatine* and *glycogen* stored in the muscle cells. However, over 95 per cent of all energy used by the muscles for sustained, long-term contraction is derived from a process known as *oxidative metabolism* which involves the combining of oxygen with the various cellular foodstuffs to liberate ATP. The foodstuffs that are consumed are carbohydrates, fats and protein.

The efficiency of any mechanism is calculated as the percentage of energy input that is converted into useful work. According to Guyton (1991) the percentage of the input energy to the muscle (the chemical energy contained in nutrients) that can be converted into useful work is less than 20 to 25 per cent, the remainder becoming

heat. The reason for this low efficiency is that about half of the energy in the foodstuffs is lost during the formation of ATP, and even then only 40 to 50 per cent of the energy in the ATP itself can later be converted into useful work.

The SMA Muscle

Consider the design of an “artificial muscle” made of SMA. A single SMA element can be regarded as the whole “muscle” or it can be part of an arrangement of numerous elements (“fibres”) of a more powerful “muscle”.

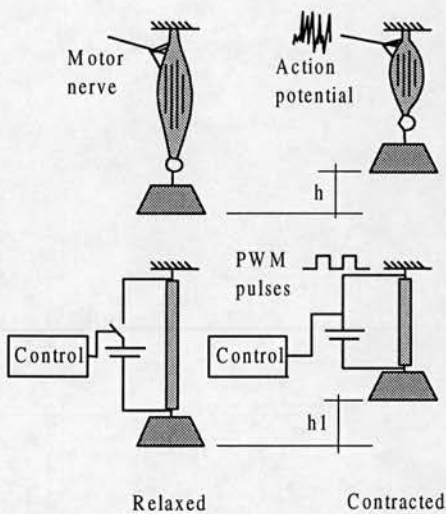


Figure 1.3: A diagram of the relaxed and contracted states of a skeletal muscle and a single SMA wire.

Figure 1.3 shows a simplified diagram of a single SMA round wire and a skeletal muscle performing work by raising a weight.

When an action potential travels along the motor nerve and reaches the muscle, a contraction will occur in the sequence described earlier. If the force developed is sufficient, the load is raised, otherwise more fibres can be recruited or the frequency of stimulation increased to increase the overall force.

The instantaneous length of the SMA wire is basically dependent on the temperature to which it is subjected (see chapter 3). Below a certain transition temperature the alloy can be easily deformed, and with subsequent heating, the original shape can be recovered. During the recovery process the alloy can develop very high levels of internal stress to overcome forces applied in the opposite direction to the shape recovery. The maximum recovery stress is a function of the cross section of the element (it also depends on the alloy composition, heat treatment and training process (see chapter 3 for more details)). The larger the cross section the higher the

recovery stress. The rise in temperature required for full shape recovery will depend on the characteristics of the alloy, but for the same SMA element under different loading conditions, the bigger the load the higher the temperature required. Also, by controlling the temperature, it is possible to adjust the rate of shape recovery, so that intermediate positions between full deformation and full recovery may be set. The heating of the element can be provided by different means, with electric heating being the most popular in the design of actuators based on SMA. A SMA element can be heated by pulses of current (such as used in Pulse Width Modulation (PWM) controllers), which allows fine adjustment of the amount of power sent to the alloy (temperature control). Therefore, fine tuning of the shape recovery is possible by using this technique. Those PWM pulses can be imagined as being similar to the action potential travelling through the motor nerve. The electronic circuits would send a signal to the “SMA muscle” to request contraction. A feedback signal can be used to monitor the status of the system and, if necessary, the power can be increased (thereby increasing the temperature and hence the recovery stress) until the load is raised. Subsequent cooling of the element allows it to be deformed into the “relaxed” position once again.

There are situations where it is not possible or viable to use one single element to develop all the necessary work. For instance, the use of larger elements may result in poor frequency response, since elements of bigger cross section usually take longer to cool. In this situation an arrangement of many wires of small cross section can be used to increase frequency response. Elements of smaller cross section generate lower levels of recovery stress, but a parallel mechanical association of elements increases the recovery stress in proportion to the number of elements. Figure 1.4 shows a possible arrangement of SMA wires.

The wires named “A” have small diameter and therefore are not very strong but can react (heat and cool) quickly, providing faster actuation. The wires named “B” have bigger diameter and are slower to cool, but can provide higher contractile forces. A very simplified analogy can be made between the operation of this system and the

multiple fibre summation in a skeletal muscle. The control system sends a signal to the smallest and faster SMA wires to contract. If those “SMA fibres” cannot generate the required forces, the control “recruits” the slower but stronger SMA wires until the load is raised. This approach can provide a smooth and quiet contraction just as observed in a muscle.

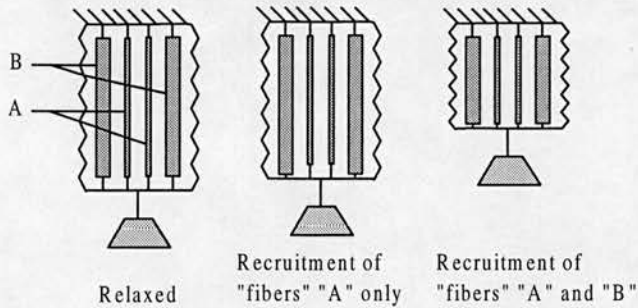


Figure 1.4: A simplified diagram of an "SMA muscle".

The efficiency of SMA actuators is usually very low. While a skeletal muscle can convert up to 25 per cent of the input energy into work, “SMA muscles” are reported to convert only around 5 per cent (for some special cases) of the input energy into work. However, a considerable amount of research is in progress to improve those figures so that, in the future, more satisfactory levels may be achieved. Nevertheless, the advantages of SMA can easily outweigh that one disadvantage to provide solutions in applications where conventional techniques are difficult to apply or are even impossible.

The previous paragraphs, describing the basic behaviour of skeletal muscles and SMA elements, reveal some interesting similarities between those two “systems”. Most notable are the smooth and quiet contractile processes used by SMA and skeletal muscles and the possibility of “recruiting” multiple elements (fibres) to increase the output force. Although we must bear in mind the limits of the analogy, those similarities raise exciting possibilities for lateral thinking by engineers.

1.4 - Aims of this Work

The specific aims of the work described in this thesis are:

- I - To investigate the main problems related to prosthetic devices paying particular attention to upper limb prostheses.
- II - To investigate the possibilities of using Shape Memory Alloys (SMA) as joint actuators for small hand prostheses and to define a methodology of designing, building and testing the actuator for that specific application.
- III - To investigate any special requirements in the design of small artificial hands so that a SMA actuator can be used to motivate their joints.
- IV - To evaluate experimentally the performance of a prototype hand prosthesis powered by a SMA actuator.

1.5 - Layout of Thesis

In order to achieve the aims described above this thesis is arranged as follows:

- Chapter 1: The present chapter. It introduces the initial considerations for this work and the motivation for the proposed investigations.
- Chapter 2: Presents a review of the field of prosthetics. The various aspects related to prosthetic devices (particularly upper limb prostheses) are described along with the main obstacles to be overcome.
- Chapter 3: An introduction of the Shape Memory Effect, its basic behaviour and a description of potential applications is given. This chapter also describes the aspects related to the use of shape memory devices, their advantages and disadvantages.
- Chapter 4: The specifications of the prototype hand are given. The basic aim is to design a hand mechanism that can be used as part of artificial arm for young

children. To achieve that, a mathematical model of the movements and forces within a chosen hand mechanism is developed and included into a computer program to simulate the behaviour of the system. The simulator is used to define the mechanical dimensions of the mechanism and to define the basic specifications of the SMA actuator to motivate the joints of the hand.

- Chapter 5: This chapter is concerned with the design and construction of the SMA actuator as specified in chapter 4. This involves the analysis of different shape memory elements, to find a suitable candidate for the application, and laboratory tests to evaluate the characteristics of those elements. The various aspects related to the design and construction of the required SMA actuator are described in detail.
- Chapter 6: An electronic system was designed to control the motion of the SMA actuator (and eventually the opening and closing of the hand) as required by the user. A set of experiments is described to investigate the characteristics of the SMA actuator and its control system.
- Chapter 7: The hand mechanism was built according to the specifications in chapter 4. A mounting frame was built to hold the hand and the actuator. The performance of the prototype was investigated through experiments.
- Chapter 8: This chapter discusses the results obtained in this research and the final conclusions are drawn. Suggestions are also given as to possible future work.
- Appendix A: Reproduction of the main code of the computer program used to simulate the behaviour of the hand mechanism.
- Appendix B: Leaflets of commercial artificial hands for young children.
- Appendix C: Publications.
- Appendix D: Practical aspects of working with shape memory alloys.
- References.

Chapter 2

Prosthetics

2.1 - Introduction

For centuries man sought to replace a lost limb by some mechanical artefact. Records of many early prostheses can be found in museums and libraries. It is considered that the earliest amputation followed by the fitting of a prosthesis was described by Herodotus (424 BC), who tells of Hegistratus of Elis, a seer who was condemned to death by the Spartans. He was tethered by his leg while waiting for execution, but escaped by amputating his foot himself. Some time later, he was again captured and put to death, but it is recorded that he had been fitted with a wooden foot (in Lamb & Law (1987)). However, the first artefact to be called an artificial limb is a Roman prosthesis dated about 300 BC. It is made of wood and bronze, and resembles the thigh, the knee and calf.

During the middle ages, while the poor and peasants wore the wooden peg prosthesis - simple, cheap and stable - richer people had the means of providing themselves with more sophisticated devices. Skilled armorers were able to produce prostheses that resembled the armour of a knight. Although these types of prostheses, fashioned in iron, were heavy, they were very functional as well as decorative.

The 16th century saw great advance in this area thanks to the work of Ambroise Paré (1510-1590). One of the most celebrated surgeons of his time, he devised and illustrated many artificial legs, arms and hands, which were of considerable complexity as shown in Figure 2.1.

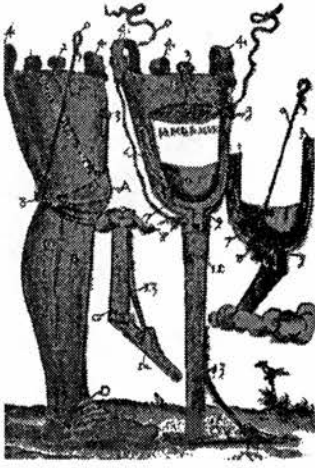


Figure 2.1: Artificial Limbs designed by Ambroise Paré - *Instrumenta Chirurgiae et Icones Anatomica* (1564).

Upper limb prostheses were also reported many centuries ago, the simple hook being the most common. Prostheses resembling the shape of the hand also appeared quite early. There are reports about one Marcus Sergius, who lost his right hand during the Second Punic War (218-202 BC) and was fitted with an iron hand (in Lamb & Law (1987)). Another rather complex artificial hand, discovered in 1800 AD along the river Rhine, is dated about 1400 AD. It is made of iron and has a rotary wrist, a rigid thumb and flexible fingers operated in pairs. The fingers were flexed passively and locked into position with a ratchet mechanism (toothed wheel).

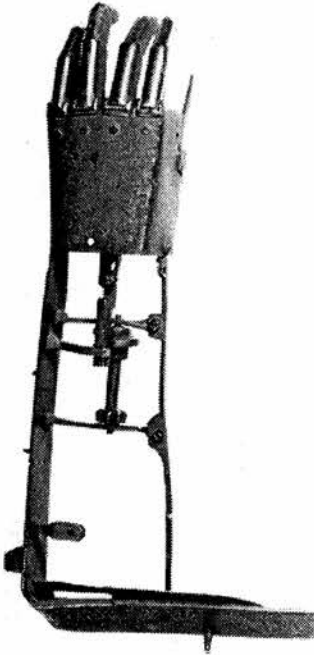


Figure 2.2: An iron artificial left hand and arm, dated about 1602. It has a fixed thumb but all fingers are moveable.

Those very elaborate hands were very heavy and depended on the opposite hand for operation. But in 1818 a Berlin dentist called Peter Ballif designed the first so called "*body powered prosthesis*". Ballif's design provided the means of powering the prosthesis by harnessing the shoulder girdle muscles¹, but was used only for forearm amputation. In 1844 Van Peetersen, applied the same principle to design an elbow flexion system. This principle evolved, and in 1855 the Comte de Beaufort demonstrated an arm with elbow flexion operated by pressure of a lever against the chest. In 1867 he published an illustration of an operating harness similar to those in use today. Another interesting alternative to powering and control was devised by

¹ The shoulder girdle consists of two bones, the scapula and the clavicle. There are seven shoulder girdle muscles which originate on the trunk and infix the scapula and/or clavicle (Pronk (1989)).

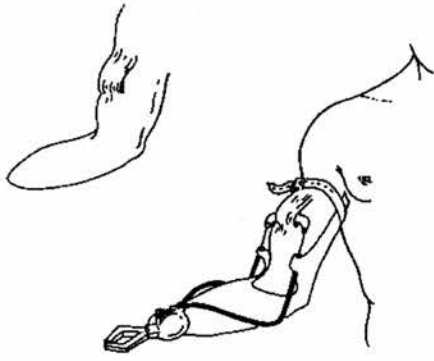


Figure 2.3: The mechanism of a Sauerbrauch prosthesis as fitted to a below-elbow limb user (in Lamb and Law (1987)).

Vanghetti in 1898. He described cineplasty² procedures in which the muscle in the stump was used to motivate the prosthesis. Following World War I, these procedures achieved great popularity and were widely applied in Germany by Sauerbrauch in 1919. One of his procedures, shown Figure 2.3, relies on a tunnel formed in the biceps, into which an insert connected to cables may be placed. Contraction of the muscle causes the hook to open and a simple spring may be used to close the prosthesis (in

Lamb and Law (1987)). Today cineplasty is considered inappropriate to power a prosthesis, since the large forces required for direct powering weaken the muscle and destroy the tunnel lining over a period of time, leaving the lesion open to infection. Another major sociological problem is that the limbs appear to be mutilated.

World War II was followed by a scientific and technological boom and, as in many other areas, the design of prostheses achieved great development. New research programs were created and funding became readily available. New techniques and new materials resulted in improved fit, lightness and more natural appearance. Development is still proceeding rapidly in many countries throughout the world.

2.2 - Background on Prostheses

In order to introduce the reader to the common definitions and jargon of the field of prosthetics, a description is given of the main components of a standard device, followed by the classification and description of the various types of prostheses.

² Cineplastics: [Kinein, to move, + Plastikos, formed]. Formation after amputation of muscles of a stump, so that it is possible to impart motion and direction to an artificial limb.

2.2.1 - The Main Parts of a Standard Prosthesis

The main parts of most prostheses are the interface, the structure, the artificial joints, the terminal devices and the cosmetic components. The characteristics and functions of each one of those may vary according to the level of limb absence and the patient's physical and psychological conditions, among many other factors.

a) The Interface

The interface components are those in direct contact with body tissues. The main interface components are:

Socket: It is the part of the prosthesis into which the stump is inserted. It must be strong enough to deal with the forces impressed upon it but also must be designed to give a good and comfortable fitting.

Controls: Provide means of operating the prosthesis. They could be simple devices such as straps and harnesses or complex techniques such as the use of electrical impulses generated by muscles to control electrical devices.

In addition to the above, any other component used to attach the prosthesis to the body and provide voluntary control or to spread the workload, is also regarded as part of the interface.

b) The Structure

This emulates the segments of a natural limb between the socket, the joints and the terminal device. External limb prostheses were originally manufactured hollow

between the joints with the loads being transmitted directly by the materials (referred to as "*exoskeletal*" structure). Nowadays many prostheses are made with an internal framework ("*endoskeletal*" structure) surrounded by a soft structure, which is solely for appearance. There are advantages and disadvantages with both types of structure. The exoskeletal structure, for example, provides more space for housing components within the dimensions of the limb. The endoskeletal structure, on the other hand, gives greater flexibility in the adjustment of axial rotation of one segment of the prosthesis with another and facilitates adjustment for length.

c) The Artificial Joints

Their primary purpose is to replace absent joints and therefore must provide the desired range of movement to the part of the prosthesis in question.

d) The Terminal Devices

This part of the prosthesis must provide the actual useful function of the prosthesis. The terminal device, whatever its shape, is the representation of the foot or the hand. Some are designed to resemble in appearance the absent hand or foot and are described as "*anthropomorphic*" prostheses. Others are designed solely for their functional use with no similarity to the human hand or foot and are described as "*non-anthropomorphic*" prostheses.

e) The Cosmetic Components

Although an artificial limb may restore some of the lost functions, the psychological impact of the loss of a limb can be the most difficult to overcome. Aware of this fact, designers often provide the prosthesis with cosmetic components which improve its

appearance and feel. The cosmetic components therefore emulate the soft tissues of the limb and give shape, as well as providing the "skin" of the artificial limb.

2.2.2 - Classification of Prosthetic Devices

Prosthetic devices can be subdivided into four main classifications, based on whether or not the prosthesis has active articulation and which source of power is used to generate the required movements:

a) *Passive Prostheses*

The articulations of this type of prostheses can be moved and set into the desired position by means of external forces. Passive prostheses may also be completely non mobile and be used only for cosmetic reasons, as shown in figure 2.4.

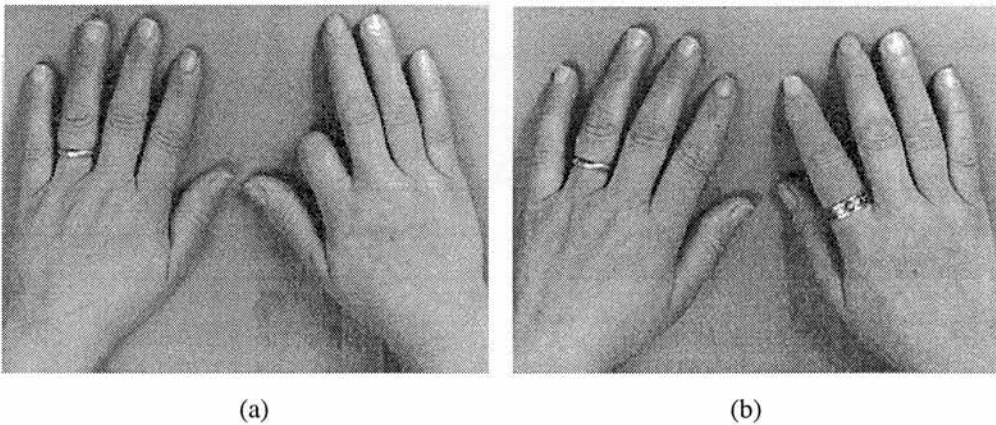


Figure 2.4: (a) Stump before attachment of cosmetic prosthesis. (b) The prosthetic finger made from silicone polymer is attached to the finger stump. The ring is included as part of the prosthesis (American Hand Prosthetics Inc., New York, N.Y., USA).

b) Body-Powered Prostheses

This type of prosthesis is operated by harnessing body movements to activate the movements of the prosthesis. Figure 2.5 shows a diagram of a body-powered prosthesis controlled by shoulder movements.

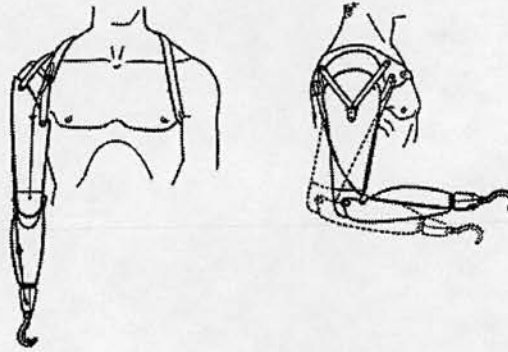


Figure 2.5: Schematic diagram of an upper limb body-powered prosthesis.

c) Externally-Powered Prostheses

In some cases it is not possible to get enough energy from the natural skeletal structures to power the prosthesis - for example when the patient has very high-level or bilateral amputation. In these situations, and according to patient's needs, it is

recommended that the prosthesis be powered by some external source of energy. At present the most common source of power is electricity provided by a battery pack (compressed gas has also been used previously). These types of prostheses are normally controlled by movements of the remaining natural structures or by electromyographic (EMG) activity for a chosen group of muscles.

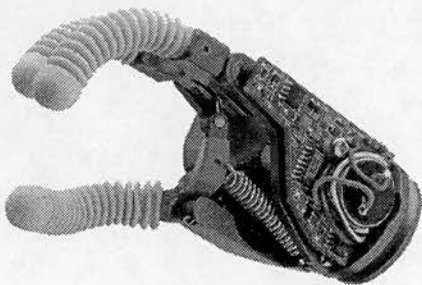


Figure 2.6: An electrically powered artificial hand (Hugh Steeper Ltd - UK).

d) Hybrid Prostheses

These type of prostheses may have body-powered parts while others are externally-powered. For example, an above-elbow limb user may be fitted with a body-powered elbow and an externally-powered hand.

2.3 - State of the Art of Prosthetics

The field of prosthetics has experienced rapid development since the end of the Second World War. However, in spite of the efforts of many research centres around the world, we are still far from producing a system that gives total satisfaction.

In the following paragraphs a brief review is presented of past and current developments in the field of prosthetics. This will be concentrated mainly on upper body prostheses, the main subject of this work. To simplify the discussion the presentation will be divided into three main parts: strategies for control, design of prostheses and acceptance and usage of prostheses

2.3.1 - Strategies for Control

This is one of the most challenging subjects of prosthetic development. A satisfactory control system for a prosthesis is yet to be achieved. The developments on the most common approaches are summarised next.

2.3.1.1 - Harnessing

As described earlier, the first prostheses were generally passive devices which relied upon a sound limb for positioning and control. In the early 19th Century the first “*body-powered*” prosthesis was developed. This very successful design provided control of the device by harnessing the shoulder girdle muscles, so that movements of the shoulder would reflect into motion of parts of the prosthesis. Since then the design has undergone some modifications, but it is basically the same as when invented. Furthermore, despite the development of other types of control, this is still the most popular system among users. The reasons for such success are not very well established, but according to Doeringer and Hogan (1995) some of the main factors are:

- It results in a cheaper prosthesis.
- The final prosthesis is not very heavy.
- The output mechanical impedance³ of the prosthesis is not high.
- It facilitates Extended Physiological Proprioception (E.P.P.)⁴. A term devised by Simpson (1974) which basically defines how much the prosthesis can be controlled as if it was an extension of the body.

The main problems of controlling and powering a prosthesis by this approach can be described as follows (Kruit and Cool (1989)):

³ How the prosthesis responds to mechanical interaction with objects in its surroundings.

⁴ The linkage of the body movement to the prosthetic component through the harness and control cable gives the user direct control over the position, velocity, and acceleration of the component and perception of the controlling physiological joint. D.C. Simpson (Edinburgh, Scotland) demonstrated empirically that linking body movements to externally-powered (pneumatic) components in a position-servo arrangement enabled children to control four degrees of freedom in such coordinated activities as feeding. He called the approach Extended Physiological Proprioception.

- The harnessing of the shoulder is generally uncomfortable.
- It requires large forces to move the prosthesis.
- The number of control inputs is limited and therefore the number of degrees of freedom of the prosthesis is limited. Nevertheless, it is possible to harness other sites such as both shoulders and abdominal muscles, which should increase the number of control inputs. However, each new independent degree of freedom of the prosthesis requires an intact degree of freedom for control, reducing the functionality of the rest of the body.
- Voluntary actuation of the device is generally restricted to one direction because the cable normally used can only carry a tensile load. Typically, gravity or an elastic device gives the required restoring force.

The large forces required for powering the prosthesis are a major problem of body powered devices, particularly for children. To overcome this problem some new techniques have appeared, such as the body-powered hand with low operating power developed by Kruit and Cool (1989). In this design the gripping force is applied by a stiff spring. When the elbow is slightly extended this spring is switched off and by further extension the hand is opened against a weak spring resulting in lower operating forces.

2.3.1.2 - Cineplasty

Although cineplastic procedures may seem a rather intrusive method of achieving control, and it is not widely applied nowadays, there are still some researches under development that rely on it to provide control of electrical prostheses.

Childress *et al.* (1995) describe their research on direct muscle attachment for multifunctional control at the Northwestern University Prosthetic Research Laboratory (USA). Small tunnel cineplasties or other surgical procedures, such as tendon exteriorisation cineplasty, can externalise the force and excursion of the

muscle. According to them, connecting the muscle to a prosthetic component via a controller that embodies the concept of Extended Physiological Proprioception enables the physiological sensory feedback inherent to the skin, muscle and other tissues of the cineplasty, to inform the user of the state of the prosthesis. They also claim that the procedure eliminates the need for proximal harnessing, can provide an additional source of control to supplement other conventional sources or can even make possible the direct control of individual fingers in prostheses for persons with wrist disarticulation or long transradial amputations.

However, there is a great debate over the advantages and disadvantages of using cineplasty and very few research groups in the field genuinely accept it as a viable technique.

2.3.1.3 - Myoelectric Control

Myoelectric control uses the electrical activity⁵ of a contracting muscle as the control signal for an externally powered prosthesis. The idea of myoelectric control is not new and started as early as 1948 (in Scott & Parker (1988)). Since then it has improved considerably thanks to the development of electronic devices needed to acquire and process the electromyographic (EMG) signal so that it can be used as a control input. Myoelectric prostheses normally do not require cables for control and in some situations (mainly for below-elbow users) there is no need for straps or harnesses for suspension. The physical effort for operation is also minimal. Those features can allow the design of self-contained, self-suspended prostheses in approximately the same dimensions and shape as the missing limb.

When myoelectric prostheses first appeared the most common EMG control system was a “two-site two-state control”. Consider the operation of an artificial hand using

⁵ A review on the physiology and mathematics of myoelectric signals is given by De Luca (1979).

this approach. Normally one pair of electrodes is placed over two muscles. Contraction of one of those muscles causes the hand to open until that muscle relaxes. The antagonist muscle is used in the same way to control the closing of the hand. As explained by Scott & Parker (1988), this strategy works in the same way as the human body - two antagonist muscles (or sets of muscles) control the movement of a joint. However, because the patient must learn how to generate independent contractions of the muscles - which requires a conscious effort - this can be difficult to learn. Also in some situations it may not be possible to find two muscles suitable for controlling the joint. In the situation where more than one joint is to be controlled, a sufficient number of muscles may not even be available. There are also other approaches such as the "one-site three-state control" (a small contraction of the muscle causes the hand to close, a large contraction causes it to open and in the absence of signal the hand stops) and the "one-site two-state control" (contraction of the muscle opens the hand and when there is no signal the hand closes).

Currently there are also a number of processing methods employing proportional control of prostheses. The EMG signal can be responsible for controlling the speed of actuation, torque and positioning of the joint. However, because of the nature of the myoelectric signal, errors and imprecision will occur for a variety of reasons (Hof (1991) and Scott & Parker (1988)).

Myoelectric signals can be detected by using basically two types of electrodes: surface electrodes placed at the surface of the skin and needle electrodes inserted in the relevant muscle site. In both cases the electrodes will produce a voltage potential with respect to ground (usually another electrode placed somewhere on the body). This voltage is the result of the asynchronous activation of hundreds of muscle fibres. The signal resembles random noise, amplitude modulated by voluntary input. Its shape depends on a number of variables such as the force and speed of activation, the electrodes, the recording site, and the electronic circuits used to collect, amplify and process the EMG signal (O'Neill *et al* (1994)).

Since one of the very first variables to affect the shape of the collected EMG signal is the electrode, many researches are dedicated to improve those devices. Nishimura *et al.* (1992) reports the use of active electrodes where a pre-amplification of the signal is done in the electrode encapsulation avoiding noises that can be inserted by cables and connectors. Filtering of unwanted noise and high frequencies is also important to provide a “clean” signal.

Further processing is usually necessary to extract as much information as possible from the EMG signal. However, the processing of biomedical signals can be a very complex task, as shown by Challis & Kitney (1990, 1991a and 1991b). The following paragraphs describe some researches using popular methods of processing EMG signals as well as non-conventional approaches.

Saridis & Gootee (1982) describe pattern recognition procedures based on statistical analysis of the EMG signals from the biceps and triceps of a below-the-humerus limb user or paralysed person. Each pattern is described by a set of features of the EMG signal, such as zero crossing and signal variance. Good separability of the classes of movements (humeral rotation in and out, elbow flexion and extension and wrist pronation and supination) is reported.

Statistical analysis is a very common approach and based on this many new mathematical techniques were developed in an attempt to understand the behaviour of EMG signals. Merletti & Conte (1995a, 1995b) introduce some techniques, review and compare different methods of analysing EMG signals and discuss their applications and limitations. The conclusion of their work is that different methods used to estimate the same parameters or variables often provide widely different results, either because they are differently affected by noise, truncation, etc., or because they define the variables of interest in different ways. As a consequence, it is important to define clearly the signal parameters of interest and to use the algorithm most suitable to the desired purpose, with full knowledge of its advantages, limitations, pitfalls and physiological implications.

Another strategy for myoelectric control classification was described by Hudgins *et al.* (1993). They have shown that in the EMG signal, collected by a single bipolar surface electrode pair, there is a set of deterministic components during the initial phase of muscular contraction - other techniques use the signal in the steady-state condition, where it is considered random (De Luca (1979)). Once these non-random components were detected, an Artificial Neural Network (A.N.N.) (Lippman (1987)) was used as a classifier. The A.N.N. was trained to recognise the relative importance of five features used to represent the myoelectric pattern: mean absolute value, mean absolute value slope, zero crossings, slope sign changes and wave form length. The A.N.N. was trained to recognise those features from four types of contractions which the limb user could reproduce reliably. Hudgins *et al.* report that the A.N.N. was capable of classifying contractions presented after the training into four categories (elbow flexion, elbow extension, wrist pronation and wrist supination) with accuracy between 70 and 98%. Further developments of this research (Kuruganti *et al* (1995)) report an improvement in the classification accuracy to 83-100% by means of using two pairs of electrodes closely spaced, but using only two of the five original features (mean absolute value and zero crossings).

Generally the methods described above involve powerful and time consuming calculations often requiring a computer. This is the main reason why those techniques still have not evolved towards clinical application. However, with the fast development in the electronics industry it is expected that the full potential of those techniques can be applied in the near future.

2.3.1.4 - Neuroelectric Control

Although the muscles normally responsible for controlling a specific function may no longer be present or are severely damaged, the peripheral nerves that contain the motor neuron for those muscles may be accessible in the remaining part of the limb (a detailed description on the neural system and conduction of signals through the

nerves can be found in Guyton (1991) and De Luca (1979)). The possibility of collecting and processing the signals directly from the nerves reveals an exciting way of improving prostheses control.

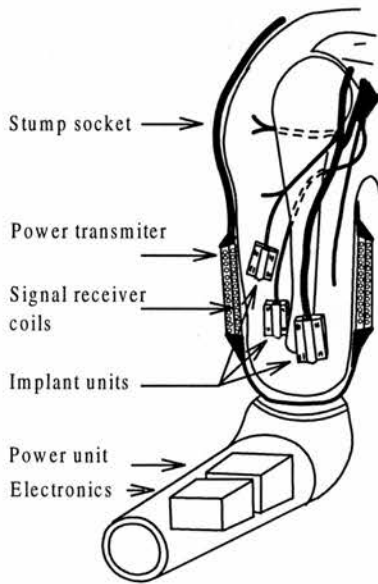


Figure 2.7: A prosthesis arrangement suggested by De Luca (1978).

De Luca (1978) presented a possible scheme for employing this methodology as shown in figure 2.7. The neuroelectric signals can be collected by special electrodes implanted in the body and attached to the relevant nerve. The Frequency Modulated (FM) signal is transmitted to a receiver placed in the socket for further processing. The power to the implanted units can be supplied via an implanted “power-receiver” powered by an external radio-frequency source. However, this interesting idea has some major problems. For instance, it is very difficult to design those special electrodes and attach them to the nerve so that they do not damage or induce degeneration of the

nerve. In the medium/long term the recorded signals may become unreliable or inconsistent.

Those difficulties are the main reason why there are not as much research in this subject as one would expect. However, with the development of new surgical techniques, new electronic devices and new prosthetic mechanisms, neuroelectric control almost certainly has a future.

2.3.1.5 - Sensory Feedback

Ideally, a prosthesis which replaces a limb should also work in closed-loop fashion with the remaining neuromuscular system. This would provide the user not only with

information about any object that the prosthesis touches but also what action it is really performing. This can enable the user to withdraw actions or even correct a wrong command. Also, feedback can provide iterative control of many parameters such as position, force, slip and overload. Current prostheses rely on the available feedback information provided by visual monitoring of the prosthesis movement, the mechanical noise, variations of vibration, pressure exerted by the socket as the prosthesis moves and Extended Physiological Proprioception (E.P.P.). Researches pursuing new methods of sensory feedback are commonly based on vibrotactile or electrotactile skin stimulation and, more recently, pressure feedback.

Geake (1994) proposed some techniques to allow the use of electrocutaneous stimulation by providing a flow of monitoring information so that the user does not have to watch the prosthesis. Data is presented as a trajectory through an array of sequentially energised electrodes. Each trajectory or pattern represents one state of the prosthesis. The research is not yet completed and major investigations are needed to evaluate potential problems with this approach such as possible tissue damage, unpleasant shock sensation, the effect of reduction or almost complete neglect of continuous sensations by the brain and possible interference with other electronic circuits such as EMG controllers.

Patterson and Katz (1992) present a review of the research activity in this field and analyse different closed-loop upper limb systems to provide the best stimulus feedback message to the body. Their initial assumption is that when grasping an object a subject does not expect noise, vibration or electrostimulation; the subject expects the natural stimulus of pressure. To explore this assumption different systems were designed and built so that five different feedback groups could be evaluated: pressure only, vibration only, vision only, pressure-plus-vision and vibration-plus-vision. The stimuli were applied to the upper arm of the subject via a pressure/vibrotactile cuff. The authors report that the conditions of pressure alone and vibration gave the greatest errors in performing some predefined tasks. Those conditions involving visual feedback had significantly lower errors, with pressure-

plus-vision having the lowest. It was also found that the conditions of vision-alone and vibration-plus-vision had approximately the same error levels. Although the experiments involved only non-handicapped volunteers, the authors concluded that, based on the experiments, an artificial sensory feedback must attempt to replicate the stimulation that one receives from the grip of a natural hand. In other words, it was considered that pressure provides a more natural feedback than other approaches such as vibration and electrocutaneous stimulation.

2.3.2 - Design of Prostheses

2.3.2.1 - Passive Prostheses

As mentioned before, passive prostheses are completely non-mobile or can incorporate passive articulations that can be moved and set into position using a sound limb. Until the advent of body-powered systems it was the only way of replacing some functionality of a lost limb. Classical examples are the wooden pegs and hooks, still used nowadays for their simplicity and low cost.

Passive prostheses are used for cosmetic and functional reasons, and to accustom users to the weight and presence of a prosthesis. Although it can provide some functionality, the main reason for fitting a passive prosthesis is cosmetic (Lamb (1993)). According to Lamb and Law (1987) the fitting of passive prostheses is indeed preferred by prosthetists in many cases where much of the natural articulation is still available (for instance, amputations distal to the elbow for a unilateral limb user).

Until recently, polyvinyl chloride (PVC) was the material most often used for covering prostheses. However, the colour and hardness of PVC does not provide good appearance and touch feeling. The use of silicone rubber has shown better

results in this regard. The processes of production of cosmetic coverings using silicone rubber are well developed and provide prostheses with startlingly realistic appearance. More recently, Aesthetic Concerns Prosthetics Inc. (1996) advertise the use of computer aided design and a special pigmented silicone matrix that allow considerable improvement in the matching of the shape and colour of the prosthesis to the user's natural limb. The prosthetic pigmentizer also allows change of the colour of the "artificial skin" to match changes in the colour of the user's skin which can happen throughout the year.

2.3.2.2 - Body-Powered Prostheses

The term "body-powered" means that the power to operate the prosthesis comes from the user's own body. The most common body-powered prosthesis is the cable-operated prosthesis. The user wears a harness that translates body motion into motion of some part of the prosthesis. In one example, the shoulder harness pulls a cable that lifts the prosthesis forearm and gravity is needed to pull it down and extend the elbow.

One way of expanding the functionality of this system is described by Lamb and Law (1987) . An elbow-locking mechanism is used to allow selection of elbow flexion or terminal device (hand) opening under the action of a single motivating cord. When the elbow is not locked, tension and movement of the motivating cord will result in flexion of the prosthetic elbow joint, while the terminal device remains closed - gravity is responsible for the extension of the elbow joint. When the elbow is locked the tension in the motivating cord is transmitted distally to the terminal device and will open it against a spring.

Although body-powered prostheses, in particular cable-operated ones, have not changed much since the end of the Second World War, they are still the most popular choice among users. Doeringer and Hogan (1995) discuss the reasons for such

popularity and analyse the performance of those devices for certain tasks. The results show that users of body-powered prostheses, specially experienced ones, were able to statically position the prosthesis as well as their unimpaired arms, but required a fairly large number of discrete movements to point the prosthesis to a given position accurately. Also the users generally could not position the prosthesis as fast as the sound limb. This is hardly surprising given the dexterity of the unimpaired human hand. It was suggested that one of the reasons for deterioration of performance is the high force necessary to power the prosthesis. According to Doeringer and Hogan, the use of a pulley system, or similar, to amplify the body forces, and improvements in the cable geometry are necessary to improve performance. However, increasing the torque alone would correspondingly reduce the range of motion of the prosthetic joint for a given amount of body movement. The use of an external power source is therefore proposed to amplify the body force without reducing motion range. Unfortunately, this also has the drawback of degrading the ability of the body of feeling an external torque - an important feedback variable to the control of the prosthesis. Those problems are yet to be solved, showing that, although body power prosthesis is a very popular design, there is still plenty room for improvement.

2.3.2.3 - Externally Powered Prostheses

So far the majority of researches in artificial limbs used two main sources of external power: compressed gas and electricity. Next, a brief review is given on researches and clinical systems using those sources of power.

i - Gas Powered or Pneumatic Prostheses

Pneumatic prostheses were under quite intense research in the past (Lamb & Law (1987) and Plettenburg (1989)). However, those devices were often too complex for

commercial manufacture. Furthermore, the use of pneumatic prostheses involved some “logistical” problems, such as:

a) The cylinders containing the gas (carbon dioxide in most cases) were heavy and big. This was necessary for safety reasons, since gas under high pressure presents a hazard which must be dealt with carefully.

b) It is not possible to supply the pneumatic actuator with gas directly from the storage cylinders. The vapour pressure is too high and varies with ambient temperature. A pressure-reducing and regulating device must be fitted to maintain the pressure of the gas supplied at a constant value. This contributes to further increase in weight and volume and also increases the energy losses of the system.

c) The containers could only be refilled by specialised centres. Transportation required special delivery as the postal services would not accept the containers in the regular mail.

d) The noise of the compressed gas exhausted to the atmosphere after the working stroke was an unwelcome feature. Silencers were developed which almost eliminated that problem. However, it also increased the weight and volume of the system.

The greatest advantage is that pneumatic “motors” (figure 2.8) can be made light, small, simple and capable of delivering a high-power output at very fast rates. When

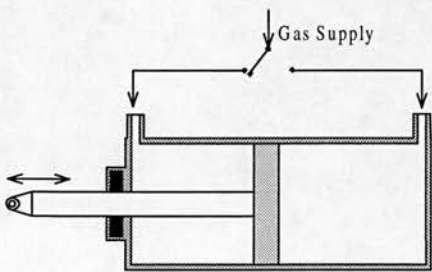


Figure 2.8: Diagram of a pneumatic actuator.

small disposable carbon dioxide gas containers became commercially available at low prices in the last decade, some researchers started once again to look for possibilities of applying this source of power in prosthetics (Plettenburg (1989)). However, no substantial work has been found by this author regarding major developments in this technique.

ii - Electrically Powered Prostheses

The development of electrically powered prostheses started shortly after the Second World War. Since then a number of prostheses have been devised but very few reached good clinical acceptance until the last decade.

The power for those prostheses is provided by secondary battery cells. Those batteries can be recharged inexpensively many times. They can also operate at high discharge currents which allows the use of more powerful DC motors. The Nickel-Cadmium rechargeable cell is the most common in prosthetic applications. It is mechanically robust, able to tolerate charging and discharging at high rates and unless badly damaged, is leakproof.

Notwithstanding the fact that there are a number of electrically powered prostheses commercially available and under development, four devices were chosen to describe some of the techniques used in upper limb prostheses: the Utah arm (Jacobsen *et al.* (1982)), the Steeper Scamp Hand (Appendix B), the VV Series VASI Hands (Appendix B) and the Southampton hand (Kyberd (1990), Kyberd *et al.* (1993), Kyberd & Chappell (1994) and Kyberd *et al.* (1995)).

The Utah arm was developed as a series of modules which can be used on persons with unilateral or bilateral amputations, ranging from wrist disarticulation up to forequarter amputation (that flexibility is one of the main reasons why this device has been so successful for a number of years). There are five modules to perform prehension, wrist articulation, elbow flexion, humeral rotation and shoulder flexion and abduction. The joint modules are interconnectable to provide maximum flexibility in fitting patients with a variety of residual capabilities. The modules also can be actuated/controlled by a number of options including electronic actuation, body-powered cables, passive joints with adjustable friction, EMG signal command systems, control switches and mechanical motion sensors.

The Steeper Scamp hand and the VV series VASI hands (see Appendix B) are commercially available electric hands designed for young children. These prostheses are powered by DC motors providing grip forces of 10 N for the Scamp hand and 20 to 38 N (depending on the model) for the VASI hands. Both hands use a “pinch attitude” (one degree of freedom) to grasp objects and are controlled by a “switch operated” electronic system.

The original Southampton hand was built in 1969. Since then, other versions of it have been developed in an attempt to produce “the next generation” of artificial hands. The Southampton hand described by Kyberd & Chappell (1994) is a five fingered device with four degrees of freedom (thumb flexion/extension, thumb abduction/adduction, index flexion/extension and flexion/extension of the other three fingers simultaneously). As the fingers flex they curl through a fixed trajectory and sensors to detect force and slip are used to control grip force. The control inputs are normally given via EMG. Kyberd *et al.* (1995) describe the design of a hand prosthesis known as MARCUS (Manipulative And Reaction Control under User Supervision), using the technology developed by the Southampton group. The design, control and functionality of the MARCUS hand are similar to the Southampton hand, but it has only two degrees of freedom (thumb flexion/extension and flexion/extension of all fingers simultaneously).

2.3.3 - Acceptance and Usage of Prostheses

The artificial limb problem is still far from a satisfactory solution. It is estimated that only 50% of those with upper limb disabilities wear prostheses, versus 75% for leg prostheses (LeBlanc (1991)). Statistics also indicate a general dissatisfaction with upper limb prostheses. Many users (mainly those with one sound arm) feel that a prosthesis offers too little cosmetic benefit and functionality to compensate for the discomfort and inconvenience of wearing the device. Of those upper limb users, it is estimated that the usage of externally powered prostheses was about 10% in 1995

(Doeringer & Hogan (1995)), although it is rising gradually as more sophisticated devices appear. This means that 90% of those who wear prostheses still use the body-powered type.

Kejlaa (1993) studied 66 upper limb users in Denmark. The research aimed to evaluate consumer concerns about their prostheses, check if these were related to cessation of use and estimate functional levels of both prosthetic users and non-users. The study involved three prosthetic systems: two active systems (body-powered and myoelectric) and one passive system. The investigation showed that users of active prostheses have a superior performance in daily living over the passive and non-users. The main problems in daily activities were reported to be hygiene, grooming and dressing. The main complaints of users about their prostheses are transcribed next.

Complaints about body-powered prostheses:

- Heavy and hot to wear.
- The suspension system caused irritation of the skin and was often wet with perspiration which could lead to operational failure.
- The control system could fail when wires slackened or broke.
- Control wires connected to the socket often damaged clothing at wrist and elbow levels.
- Underwear such as undershirts were also damaged by the suspension system.
- Users undertaking heavy work experienced socket problems sometimes leading to pressure sores and loosening of the prosthesis.

Complaints about myoelectric prostheses:

- Heavy and hot to wear and the cosmetic gloves were difficult to keep clean.
- Slow in action and difficult to control.
- The close fitting sockets could give discomfort with heavy loads.

- When there was a prosthesis failure it was always necessary to contact a prosthetic centre or a prosthetist.

Complaints about passive prostheses:

- Hot to wear and the cosmetic gloves were difficult to keep clean.
- Some damage of clothing by the suspension system.

The causes of cessation of use of body-powered prostheses were reported as: prosthetic discomfort, delayed prosthetic supply, the prosthesis was not essential, illness and psychological reasons. Myoelectric prostheses were rejected mainly for prosthetic failure and discomfort. Only one user of passive prostheses stopped using the device.

2.4 - Problems to be Overcome

As shown above, there is still a considerable amount of problems to overcome so that a satisfactory artificial limb can be produced. The next paragraphs discuss some of the major obstacles which prosthetists have to face when designing artificial devices.

2.4.1 - Actuators

Although body-powered prostheses are commonly used, it is unlikely that a sophisticated device, such as a multifunctional arm/hand system, can be designed solely based on that principle. Pneumatic actuators would provide a possible solution, but their present stage of development is also not satisfactory. Electric DC motors are the most common choice to provide multifunctional actuation. However, they still can be noisy, do not provide a natural motion of the joint (at least not without the use

of sophisticated control systems), the power consumption is much higher than desired for the current battery power supplies and the power/weight and power/volume ratios are still very low. This means that DC motors, and sometimes the necessary gear boxes, powerful enough to provide motion of a joint, are still heavy and occupy a great deal of space within the already small volume of a prosthetic device such as an artificial hand.

2.4.2 - Power Supply

The design of externally powered prostheses is also affected by the current state of the art of power supplies. A portable and rechargeable source of energy is the desirable alternative for externally powered prostheses. The more energy which can be stored per unit of volume and weight on a portable unit, the better. As described before, gas cylinders used in pneumatic prostheses did not achieve great popularity and the use of battery cells is almost standard in most current applications. However, battery cells are still heavy, large and cannot deliver the necessary power for some applications.

2.4.3 - Adaptation of New Techniques for Clinical Use

The miniaturisation and development of new and faster electronic components is another important issue. Most of the new techniques under development, which aim to provide better control of the prostheses, rely heavily on complex software and hardware. The use of such techniques in clinical applications will require the necessary computational power to be compacted and fitted into the dimensions of artificial devices.

2.4.4 - User's Control and Feedback

As described earlier, this is maybe the area where new developments are most needed. Harnessing joint movements to provide control and feedback is not ideal for the reasons described before. Cineplastic procedures may offer an interesting solution, but they do not attract much interest currently, since they are very dependent on the development of new surgical techniques and reliable interfacing mechanisms between the cineplastic tissues and the prosthesis. Also, cineplastic techniques seem to be feasible only in a limited number of cases such as wrist disarticulations. The development of new surgical techniques, new electronic devices and new processing techniques is also essential to future development of neuroprostheses and new EMG control systems.

The sensory feedback provided by most of the current prostheses is still minimal or non-existent. It is not intended here to postulate that a sensory feedback as sophisticated as that of the human hand must be developed. However, the more information the user can get about the state of the prosthesis the better he can control the device in a more natural way.

2.4.5 - Natural Behaviour

In spite of the effort of many researchers, current artificial limbs still do not behave in a natural fashion. The movements are normally rough and "robot-like" demanding considerable effort for control. The motion of electrical prostheses is generally accompanied by the noise of the electric motors, another highly undesirable feature. Such problems have also to be addressed carefully if it is intended to provide a more realistic artificial substitute for a lost limb.

2.5 - Benefits and Possible Applications of Shape Memory Alloys in Prosthetics

A detailed description of the shape memory phenomenon and its applications is given in chapter 3. Shape Memory Alloys (SMA) can allow the development of devices which occupy very little space, are extremely light, can generate large forces per unit of weight, are noiseless in operation and can be shaped to suit the needs of the designer. Therefore, it is not surprising that one can visualise the development of prosthetic devices using SMA. This section will present some possibilities of using those alloys in the various areas of prosthesis design. No attempt is made to demonstrate how to implement the devices described below using the current technology.

The potential use of SMA to mimic the behaviour of a human muscle has been described (chapter 1). A “SMA muscle” would contract and extend in similar fashion to the human muscle and can even be composed of hundreds of “SMA fibres”. Smaller fibres can be recruited for fast actuation at lower forces and, as the load increases, bigger fibres can be recruited to sustain the load demands.

Because the resistivity of SMA changes as its shape changes through deformation or shape recovery, it is possible to monitor the “status” of the SMA element by monitoring its electrical resistivity. This means that a joint powered by a SMA actuator would not need a position sensor, since the SMA element can act as actuator and sensor. This eliminates the sensor from the control system, contributing to the reduction of volume and weight of the overall system.

The SMA element can be shaped to suit the needs of the designer. This can allow the design of new braking or locking systems for artificial joints based on SMA. Two possible arrangements are shown in figure 2.9.

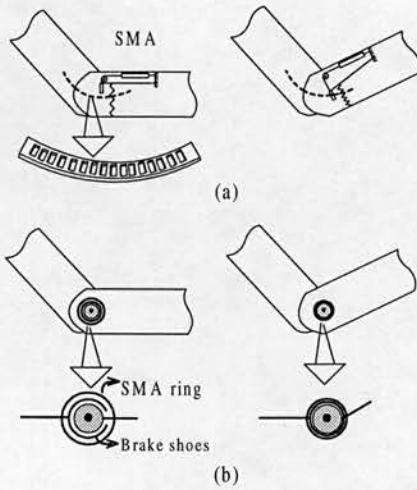


Figure 2.9: Possible schemes of locking or braking systems using SMA.

Figure 2.9(a) shows a mechanical lock using a standard one-way shape memory alloy. As the SMA is heated it contracts (shape recovery) pulling the lever and releasing the locking so that the joint is free to rotate. When the joint reaches the desired position the power to the SMA is removed and as it cools down a spring pulls the lever to lock the joint and deform the SMA element. Figure 2.9(b) shows a two-way SMA element shaped as a ring. If the temperature of the SMA ring is below its transition temperature, the ring has a diameter larger than the diameter of the “brake shoes”,

and the joint can rotate freely. Heating the ring causes it to contract, reducing the diameter around the “brake shoes”. The forces generated are such that the “brake shoes” would prevent any movement of the joint. When the temperature is again below the transition temperature the ring automatically changes shape again to the larger diameter.

Another application described by Kuribayashi (1986b) uses SMA elements to provide tactile control for artificial hands (Kuribayashi applies the principle in robotic hands). He describes a three fingered hand with three joints in each finger. Stepping motors are used for rough positioning. As the finger touches the object the motors are stopped and the controller uses the SMA elements for fine control of the position. However, the main advantage is that, by controlling the temperature of the elements, what is really being controlled is the recovery stress of the SMA. Therefore, it is possible to fine tune the force applied to the object.

SMA actuators can be small, light and yet very powerful. Those are highly desirable characteristics of any joint actuator, specially those dedicated to very small devices such as children’s prostheses. Nowadays, if someone loses a finger or thumb, he/she

would most certainly be fitted with a passive cosmetic device such as the one shown in figure 2.4. This is considered satisfactory since the loss of a finger does not significantly reduce the functionality of the hand. But there are more severe cases such as partial amputation of the hand or when most of the fingers are lost. In those situations the development of active fingers/thumb is desirable. In other words, any device used to promote motion of the joints must be fitted inside the volume of the fingers/thumb. With prostheses for children the problems are very much the same. There is not much room for components, the prosthesis must be as light as possible, noiseless motion is a welcome feature, and still the actuator must provide reasonable force.

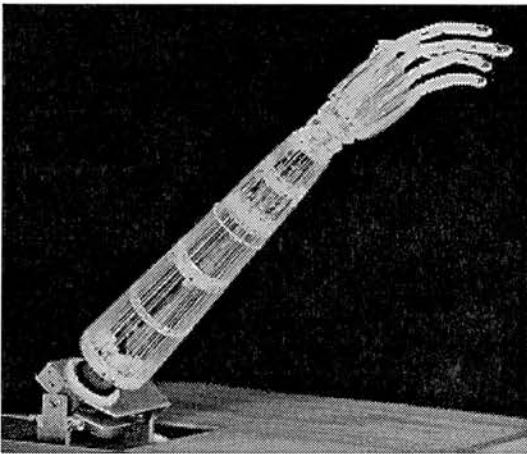


Figure 2.10: The prosthetic arm from Oaktree Automation - USA

Finally, the ultimate dream of a prosthetist who is also an “SMA enthusiast” would be the development of a complete prostheses using solely “SMA muscles”. The actuators could be spread around the “artificial skeleton” providing motion to every joint of a human like prosthesis. This “dream” is unlikely to be realised in a very near future since current SMA elements require a considerable amount of energy for shape recovery and

the efficiency is very low. However, the principle has already been demonstrated by Oaktree Automation (Boggs (1993)). Their human-like prosthetic arm (figure 2.10) has 36 actuators (using a total of one hundred and eight 250 μm FlexinolTM Nickel-Titanium SMA wires) located within the hollow forearm and hand. In a similar fashion to the natural joints, opposing pairs of actuator wires power each finger. Unfortunately, this arm is not feasible as a real prosthesis due to factors such as the high power required and the complex system required for controlling the device. However, monitored by a computer system, the arm duplicates the motion of a

human hand so accurately that it can form sign language symbols (this hand is also known as “The Fingerspelling Hand”).

2.6 - Conclusion

This chapter provided some background on the area of prosthetics, describing past and current developments along with some of the most important problems affecting the design and usage of prosthetic devices. A short discussion on some possible applications of Shape Memory Alloys (SMA) in prosthetics was given. Chapter 3 introduces the Shape Memory Effect and other aspects related to the use of SMA devices.

Chapter 3

Shape Memory Alloys and Actuators

3.1 - Introduction

During the past two decades Shape Memory Alloys (SMA) have proved to be very useful in a number of different applications. Nowadays many devices taking advantage of the characteristics of those alloys are a commercial success world-wide. Actuators based on SMA have a very high power/weight ratio, which favours them in applications demanding high forces but very low weight. Although many different actuators have been produced, little has been said about the problems one should expect when designing and developing such systems. This chapter describes the Shape Memory Effect (SME), its applications and the various considerations to be taken into account when using SMA.

3.2 - Background

The so called Shape Memory Effect can be seen in certain alloys, such as Ni-Ti and Cu-Zn-Al (Kennon & Dunne (1981) and Wayman (1993)). This effect is associated with internal transformations of the alloy, known as *thermoelastic martensitic transformations* (Wayman & Duerig (1990)), which allow these alloys to convert thermal energy into kinetic energy. This martensitic transformation is the kind of

transformation in crystal structures which occurs in the heat treatment of steels to give them hardness and strength. In shape memory alloys, the martensite, unlike the martensite in steel, is thermoelastic, that is, it continually appears and disappears with falling and rising of temperatures.

There are two very distinct phases in the SME: the *Martensite Phase* and the *Austenite Phase* (Wayman & Duerig(1990) and Tanaka (1990)). In the martensite phase the alloy is easily deformed if under stress (Figure 3.1 (a) -> (b)). Provided that the strain does not exceed a certain amount (usually around 6-10% for NiTi), the original shape can be fully recovered upon heating (c), when the alloy enters the austenite phase (reverse transformation of the martensite phase). An important feature related to this phenomenon is that the deforming stress below the *Martensite finish* (M_f) temperature is considerably smaller than the recovery stress. This is one of the most valuable properties in the development of actuators based on SMA.

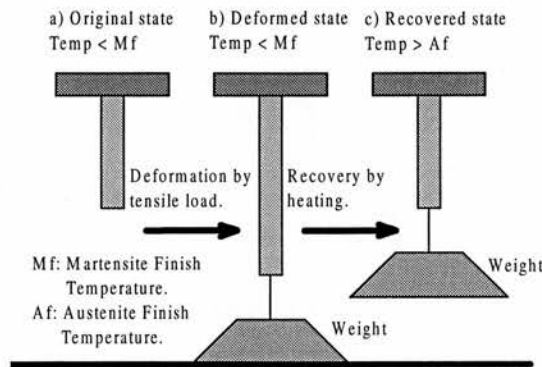


Figure 3.1: The Shape Memory Effect.

In order to specify a useful SMA actuator one must be familiar with some basic aspects of SMA behaviour. Therefore, before going into the design itself, a brief background will be given. It is not intended to explain fully the shape memory phenomenon, since it is a complicated matter outside the scope of this work. The discussions will be concentrated mainly in those points which will affect the design of SMA actuators. However, a good understanding of the shape memory

phenomenon is vital for any successful design, and the reader is encouraged to look into more specific references.

3.2.1 - The Shape Memory Effect

The Shape Memory Effect is a property of some special alloys and has been known for more than 50 years. Nevertheless, it is only within the past 25 years that substantial progress has been made in the development of such alloys. SME can occur in many binary and ternary alloy systems (Ni-Al, Cu-Zn, Cu-Al, Cu-Zn-Al, Mn-Cu, Fe-Pt, and others) but the most successful alloy to date is the near equiatomic Nickel-Titanium (NiTi) alloy. This alloy, discovered at the Naval Ordnance Laboratory in the USA (hence its commercial name NITINOL), can revert deformations of more than 10% strain when heated above the *Austenite finish* (A_f) temperature.

The alloy fabrication is a laborious task and involves precise control of every step. Although this matter is not discussed in this work, the reader must be aware that the fabrication technique is vital for the desired application. Many factors contribute to the final properties of the alloy, of which the most sensitive is the chemical composition. SMAs can be supplied in many different shapes to fit different applications but the most common shapes for actuators are round and flat wires and coil springs. The choice of the correct alloy and its shape are paramount to the application in mind.

3.2.1.1 - Microscopic Analysis

The SME must always be analysed by its microscopic and macroscopic changes. Figure 3.2 shows a very simplified diagram of what happens in the microscopic world. The grid shows a two dimensional picture of a typical crystal structure,

representing the arrangement of the alloy's component metals. In this case it could be Nickel and Titanium.

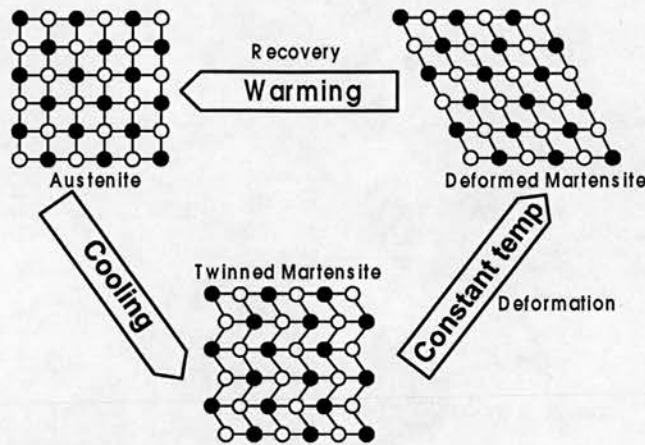


Figure 3.2: Crystal structure.

There are two distinct phases: a high temperature phase called *parent phase* or *austenite* and a low temperature phase called *martensite*. The ability of the SMA to easily transform to and from martensite is the basis of the shape memory effect.

Consider a SMA sample in its high temperature austenite phase, showing its original shape. By cooling it down the crystal structure will change to a *twinned martensite* structure but, although the crystal structure has changed, its shape has not. From this point the material can be easily deformed, leading to a *deformed martensite* state. The shape recovery can be achieved by heating the specimen until it reaches its high temperature austenite phase. Note that, although the atoms within the structure move, they do so by a pivoting action, so that, after the deformation, each one keeps the same neighbours. This diffusionless transformation is the key to the SME, since it allows the atoms to return to their original positions when the specimen is heated.

3.2.1.2 - Macroscopic Analysis

Figure 3.3 illustrates a very simple experiment using a SMA wire. The upper end is fixed and a weight is attached to the other end. Starting the experiment with the material in its high temperature austenite phase and assuming that the load is below a maximum limit, one can expect the wire to show its original length. By steadily

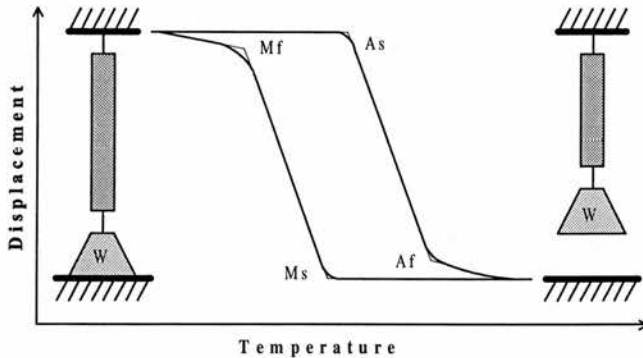


Figure 3.3: Changes of shape under constant load conditions.

decreasing the temperature the material will enter the twinned martensite state and the tensile load will elongate the wire. By increasing the temperature the recovering process starts and, when the temperature rises above Af, the sample will fully recover its original shape.

The transformation from one state to another does not occur at the same temperature on heating and cooling, but follows a hysteresis cycle. This hysteresis gap is described by the transformation temperatures M_s , M_f , A_s and A_f (*Martensite start*, *Martensite finish*, *Austenite start* and *Austenite finish*) and it is normally in excess of 10 °C for most alloys.

3.2.1.3 - The Rhombohedral Phase

The previous paragraphs described the SME basically as a martensitic transformation associated with a rather large temperature hysteresis. However there is a competing transformation that can occur prior to the martensitic transformation called *Rhombohedral phase* or, as it is commonly known, *R-Phase*. It can be realised by suppressing the martensitic transformation relative to the R-Phase, by means of

special processing and treatment (Otsuka (1990)). This phase is mainly detected during the *Austenite* \rightarrow *Martensite* phase transition, as shown in figure 3.4. However, Goubaa *et al.* (1991) demonstrated that, for TiNi and TiNiCu alloys, the R-Phase is always present. Its detection or not depends on the method used to measure it and the possibility of interference between the R-Phase and the martensite phase. The results also showed that the R-Phase can also be observed upon heating. In similar research, Jordan *et al.* (1994) proved that, whatever the NiTi alloy is, binary or ternary, there is always the transformation sequence: *Austenite* \leftrightarrow *R-Phase* \leftrightarrow *Martensite*. If this sequence is not observed, it is only because the R and martensite transformations proceed in a too narrow temperature interval (as it generally occurs on heating).

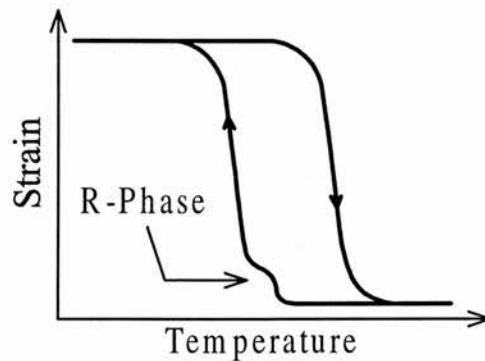


Figure 3.4: Detection of the R-Phase during cooling.

The main advantage of the R-Phase is that the hysteresis is around 1.5 °C. For this reason many researchers use this special transformation rather than the martensitic transformation to perform precise proportional control of devices based on SMA (Ikuta *et al.* (1994)). However, the disadvantage is that the recovery strain is usually around 0.5%, which is quite small compared to the martensitic shape memory. Otsuka (1990) has also demonstrated that it is necessary to keep the load very small, since large loads will produce larger hysteresis, indicating the inducement of martensite. Those disadvantages have limited the use of the R-Phase to only a few

useful devices. Nevertheless, it is an excellent option if the application involves small strain and small loads.

3.2.1.4 - The Two Way Effect

A SMA sample that displays the two-way effect is able to memorise its hot (austenite) and cold (martensite) shapes. This can be achieved by means of variations in the fabrication process and some thermomechanical treatment. As it will be explained later, the sample must be heat treated (to fix its “hot shape”) so that, after deformation, it can recover that “hot shape” when heated above A_f . By heavily deforming the specimen in the martensite state or by heating under constraint after it has been deformed in the martensite state, it is possible to train it to remember its martensite shape (other techniques to achieve the two-way effect are also shown by Suzuki (1987) and Perkins & Hodgson (1990)). In so doing, when the sample is heated above A_f , it will show its original hot shape and, upon cooling below M_f , it will spontaneously deform into the trained cold shape. At this point it is important to mention that all SMA samples display the two-way effect to some extent. This tends to increase with the number of cycles, particularly if the sample suffers the same deformation throughout the cycling and it is under high stress.

Although the two-way effect is a very interesting phenomenon, it is not yet very well developed and the forces involved, mainly upon cooling, are not large enough to produce any reasonable work. Those problems are the main reasons why the applications of the two-way effect are limited to very few areas (Escher *et al.* (1992) and Ivshin & Pence (1992)).

3.2.1.5 - Superelasticity

In the SME the strain induced at temperatures below A_s is removed by heating the specimen to temperatures above A_f . In the superelastic or pseudoelastic effect the strain induced at temperatures above A_f is eliminated just by removing the stress. This can be achieved because, even at temperatures higher than M_s , it is possible to induce a martensitic phase by applying stress to the specimen (Shimizu & Tadaki (1987)). The martensite phase is therefore called *Stress Induced Martensite* (SIM) and is the basis for the superelastic effect. Figure 3.5 shows the relationship between

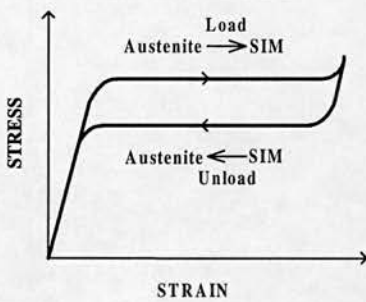


Figure 3.5: Superelastic effect

stress and strain for an ordinary superelastic SMA.

When deformed at temperatures higher than A_f , the specimen undergoes a transformation from the austenite phase to SIM phase. The reverse transformation to the austenite phase will occur upon removing the stress at the same temperature. Note that the superelastic effect is a completely isothermal event.

3.2.2 - Measuring the Transformation Temperature

The Transformation Temperature (TTR) is the one of the most important parameters when working with SMA. It defines the temperature at which the alloy changes from high temperature austenite to low temperature martensite or vice-versa. The TTR varies considerably depending on the processing of the alloy and the operational conditions. However, the chemical composition is the most important parameter that will affect the TTR. For instance, for the near equiatomic Ni-Ti alloy, the transformation temperature can be adjusted within a range of -200 to $+100^\circ\text{C}$ by changing the proportion of titanium.

Although the TTR is basically set during manufacture, it can shift from that set point because of a number of reasons, such as the operational stress and strain. Therefore it is important to measure the TTR under different operational conditions. Many approaches have been tried (Honma (1987)) but the following methods are very common, simple and widely used:

a) Constant Load

Starting with the material in its original shape, a deformation force is applied to the alloy and the changes of shape are monitored simultaneously with the temperature as the alloy is cooled and heated through the hysteresis cycle. A curve should be obtained, as shown in Figure 3.3, with the four main temperature points (M_f , M_s , A_s and A_f). Any of those may be used as TTR. Some researchers also monitor the changes in other characteristics of the alloy such as electrical resistivity and magnetic susceptibility, but those methods normally demand a very precise and expensive range of test equipment.

b) Differential Scanning Calorimeter

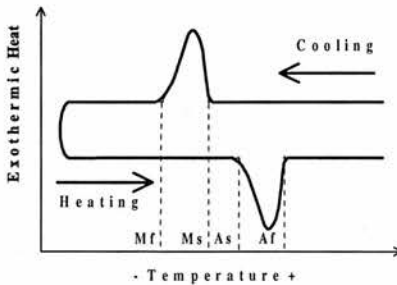


Figure 3.6: Measuring TTR using DSC.

A very precise measurement of the transformation temperature at zero stress can be made by using a Differential Scanning Calorimeter (DSC). This measures the amount of heat given off or absorbed by the sample as it is cooled or heated through the temperature transformation range. A typical plot from a DSC is shown in Figure 3.6.

Note that the transformation temperature is a stress dependent parameter (Wayman & Duerig (1990)) and therefore it will shift depending on the stress applied to the material. Under normal conditions, the higher the stress the higher will be the transformation temperature. Figure 3.7 shows a typical effect upon the transformation temperature of applying different levels of stress.

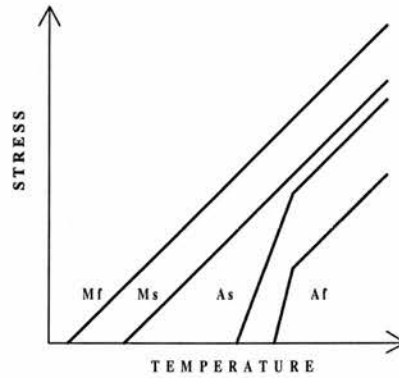


Figure 3.7: Effect of stress upon TTR.

3.2.3 - General Applications

Since their early days SMAs have been considered a metallurgic solution waiting for future problems. Nowadays the use of SMA is widely spread in many different areas. In an attempt to define product screening criteria, Duerig *et al.* (1990) divided the SMA systems into five categories according to the functions they perform:

I - Free Recovery Devices

If nothing interferes with the shape recovery, the process is referred to as *free recovery* and therefore the only function of the element is to cause motion or strain.

II - Constrained Recovery Devices

This includes applications in which the element is prevented from recovery and therefore will generate a stress. The use of constrained recovery in pipe couplings, fasteners and connectors (Borden (1991) and Schetky (1994)) is currently one of the most successful application of SMAs

III - Actuators

In an actuator the SMA element recovers its shape against a stress. This has been considered to be the application with the greatest potential but, as it will be shown later, reliable SMA actuators are not easy to achieve. Actuators based on SMA can be divided into three categories, according to the method of changing the temperature of the alloy:

a) Thermal Actuators

Thermal actuators are heated by changes in the ambient temperature. Therefore they can be used to respond to a change in the ambient temperature. In such applications (Stoeckel (1990) and Stoeckel & Wayman (1991)) they operate as a combined temperature sensor and actuator.

b) Heat Engines

This type of actuator is used to transform thermal energy into mechanical energy. Although it seems a very interesting idea and there are many ingenious designs in the literature (Banks (1981) and Ginell *et al.* (1979)), the levels of work delivered by these devices are not yet good enough to attract any commercial exploitation.

c) Electric Actuators

These actuators are heated by passing electric current directly through the SMA. Various reports (Schetky (1984), Nakano (1984), Kuribayashi(1986a and 1986b), Besselink *et al.* (1991), Hesselbach & Stork (1994) and Hodgson (1990)) have shown that, by controlling the current, it is possible to control these devices very accurately.

IV - Superelastic Devices

The superelastic effect has already been described in this work as being isothermal and involves the storage of potential energy (Otsuka & Shimizu (1981)). Proper use of superelasticity requires care and has some limitations, since it cannot be used over a wide range of temperatures. For this reason the biggest commercial success to date has been in medical applications (Melzer & Stöckel (1994) and Poncet & Zadno (1994)), where the temperatures of operation are usually body temperature and do not vary too much.

V - High Damping Capacity Devices

Damping refers to the process of converting some of the energy associated with a given oscillation into a different form of energy. Hodgson & Krumme (1994) have shown the possibilities of using microstructural processes which occur in the SMAs that can convert mechanical energy into thermal energy. By using the internal friction that occurs close to the transformation temperature (either in the martensite deformation or the stress induced martensite) they showed that SMAs have a number of advantages over other damping materials. SMAs are not subjected to atmospheric degradation, are not unduly temperature sensitive, are corrosion resistant, have good fatigue properties, and are able to absorb a large amount of energy when compared with traditional damping materials.

3.2.4 - Considerations on Using SMAs

It has already been stated that certain parameters, such as the fabrication method and the operational conditions, affect the characteristics of the SMAs. However, there are many other important factors that must be taken into consideration when using this material. The following paragraphs will review those most important aspects and how they can affect the properties of the specimens.

3.2.4.1 - Heat Treatment

The heat treatment aims primarily to set the custom “hot shape” of the SMA element so that, after some deformation, it can be recovered upon heating above A_f . The most common ‘recipe’ for the heat treatment is described next:

- 1 - Begin with the material in its draw state (there is no shape memory effect as yet).
- 2 - Form the desired hot shape and clamp it.
- 3 - Apply the “memory heat treatment” to fix the “hot shape”. For the NiTi alloy this is usually done by keeping the sample at a constant temperature between 400-500°C for about one hour then letting it cool. In general, temperatures as low as 400 °C and times as short as 1-2 minutes can set the shape, but temperatures closer to 500 °C and times over 5 minutes are commonly used. Also rapid cooling is preferred via water quench or rapid air cool when possible.

The heat treatment affects many different characteristics of the alloy, such as the deformation and recovery forces and the phase transitions (Ikuta *et al.* (1994) and Jordan *et al.* (1992)). For instance, higher heat treatment times and temperatures will increase the actuation temperature and often gives a sharper thermal response. However, there is usually a concurrent drop in peak force (for shape memory elements), accompanied by a decrease in the ability of the element to resist

permanent deformation. Therefore, it may be necessary to try different variations of heat treatment, until the shape memory behaviour is fine tuned for the application.

Also, since the desired shapes and properties are imparted largely by the *time at the maximum temperature*, it is important to make sure that the sample actually reaches the desired temperature and time.

3.2.4.2 - Training

The final step in the preparation of the sample¹ is the training process. After the heat treatment, it is necessary to perform a thermal cycling of the specimen (normally around 100 cycles for NiTi) at the desired operational strain. This aims to stabilise the characteristics of the specimen as they can shift during the first few cycles (Watanabe *et al.* (1993), Suzuki (1987), Jordan *et al.* (1994) and Strnadel *et al.* (1995)).

3.2.4.3 - Joining to Mountings

The method used to attach the SMA element to other components is vital to the performance of the device. For instance, overtightening or sharp bends can lead to future fractures. The most common methods of joining the SMA element to an anchor point or surface normally use crimped bonds, screws and similar techniques.

¹ Normally manufacturers of SMAs can also supply samples already heat treated and/or trained at the desired operational strain.

3.2.4.4 - Operational Temperature

As explained before, the TTR can be affected by many different factors. Under normal operational conditions great care must be taken regarding the temperatures to which the alloy is subjected. High temperatures should not be maintained for too long, since this may shift TTR and the shape at that temperature can be partially memorised, or in extreme cases the shape memory effect can be completely destroyed.

3.2.4.5 - Environment

Normally, when working with a metal, great care must be taken regarding corrosion. In some SMAs, such as Cu based alloys, this can be an important aspect but in others, like NiTi, this is not a problem. NiTi is more noble than stainless steel (almost as good as pure titanium) and it is virtually non magnetic.

Because the SME relies heavily on temperature changes, it is understandable that the ambient temperature to which the SMA elements will be exposed must be taken into consideration during the design phase. For actuators it is desirable that this temperature is well below M_f so that full martensite phase can be accomplished.

3.2.4.6 - Fatigue and Degradation

Fatigue properties of SMAs are affected by many different aspects such as the alloy composition, annealing temperature, strain and applied load (Miyazaki *et al.* (1992), Gilbertson (1992) and May *et al.* (1992)). Van Humbeeck (1991) presents an overview of the various observations related to cycling effects, fatigue and degradation of SMA. He states that three main types of fatigue may be observed when working with SMA: (1) failure by fracture due to stress or strain cycling at a

constant temperature; (2) changes in physical, mechanical and functional properties such as the transformation temperature and the two-way effect; and (3) the degradation of the shape memory effect due to stress, strain or temperature cycling.

3.2.4.7 - Young's Modulus

Young's Modulus is a constant that describes the material's ability to endure strain. Its prior knowledge is very important to the design of SMA actuators. For SMAs this value varies greatly with the type of alloy, the deformation and the operational temperature (Carballo *et al.* (1995)). For instance, for the equiatomic NiTi alloy the Young's Modulus is about 28 GPa in the martensite phase (like lead) and about 75 GPa in the austenite phase (like aluminium).

3.2.4.8 - Stress

If the material is heated while the transformed strain is held constant or while it is under the stress of an external load, a recovery stress appears. Although that is exactly what we want to produce for an actuator, great care must be taken to guarantee reliability. For instance, the maximum recovery force for NiTi is about 600 MPa but it is normally recommended that it is kept below 1/3 of that value (200 MPa) for longer lifetime. Reynaerts & Van Brussel (1994) report fatigue tests using a 0.17 mm air cooled NiTi wire, loaded with a cyclic load of 130 MPa at a frequency of 1 Hz. After 60000 cycles the trained strain of 3.5% was reduced to 3.4% with no further reduction when increasing the number of cycles. However, when using a load of 150 MPa the wire broke after 150000 cycles. For those reasons they considered that 100 MPa is a safe design value for their SMA actuators, and that degradation will occur faster when the SMA is required to provide more work (stress) during heating. However, those values may vary depending on the fabrication process, heat treatment, training and working conditions.

3.2.4.9 - Strain

Although SMA can withstand high levels of strain, there is a maximum limit from which the material can recover its shape upon heating. This limit, usually around 6-10% for NiTi, is called the *Strain Limit* for complete recovery (ϵ_L) and it defines a critical value of induced strain which, if exceeded, leads to true plastic deformation. Also, even when cycling the specimen below ϵ_L , the closer the applied strain is to this value the more deterioration in performance and lifetime can be expected. Many experiments using NiTi have shown that if the strain is below 1% the lifetime can extend to millions of cycles. For 2% strain, the lifetime will be well above 10^5 cycles and for 6% it is usually around a few hundreds. However if the strain is above 10% the specimen can only be used in “single-shot” applications and full shape recovery may not be possible.

Also, for NiTi alloys, the reactive stress depends on the level of tensile pre-strain of the specimens. The higher the pre-strain the higher the recovery stress (Filip & Mazanec (1995)). Therefore, if the device is intended to produce work, there must be a compromise between the maximum strain (for satisfactory lifetime) and the minimum recovery force required.

3.2.4.10 - Deformation Force

Figure 3.8 shows a typical stress-strain curve for the NiTi SMA in the martensite state. When tensile stress is applied to the sample an elastic deformation appears (1) yielding in a plateau of approximately constant stress (2) where the deformation will be similar to a normal plastic deformation (Suzuki (1987)). If the stress is removed on this plateau, the elastic portion of the strain is recovered but the apparent plastic deformation remains (3). This can be removed by heating the specimen. If the strain is increased further the stress will increase (4). At this point if the load is removed (5) the strain will not be fully reverted upon heating (6). This incomplete recovery is

often called *amnesia strain*. It will increase with the increase in the deformed strain until it reaches levels above (7) which may result in the elimination of the SME and fracture of the sample.

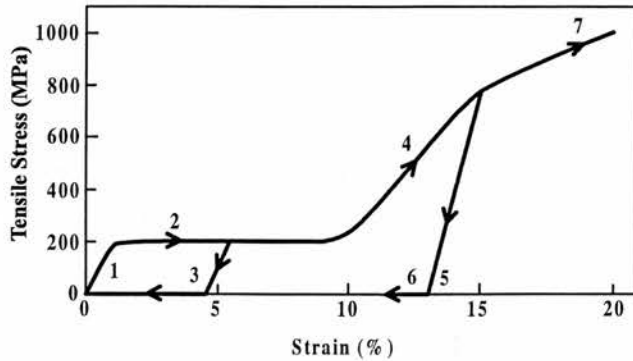


Figure 3.8: Stress-Strain curves for NiTi SMA.

The deformation strain can be controlled either by limiting the displacement of the system or by limiting the deformation force. As shown in Figure 3.8 for this specific NiTi element, a stress of about 200 MPa is enough to overcome the yielding point and reach the plateau of apparent plastic deformation.

3.2.4.11 - Bend Radius

In some applications it may be necessary to bend the SMA. One must be aware that the different points of the bending area will be under different stresses and different

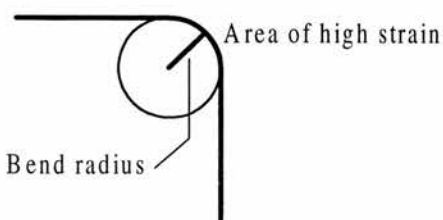


Figure 3.9: Bending a SMA wire.

strains, as shown in Figure 3.9. Depending on the shape of the specimen, the bend radius must be limited to avoid very high levels of stress and strain on the bent area. It is normally recommended that for round wires the bend radius must be at least 20 times the radius of the wire itself.

3.3 - Basic Considerations on Using SMA as the Driving Element for Actuators

Before starting to design a SMA actuator one must be aware of what this approach has to offer and what kind of difficulties may appear. The following paragraphs present a description of the most important advantages and disadvantages of using SMAs and the most common shapes for the SMA elements.

3.3.1 - Advantages

High Power Density: In general SMA elements are very light, which allows the development of SMA actuators with very high *power/weight* and *power/volume* ratios when compared to conventional actuators.

Smooth and Quiet Movements: Because of its nature, the deformation and recovery of the SMA element is absolutely quiet and the movements involved can be very smooth.

Control of Force and Position: Kuribayashi (1986a) was one of the first researchers to demonstrate that it is possible to achieve controllable actuation and continuous position or force control. In some applications it is also possible to use resistive feedback from the SMA element which eliminates the need for external position sensors (Ikuta *et al.* (1994)).

Very Robust to Environmental Influences: Another great advantage of SMA is that its operation is not influenced by any environmental or ambient factor other than temperature.

3.3.2 - Disadvantages

Low Levels of Strain: Even though SMA can endure extremely high levels of strain compared to other metals, this still can be quite small for many applications.

Need for Protection: In order to achieve reliable operation and good fatigue properties, it is necessary to provide protections against overloading, overstraining and overheating.

Sensitive to Changes in the Ambient Temperature: Since the behaviour of SMA is based on changes in temperature, variations in the ambient temperature may present a problem to the design of SMA actuators.

Low Efficiency: It has been demonstrated (Hashimoto *et al.* (1985), Reynaerts & Van Brussel (1991) and Reynaerts & Van Brussel (1994)) that the efficiency of such devices is very low (around 5% at best) compared with conventional actuators such as DC motors which have efficiencies around 60 to 75%.

Difficulty of Achieving High Frequency Response: The frequency response of SMA actuators is defined by the rate of heating and cooling of the SMA elements. Normally, heating is a minor problem and it can be achieved very quickly by passing electric current through the SMA. However, cooling is not so straight forward and may require the assistance of some sort of cooling system, such as forced air, to speed up the response. This may be a major disadvantage since it will increase the weight and the volume of the actuator. In some cases it may not be possible to include a cooling system into the device.

Need for Reset: Another problem that may appear when using SMA is that it will require a deformation force to “reset” the actuator (assuming that it does not use the two-way effect). Although this can be achieved quite easily by means of a bias-spring

or some other device, this will certainly contribute to a reduction of the power density of the device.

Hysteresis: Its existence may be a problem for many applications since the deformation and the recovery follow two different pathways that will also depend on other aspects such as the stress applied in that specific cycle. Those problems may represent a challenge to the development of the control system as shown by Kuribayshi (1986a).

3.3.3 - Typical Shapes for the SMA Elements

SMA elements can be shaped to fit almost any application but some shapes are more popular than others for reasons that range from simplicity of design to higher levels of work production. To date the majority of SMA actuators use elements shaped as coil springs or wires.

Coil springs have the advantage of requiring a small microscopic displacement of the SMA elements for a large macroscopic displacement of the spring, which means that the overall length of SMA coil springs can be smaller than the overall length of SMA wires for the same level of strain. However, SMA springs generally have a larger diameter and therefore occupy more volume than SMA wires. Other disadvantages of SMA springs are the non uniform stress distribution, a considerable two way effect and a very low energy efficiency when compared to SMA wires. Since the convection area is generally small, the cooling rate of SMA elements (particularly in still air) is low, often requiring the use of some auxiliary cooling system to improve the frequency response of SMA actuators. Nevertheless, whatever the shape of the SMA elements, they can be made very light and heated very quickly. Table 3.1 shows a summary of the aspects discussed above. Note that the ratings given are only simple guidelines, collected from general designs, and can vary depending on the application.

	Coil Spring	Wire
Overall diameter	greatest	least
Overall volume	greatest	least
Two way effect	greatest	least
Macroscopic displ.	greatest	least
Microscopic displ.	least	greatest
Overall length	least	greatest
Recovery stress	least	greatest
Efficiency	least	greatest
Weight	low	low
Convection area	low	low
Cooling rate	low	low
Heating rate	high	high
Stress distribution	non uniform	uniform

Table 3.1: Comparison between SMA coil springs and SMA wires.

3.4 - Conclusion

A few years ago SMAs were regarded as excellent driving elements for almost any kind of actuator. Nowadays, because of the problems stated earlier, researchers are much more careful with its use. SMA actuators unveil a whole new set of applications that are very difficult or even impossible to accomplish with conventional methods. However, depending on the application, its proper use may require a great deal of skill and careful design.

Chapter 4

The Design of an Artificial Hand Powered by SMA Actuators for Young Children

4.1 - Introduction

The design and manufacture of prostheses is a complex task. Chapter 2 showed that there are a number of variables to be considered in the design and prescription of prostheses. When this involves artificial limbs for young children, many other new parameters also need to be addressed. This chapter describes those parameters and how to design an artificial hand taking all those aspects into account. The motivating power for the joint mechanisms will be provided by a SMA actuator to demonstrate the potential of such devices in the area of prosthetics.

4.2 - Initial Considerations

Fitting children with prostheses is a challenging issue that must be addressed carefully. The assumptions and techniques used for adults are not always valid for children. It is not only a matter of reducing the size of an adult prosthesis since many additional factors will now contribute to the success or failure of the prosthetic

device. This section will discuss some important variables involved in the design, fitting and management of children with prostheses.

As opposed to adults, the majority of limb disabilities in children are due to congenital anomalies (around two-thirds according to Krebs *et al.* (1991)). Therefore, it is important that the clinicians are well trained to identify those patients who may benefit from early prosthetic fitting.

Parental support plays a vital role in the success of the prosthesis. Parents are the ones who decide in favour of fitting the prosthesis in first place. The initial expectation is normally to disguise the amputation, which demands a device with good cosmetic appearance. It is important that the parents know how to assist their child so that he/she can get maximum benefit from the prosthesis. Parents also must be able to operate, care for and maintain the device. Parental support is such an important issue that most specialised clinics include a programme of training courses and try to keep the therapists in close contact with the parents (Hermansson (1991)).

The best age for fitting the prosthesis normally depends on a number of factors. It is commonly accepted that there is little functional need for a prosthesis prior to 6 months of age, so the first fitting generally occurs when the child shows interest in standing, can sit and starts to use the hands to explore and manipulate objects. At six to eight months the child is too young to operate a terminal device such as an active artificial hand. However, a passive device to hold objects inserted by an adult will draw the child's attention to the prosthesis (Krebs *et al.* (1991)). Also, it is accepted that children with bilateral amputations should be fitted with prostheses later than usual to allow the development of other important functions. For instance, a child with bilateral arm amputation often will learn to use the feet to perform many activities such as picking objects, eating and even writing.

As the child grows older new prostheses are fitted to allow prehensile control. Many centres will fit the child with passive prostheses, then a cable-driven prehensor and,

later, when he/she proved to be a good operator of the cable-operated prostheses, a myoelectric prehensor may be fitted. Once again the best age for fitting active devices is debatable and heavily dependent on the needs of each child.

An important factor for the success of a prosthetic device is that it can be used in a natural way. The need for harnesses is an undesirable feature in this sense, since a harness normally constrains the movements of the user and is not very comfortable. However, the weight of the prosthesis represents a major problem to be solved. Children in particular require that the prosthesis is light-weight so that it can be used in a natural way. The forces that the weight of the device exert upon the stump can be uncomfortable and sometimes unacceptable, leading to the complete rejection of the prosthesis. Careful analysis of the stress distribution within the socket is also vital for the health of the skin on the interface region (Sanders (1995)).

Consider the situation of a below-elbow limb user fitted with an artificial hand holding it with the elbow flexed at 90° as shown in figure 4.1. The weight of the prosthesis generates a moment $W * b$ Nm about the elbow joint. This is resisted by the force generated by the elbow flexors and produces forces (F) distributed along the socket. Also, a further reaction force (R) is produced in the dorsal surface of the socket. Keeping the elbow flexed at 90° and applying the equations of equilibrium:

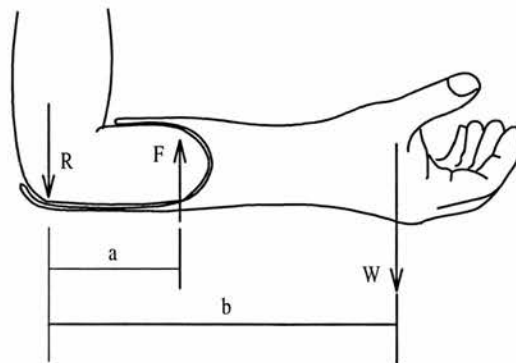


Figure 4.1: Schematic force distribution with a standard artificial hand.

$$a) F * a - W * b = 0 \quad (\Sigma \text{moments about the elbow joint} = 0)$$

$$F = W * b / a$$

$$b) R + W - F = 0 \quad (\Sigma \text{Forces} = 0)$$

$$R = F - W$$

Suppose that the length of the arm (b) is about three times that of the stump (a), and that the prosthesis weighs 300 grams ($W = 2.94 \text{ N}$).

$$F = 2.94 * 3 * a / a \Rightarrow F = 8.82 \text{ N}$$

$$R = 8.82 - 2.94 \Rightarrow R = 5.88 \text{ N}$$

In this situation the forces on the elbow joint are considerably greater than the weight of the prosthesis itself. If the hand is holding an object or applying forces on it or if the stump is shorter, those effects are even more pronounced. Normally, the designer of the prosthesis tries to minimise those effects by means of solutions such as a better socket that makes the distribution of forces more even through the stump and by shifting the centre of gravity of the prosthesis to a more proximal point. However, there is little doubt that the best solution is to keep the overall weight of the prosthesis as low as possible.

4.3 - Specification and Design of the Artificial Hand

Consider the design of an artificial hand to be used as part of an above elbow prosthesis for children under 24 months old. There are normally a number of restrictions upon the hand and the joints actuators, as described before. With those restrictions in mind, a small artificial hand will be designed so that its motion is as smooth and natural looking as possible. Current commercially available artificial

hands for this age group (see appendix B) weigh between 130 and 150 grams (excluding gloves, batteries and suspension devices). This work will use those values as guidelines for the design. Some basic dimensions for the intended prosthesis are shown in figure 4.2.

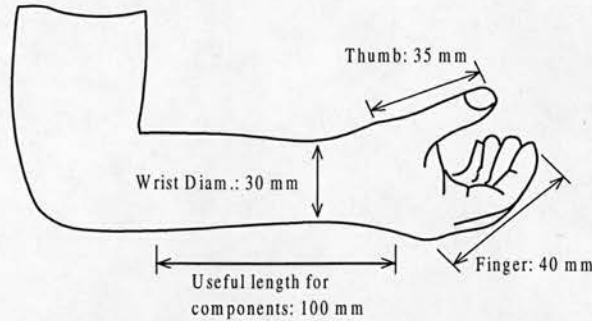


Figure 4.2: Basic dimensions of a small above elbow prosthesis.

The actuator for the joint mechanism must be designed so that it is as light and compact as possible, leaving enough room for the other components of the prosthesis (such as mechanical parts and electronics). It is accepted that the main reason for fitting very young children with artificial limbs is to provide them with a “training device” and accustom them to wearing prostheses. With this in mind, it was decided that the actuator should provide a grip force of 3 N (without cosmetic glove) and 1.5 N for opening the hand against a cosmetic glove (both values measured at the tip of the fingers and thumb). A minimum lifetime of 72000 cycles was considered satisfactory for the actuator. This value is not necessarily related to the lifetime of the prosthesis itself, but was chosen to give approximately 4 months of continuous use at a rate of 600 cycles a day. Although 72000 cycles is a low value for conventional prostheses it would be adequate if the actuator is not very expensive and could be replaced (if necessary) when the prosthesis is returned to the prosthetic centre for review (which, for this range of prostheses, normally happens every three months). In addition to the above, other specifications for the actuator would be:

- It must fit into a volume of 30 mm x 30 mm x 100 mm.

- It must weigh less than 50 grams.
- The actuator must be able to stand high levels of vibration and work in any position.
- Time to open the hand: 1.5 seconds.
- Time to close the hand: 2 seconds.
- Working temperature: 0 - 35 °C.
- Must provide an opening width of the hand of around 25 mm.

The specifications above suggest that SMA may be a good candidate for the development of the desired actuator. Note that it is not intended to prove that SMA is the only solution for this particular problem. The aim is to evaluate whether or not SMA is a viable alternative to conventional techniques.

4.3.1 - The Hand Mechanism

The hand mechanism chosen for the purpose of this work is similar to designs used in some existing prostheses. Two fingers (medium and index) are locked together to grasp or pinch an object against the thumb. The other two fingers are basically for cosmetic reasons and just follow the movements of the “active” fingers. Figure 4.3 shows a diagram of such a scheme.

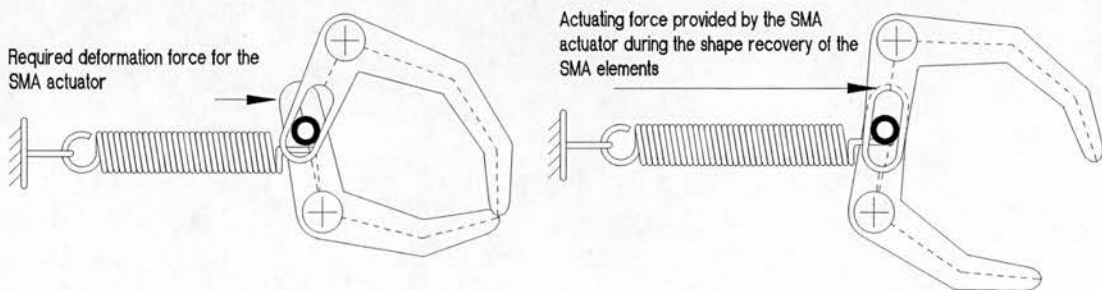


Figure 4.3: The chosen hand mechanism.

The fingers and thumb are linked so that moving the thumb will result in motion of the fingers and vice-versa. An ordinary spring will be used to provide the closing/grasping force and a SMA actuator will be used to open the hand against the spring. As explained in detail in chapter 5, this system will use a *bias SMA actuator*, which requires an external force to deform the SMA elements. In this design the bias force will be provided by the same spring responsible for the grip force. The necessary power for the SMA actuator will be provided by a rechargeable battery pack. The main advantage of this arrangement is that the SMA actuator will be powered only while opening the hand. Since the device is closed or holding an object most of the time (grip force provided by the spring), this will extend the operating time between charges of the battery.

The next step is to construct the mechanism and determine the required spring and the characteristics of the SMA actuator. A very common approach is to construct a hand mechanism based on the preliminary specifications, fit a spring and an actuator and check if it works as intended. If the results are not satisfactory the system is “refined” and rebuilt. In other words, once the initial specifications and ideas are collected, the design has to be optimised until the results are within the requirements. This is usually a very laborious job involving a number of modifications and adjustments. Also, one must make sure that the SMA actuator will be used as efficiently as possible. Therefore, instead of using the approach described above, it was decided to simulate the movements and forces within the hand mechanism shown in figure 4.3. The mathematical model of the system was obtained and a computer program (appendix A) was written to simulate the operation of the device. The program proved to be a very useful tool, allowing the user to analyse the design and evaluate the consequences of modifying any parameter without actually building anything. The mathematical modelling of the system is shown next, followed by a detailed description of the program and how it was used to optimise the design of the hand and to specify the spring and the SMA actuator.

4.3.2 - Simulation of the Hand Mechanism

4.3.2.1 - Motion

The equations described in this section will be used to find the position of the main points of a general hand mechanism as shown in figure 4.4.

Note that the elements of the hand are considered to lie in the same plane (coplanar system). This means that both fingers are represented as one imaginary finger placed in an intermediary position between the actual fingers. Also, the Y axis is inverted for compatibility with the convention used for computer screens.

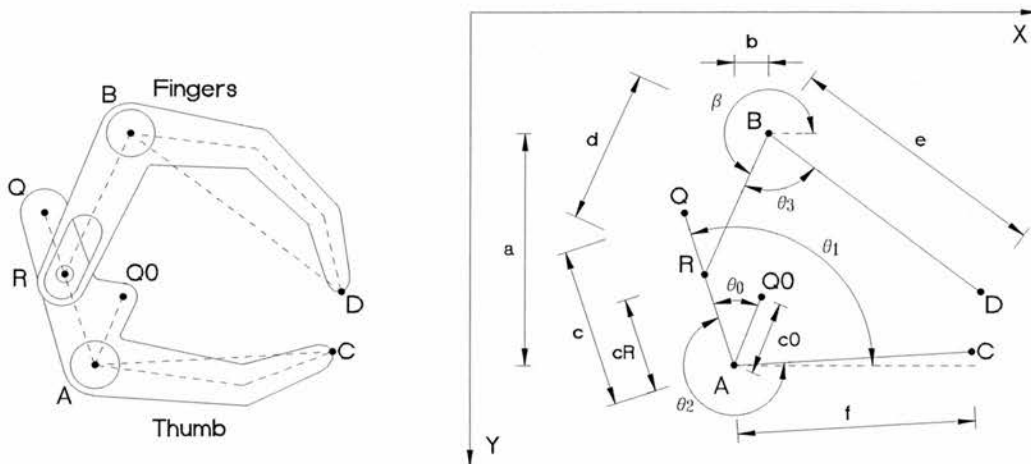


Figure 4.4: Main points within the hand mechanism.

The motion of the mechanism will be described in terms of the following set of parameters:

- A: Pin around which the thumb rotates.
- B: Pin around which the fingers rotate.
- C: Tip of the thumb.

D: Tip of the fingers.

R: Centre of the barrel linking the movements of the thumb and fingers.

Q: Connection point to the SMA actuator.

Q0: Connection point to the main spring.

a (height): vertical distance between A and B.

b (offset): Horizontal distance between A and B.

c: Length of the lever AQ.

c0: Length of the lever AQ0.

cR: Length of the lever AR.

d: Length of the lever BR.

e: Linear length of the fingers (BD).

f: Linear length of the Thumb (AC).

θ_0 : Angle between the lever AQ and the lever AQ0 (+: counter-clockwise from AQ).

θ_1 : Angle between the lever AQ and the horizontal axis.

θ_2 : Angle between AQ and AC.

θ_3 : Angle between BQ and BD.

In the calculation of motion the dimensions of the device (a, b, c, c0, cR, d, e, f, θ_0 , θ_1 , θ_2 and θ_3) are previously defined and will be used to calculate the co-ordinates of the main points of the hand mechanism, as follows:

$$B_x^1 = 50 + b \quad [1a]$$

$$B_y = 30 \quad [1b]$$

$$A_x = B_x - b \quad [2a]$$

$$A_y = B_y + a \quad [2b]$$

$$C_x = A_x + f * \cos(\theta_1 + \theta_2) \quad [3a]$$

$$C_y = A_y - f * \sin(\theta_1 + \theta_2) \quad [3b]$$

$$Q_x = A_x + c * \cos\theta_1 \quad [4a]$$

¹ Pin B is fixed in the XY plane in the co-ordinates (50 + b , 30) as the starting point for the calculations.

$$Q_y = A_y - c * \sin\theta_1 \quad [4b]$$

$$Q_{0x} = A_x + c_0 * \cos(\theta_1 + \theta_0) \quad [5a]$$

$$Q_{0y} = A_y - c_0 * \sin(\theta_1 + \theta_0) \quad [5b]$$

$$R_x = A_x + cR * \cos\theta_1 \quad [6a]$$

$$R_y = A_y - cR * \sin\theta_1 \quad [6b]$$

$$D_x = B_x + e * \cos(\theta_3 + \beta) \quad [7a]$$

$$D_y = B_y - e * \sin(\theta_3 + \beta) \quad [7b]$$

$$\beta = \pi + \tan^{-1}\left(\frac{R_y - B_y}{B_x - R_x}\right) \quad [7c]$$

Opening width of the hand:

$$CD = \sqrt{(D_x - C_x)^2 + (D_y - C_y)^2} \quad [8]$$

For the purpose of this system, movement occurs by moving Q by δS mm. Note that δS is the length of the arc described by Q (since it is situated on the thumb lever it will rotate around pin A). Therefore, the new θ_1 can be calculated by:

$$\text{New}\theta_1 = \text{Old}\theta_1 - \delta\theta_1 \quad [9]$$

where:

$$\delta\theta_1 = \frac{\delta S}{c} \text{ [rad]}$$

Now the new co-ordinates of the moveable points (equations 3a to 7b) and the opening width of the hand (equation 8) can be calculated by substituting θ_1 for $\text{New}\theta_1$.

4.3.2.2 - Forces

In order to develop the mathematical equations for force analysis, the system will be considered in equilibrium when the hand touches an object or it is opened against an external obstacle such as a cosmetic glove. It is desired to calculate the force exerted upon an object or the cosmetic glove during the actions of opening and closing the hand. Other forces, such as the forces exerted by pins A and B upon the structure of the hand, must also be considered. In the same way as before the forces will be calculated assuming a coplanar system.

The Free Body Diagram (FBD) of the hand mechanism shown in figure 4.5 will be used to analyse the force distribution in the system.

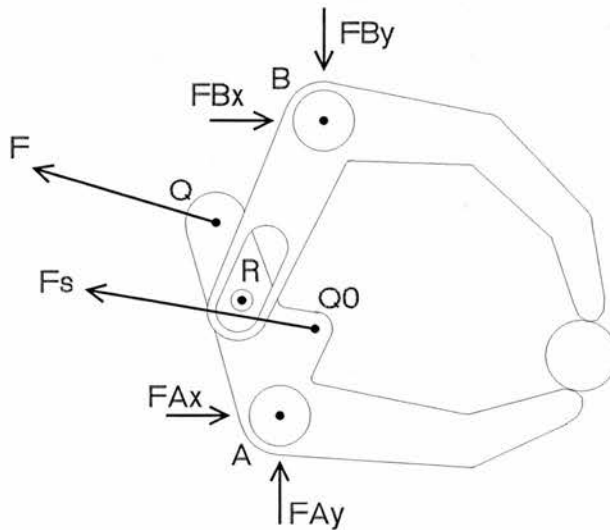


Figure 4.5: FBD of the hand mechanism holding an object.

The following assumptions are considered in this model:

- The direction of the forces used in the equations follow the convention adopted in figure 4.5
- R is a barrel and slides through a smooth slot (no friction considered).

- A and B are frictionless pins.
- The sides of the slot and its central line are parallel to the line RB.
- F_{Ax} and F_{Ay} are the components of the force exerted on the structure by pin A.
- F_{Bx} and F_{By} are the components of the force exerted on the structure by pin B.
- The system is in equilibrium when the tip of the fingers/thumb touches an object during opening or closing the hand.
- F is an external actuating force applied to Q.
- F_s is an external actuating force applied to Q0. If F_s is generated by an ordinary spring it is calculated by:

$$F_s = F_{s0} + K_s * \text{SpringDispl} \quad [10]$$

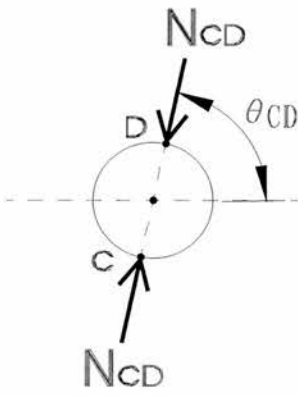
where:

- F_{s0} is the tension on the spring (N) with the hand fully closed.
- K_s is the spring rate (N/mm).
- SpringDispl is the displacement of the spring and will be approximated to the length of the arc described by Q0 (δS_{Q0}), as shown below (note that since Q and Q0 are located in the thumb, both will rotate around pin A in the same direction and describing the same angle ($\delta\theta_1$)):

$$\text{SpringDispl} = \delta S_{Q0} = C0 * \delta\theta_1 \quad [\delta\theta_1: \text{angle (rad) described by Q0}]$$

The FBD of the whole system is of little use here since it does not show the forces exerted upon the object. The system must therefore be “broken apart” to generate enough equations to calculate all the unknown variables.

The Object



Assuming that the object is held in equilibrium by two forces applied by the finger and the thumb, its analysis can be simplified by the application of the two-force principle: *If an object is held in equilibrium by two forces, the resultant forces must be equal in magnitude and opposite in direction along the same line of action.* The two-forces of equal magnitude (N_{CD}) are the forces applied by the finger and the thumb at points D and C (figure 4.6) at an angle θ_{CD} :

Figure 4.6: FBD of the object.

$$\theta_{CD} = \tan^{-1}\left(\frac{Cy - Dy}{Dx - Cx}\right) \quad [11]$$

The Finger

Figure 4.7 shows the FBD of the finger and the forces related to it.

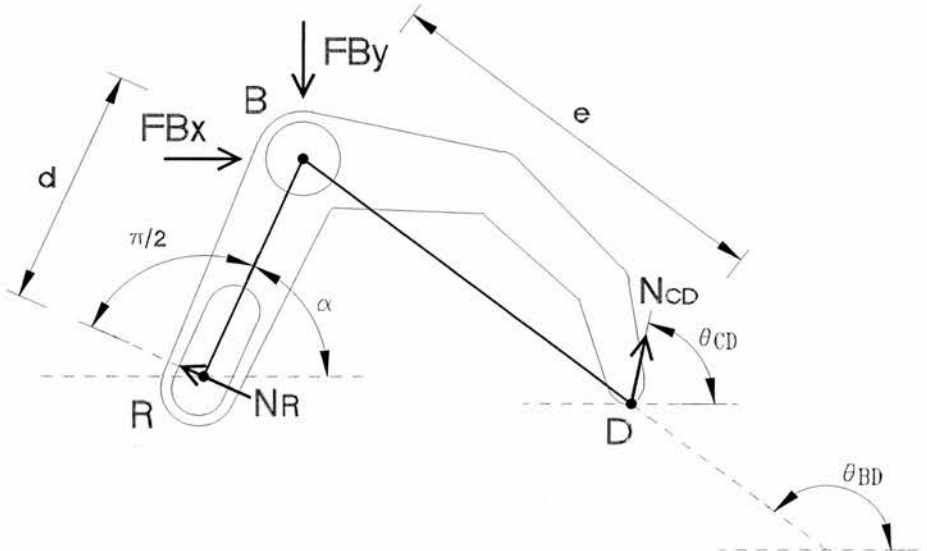


Figure 4.7: FBD of the finger.

Applying the equations of equilibrium at point B:

$$\Sigma M_B = 0$$

$$N_R * d - N_{CD} * \sin(\theta_{BD} - \theta_{CD}) * e = 0 \quad [12]$$

$$\Sigma F_X = 0$$

$$FB_X + N_{CD} * \cos \theta_{CD} - N_R * \cos\left(\frac{\pi}{2} - \alpha\right) = 0$$
$$FB_X + N_{CD} * \cos \theta_{CD} - N_R * \sin \alpha = 0 \quad [13]$$

$$\Sigma F_Y = 0$$

$$N_R * \sin\left(\frac{\pi}{2} - \alpha\right) - FB_Y + N_{CD} * \sin \theta_{CD} = 0$$
$$N_R * \cos \alpha - FB_Y + N_{CD} * \sin \theta_{CD} = 0 \quad [14]$$

where:

- N_R is the normal force exerted by the barrel on the slot.
- N_{CD} is the force exerted on the tip of the finger by the object.
- $\alpha = \beta - \pi$

The Thumb

Figure 4.8 shows the FBD of the thumb.

Applying the equations of equilibrium at point A:

$$\Sigma M_A = 0$$

$$\begin{aligned}
& FR_Y * \sin\left(\theta_1 - \frac{\pi}{2}\right) * cR - FR_X * \sin(\pi - \theta_1) * cR - F * \sin(\theta_F - \theta_1) * c - \\
& F_S * \sin(\theta_{FS} - (\theta_1 + \theta_0)) * c0 + N_{CD} * \sin(\pi - \theta_{AC} + \theta_{CD}) * f = 0 \\
& N_{CD} * \sin(\theta_{AC} - \theta_{CD}) * f - FR_Y * \cos\theta_1 * cR - FR_X * \sin\theta_1 * cR - \\
& F * \sin(\theta_F - \theta_1) * c - F_S * \sin(\theta_{FS} - (\theta_1 + \theta_0)) * c0 = 0
\end{aligned} \tag{15}$$

$$\Sigma F_X = 0$$

$$\begin{aligned}
& FA_X - F * \cos(\pi - \theta_F) - FR_X - F_S * \cos(\pi - \theta_{FS}) - N_{CD} * \cos\theta_{CD} = 0 \\
& FA_X + F * \cos\theta_F - FR_X + F_S * \cos\theta_{FS} - N_{CD} * \cos\theta_{CD} = 0
\end{aligned} \tag{16}$$

$$\Sigma F_Y = 0$$

$$FA_Y + F * \sin\theta_F + FR_Y + F_S * \sin\theta_{FS} - N_{CD} * \sin\theta_{CD} = 0 \tag{17}$$

where:

- N_{CD} is the force exerted by the object upon the thumb.
- FR_X and FR_Y are the components of the force exerted by the barrel upon the thumb.
- $\theta_{AC} = \tan^{-1}\left(\frac{Cy - Ay}{Ax - Cx}\right)$
- $\theta_F = \pi - \sin^{-1}\left(\frac{Fhi - (Ay - Qy)}{Flen}\right)$
- $\theta_{FS} = \pi - \sin^{-1}\left(\frac{Fshi - (Ay - Q0y)}{Fslen}\right)$

Note that the inclination of F and F_S will change as the thumb rotates around pin A. In the equation θ_F , $Flen$ is the current distance between Q and the moveable part of the SMA actuator (see chapter 5 for details) and Fhi indicates the vertical distance of that moveable part to a horizontal line passing through point A. In the equation θ_{FS} , $Fslen$ is the current length of the spring (from $Q0$ to the fixed end of the spring) and

F_{shi} indicates the vertical distance of the fixed end of the spring to a horizontal line passing through point A.

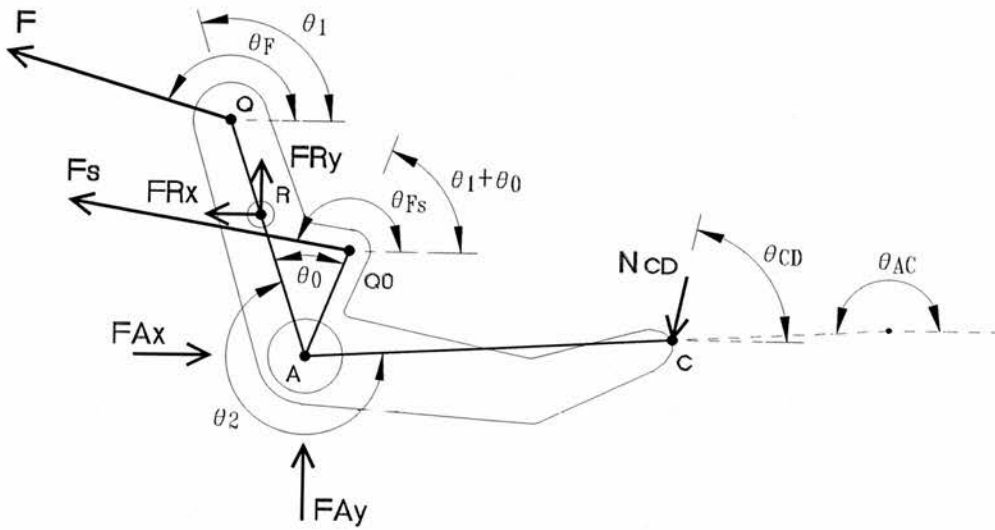


Figure 4.8: FBD of the thumb.

The Barrel

In the FBD this element is represented only by its central point (R) where all the forces act. Figure 4.9 shows such representation.

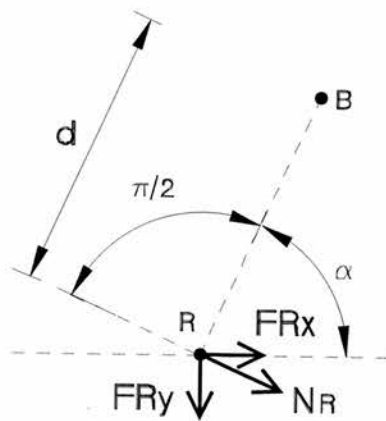


Figure 4.9: FBD of the linking barrel.

Applying the equations of equilibrium for point R:

$$\Sigma F_x = 0$$

$$FR_x + N_R * \cos\left(\frac{\pi}{2} - \alpha\right) = 0$$

$$FR_x + N_R * \sin\alpha = 0 \quad [18]$$

$$\Sigma F_y = 0$$

$$FR_y + N_R * \sin\left(\frac{\pi}{2} - \alpha\right) = 0$$

$$FR_y + N_R * \cos\alpha = 0 \quad [19]$$

Where:

- N_R is the force exerted upon the barrel by the slot.
- FR_x and FR_y are the components of the force exerted by the thumb upon the barrel.

Solving the system

Simplifying some common terms:

$$K1 = \sin(\theta_{BD} - \theta_{CD}) * e$$

$$K2 = \sin(\theta_F - \theta_1) * c$$

$$K3 = \sin(\theta_{FS} - (\theta_1 + \theta_0)) * c0$$

$$K4 = \sin(\theta_{AC} - \theta_{CD}) * f$$

Substituting into equations [12] and [15]:

$$N_R * d - N_{CD} * K1 = 0 \quad [12']$$

$$N_{CD} * K4 - FR_y * \cos\theta_1 * cR - FR_x * \sin\theta_1 * cR - F * K2 - F_S * K3 = 0 \quad [15']$$

from [18] and [19]:

$$FR_x = -N_R * \sin\alpha \quad [20]$$

$$FR_y = -N_R * \cos\alpha \quad [21]$$

Substituting FR_x and FR_y into [15']:

$$N_R * \cos\alpha * \cos\theta_1 * cR + N_R * \sin\alpha * \sin\theta_1 * cR - F * K_2 - F_S * K_3 + N_{CD} * K_4 = 0$$

solving the equation for N_R :

$$N_R = \frac{K_2 * F + K_3 * F_S - K_4 * N_{CD}}{K_5} \quad [22]$$

where:

$$K_5 = cR * (\cos\alpha * \cos\theta_1 + \sin\alpha * \sin\theta_1) = cR * \cos(\alpha - \theta_1)$$

Substituting [22] into [12']:

$$\frac{K_2}{K_5} * d * F + \frac{K_3}{K_5} * d * F_S - \left(\frac{K_4}{K_5} * d + K_1 \right) * N_{CD} = 0 \quad [23]$$

Equation [23] relates F , F_S and N_{CD} and can be solved as follows:

Knowing F_S and F :

$$N_{CD} = \frac{\frac{K_2}{K_5} * d * F + \frac{K_3}{K_5} * d * F_S}{\frac{K_4}{K_5} * d + K_1} \quad [24a]$$

Knowing F_S and N_{CD} :

$$F = \frac{\left(\frac{K4}{K5} * d + K1\right) * N_{CD} - \frac{K3}{K5} * d * F_S}{\frac{K2}{K5} * d} \quad [24b]$$

Knowing F and N_{CD} :

$$F_S = \frac{\left(\frac{K4}{K5} * d + K1\right) * N_{CD} - \frac{K2}{K5} * d * F}{\frac{K3}{K5} * d} \quad [24c]$$

Once the external forces (F , F_S and N_{CD}) are known, F_{Rx} , F_{Ry} and N_R can be calculated by [20], [21] and [22] respectively. The forces upon the structure of the hand mechanism can be resolved as follows:

Forces on pin B

Solving equation [13] for F_{Bx} :

$$F_{Bx} = N_R * \sin\alpha - N_{CD} * \cos\theta_{CD} \quad [25a]$$

Solving equation [14] for F_{By} :

$$F_{By} = N_R * \cos\alpha + N_{CD} * \sin\theta_{CD} \quad [25b]$$

Forces on pin A

Solving equation [16] for F_{Ax} :

$$F_{Ax} = F_{Rx} - F * \cos\theta_F - F_S * \cos\theta_{FS} + N_{CD} * \cos\theta_{CD} \quad [26a]$$

Solving equation [17] for F_{Ay} :

$$F_{Ay} = N_{CD} * \sin\theta_{CD} - FR_y - F * \sin\theta_F - F_s * \sin\theta_{FS} \quad [26b]$$

4.3.2.3 - Software

Once the required equations were defined, a computer program was written to simulate the operation of the hand mechanism based on those equations. The program, which can be found in appendix A, was written in Delphi 2.0 for Windows 95 (IBM PC compatible). A user interface (main screen shown in figure 4.10) was designed to allow the user to select and change any parameter of the model, initiate the movements of the hand and evaluate the responses. A description of the main components of the user interface is given next.

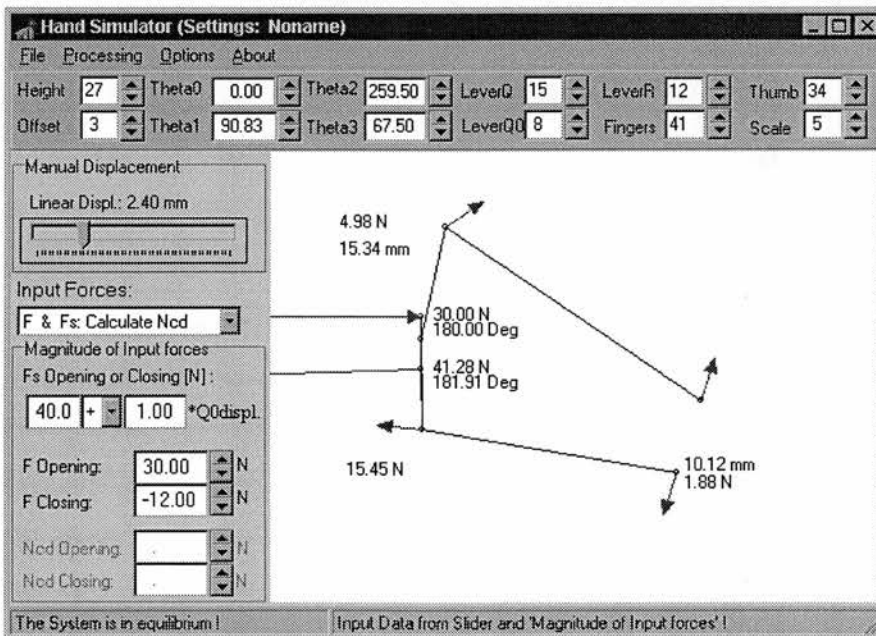


Figure 4.10: Snap shot of the user interface (main screen).

Image area: As the hand moves, a simplified diagram of the current state of the hand is shown along with the position of the fingers and thumb, forces applied to the main

points of the mechanism, opening width of the hand and the angles of the external actuating forces.

Height (mm): Specifies the vertical distance between pins A and B of the hand mechanism.

Offset (mm): Horizontal distance between pins A and B of the hand mechanism.

Theta0 (deg.): Angle between the lever AQ and the lever AQ0 (+: counter-clockwise from AQ).

Theta1 (deg.): Angle between the lever AQ and the horizontal axis (updated as the hand moves).

Theta2 (deg.): Angle between the lever AQ and the line AC.

Theta3 (deg.): Angle between the finger lever BQ and the line BD.

LeverQ (mm): Length of the lever AQ.

LeverQ0 (mm): Length of the lever AQ0.

LeverR (mm): Length of the lever AR.

Fingers (mm): Specifies the linear length of the fingers (BD).

Thumb (mm): Specifies the linear length of the thumb (AC).

Scale (pixels/mm): Adjust the scale of the image.

Manual Displacement (mm): A slider is used to apply a linear displacement to point Q and start the evaluation of the mathematical model for that situation. The current linear displacement (which is equal to zero with the hand fully closed) is shown on top of the slider.

Input Forces (N): Allows the user to select two known forces and calculate the unknown. As described before, there are three possible combinations:

- Knowing F and F_s calculate N_{CD} .
- Knowing F and N_{CD} calculate F_s .
- Knowing F_s and N_{CD} calculate F.

Magnitude of Input Forces: In this group of fields the user must enter the value of the known forces (those fields related to the unknown force are disabled).

F_s Opening or Closing: The user must specify the equation of the spring to be used:

$$F_s = F_{s0} +/- K_s * SpringDispl$$

- F_{S0} (N): Initial force with the hand fully closed
- K_s (N/mm): Spring rate
- SpringDispl (mm): Displacement of point Q0 (calculated by the program).

F Opening (N): Magnitude of the external actuating force (F) applied to Q when the hand is opening.

F Closing (N): Magnitude of the external actuating force (F) applied to Q when the hand is closing.

Ncd Opening (N): Required magnitude of the force at the tip of the fingers and thumb when the hand is opening.

Ncd Closing (N): Required magnitude of the force at the tip of the fingers and thumb when the hand is closing (grip force).

Graphic Outputs: The software can produce graphic outputs showing the curves for all variables during the operation of the hand mechanism.

Other standard features such as file manipulation are also available.

4.3.3 - Using the Simulator in the Design of the Device

The next paragraphs explain how the software was used in the design and optimisation of the hand mechanism. The importance of the simulation in determining the basic specifications of both the main spring and the SMA actuator is also illustrated.

Using the specifications of the prosthesis shown in figure 4.2 as basic guidelines, initial estimations for the dimensions of the hand mechanism were defined as follows:

- Height: 28 mm
- Offset: 12 mm

- Theta0: 0 °
- Theta1: 101 °
- Theta2: 256 °
- Theta3: 85 °
- LeverQ: 15 mm
- LeverQ0: 8 mm
- LeverR: 15 mm
- Fingers: 37 mm
- Thumb: 34 mm

A maximum of 6 mm displacement for point Q was initially considered satisfactory. This displacement was defined based on an actuator with SMA wires 200 mm long strained up to 3% of their initial length.

F and Fs were defined as input forces and Ncd was to be calculated. The input forces were defined as:

- “Fs Opening or Closing” was to be provided by a commercially available spring. Based on the dimensions of the required mechanism a spring was chosen from the range of products of SPEC[®] Associated Spring (UK). The spring (type E0240-041-2500S) was to be fitted so that when the hand was fully closed it should pull the thumb lever (point Q0) with a force of 30 N (“Initial FsLength” = 81 mm; “Spring Rate” = 1.46 N/mm).
- The actuating force F was to be provided by a SMA actuator and “F Opening” was defined as the force the actuator should provide for opening the hand. “F Closing” should be the force required to deform the SMA elements. Those values were initially set to 24 N (F Opening) and 9.5 N (F Closing). Such forces were compatible with a SMA actuator with 8 SMA wires Flexinol 150HT mechanically in parallel (see chapter 5 for details of those wires).

Once all the required parameters were specified, the force and movements within the hand could be calculated. Figure 4.11 shows a snap-shot of the main screen of the computer simulation program with all parameters set as detailed above. Figures 4.12(a) and 4.12(b) show the graphic outputs for the opening and closing of the hand respectively.

The graphic outputs show that, during opening and closing of hand, the forces and movements obtained with this setup are not satisfactory. The following problems were identified:

- The maximum opening width of the hand for 6 mm displacement of point Q is only 22.1 mm.
- The opening force starts at 2.8 N with the hand still closed but decreases to 1.32 N at maximum opening width.
- The grip force during closing of the hand is below the specifications (it reaches a maximum of 2.5 N with the hand fully closed).

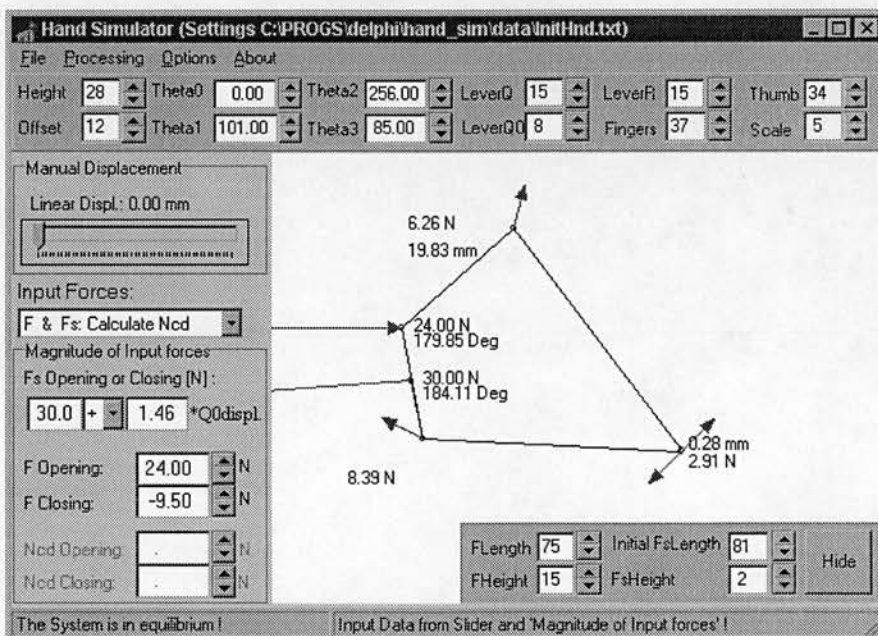
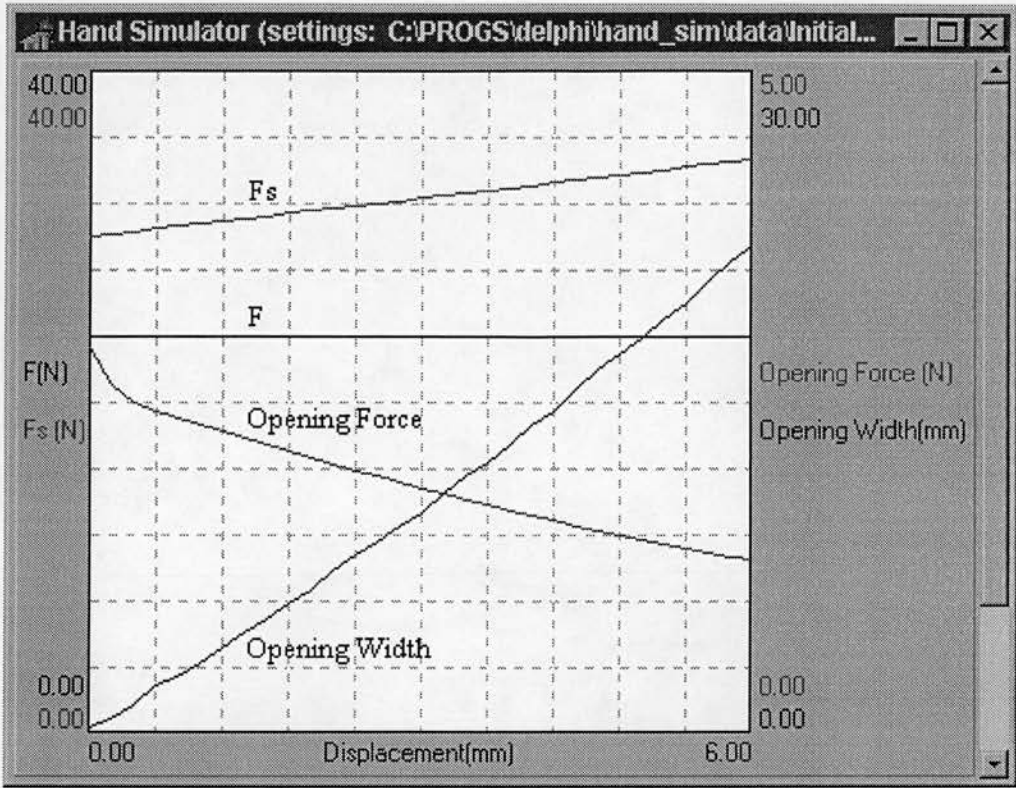
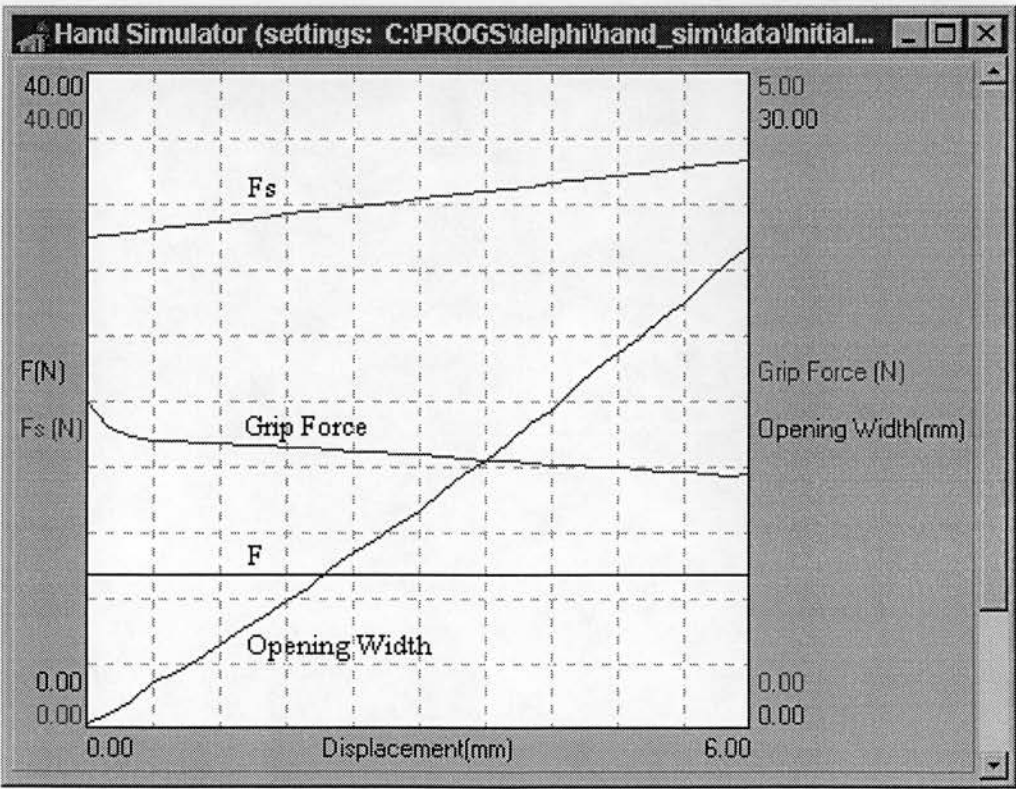


Figure 4.11: Snap shot of the main screen for the initial setup.



(a)



(b)

Figure 4.12: Results of the simulation of the initial hand mechanism. (a) Hand opening; (b) Hand closing.

Since the movements and forces obtained from that initial set of parameters are not satisfactory, the design must be optimised. This optimisation involves choosing another spring, trying different configurations for the SMA actuator and modifying the mechanical dimensions of the mechanism. After each modification the software was executed and the results evaluated, until a satisfactory combination was found. This process aimed to achieve maximum motion and maximum grip/opening forces with minimum variation during closing/opening of the hand mechanism. Note that the choice of the spring and the SMA actuator are very much interconnected and restricted by a number of factors, such as:

- The SMA actuator provides the necessary force for opening the hand against the spring. However, there are compromises between the maximum force provided by SMA electric actuators and factors such as power consumption and frequency response. The bigger the SMA elements (or the higher the number of SMA elements in parallel) the more power has to be supplied for shape recovery and the longer it will take to cool. Keeping those restrictions in mind, a number of experiments were developed to study suitable configurations for the SMA actuator. It was found that very thin SMA wires must be used if the requirements for time response were to be met (see chapter 5 for details). Also the maximum power consumption was limited to about 20 W, which also limits the maximum number of SMA wires that can be placed in parallel.
- The spring must be chosen from a range of products of standard suppliers to provide the necessary deformation force for the SMA elements and also to generate the required grip forces.

The process of optimisation was executed according to the following sequence:

Step 1. The configuration of the SMA actuator was defined according to the restrictions above.

Step 2. The spring was chosen as specified above.

Step 3. In the “simulator”, the following fields were completed:

- F_s Opening or Closing (N): Based on the specifications of the spring.
- Initial F_s Length: Length of the spring with the hand fully closed.
- F_s Height: Vertical distance of the fixed end of the spring to a horizontal line passing through point A.
- $F_{Opening}$ (N): Recovery force provided by the SMA elements.
- $F_{Closing}$ (N): Deformation force required by the SMA elements.
- F Length: Distance between point Q and the moveable part of the SMA actuator.
- F Height: Vertical distance of the moveable part of the SMA actuator to a horizontal line passing through point A.
- The remaining fields were kept as for the initial setup.

Step 4. The software was executed and the results for opening and closing of the hand mechanism were analysed. If the results were satisfactory the optimisation process was terminated, otherwise the setup was modified. For every item modified, the program was executed and the results re-evaluated. The items were modified in the following order:

I. Mechanical dimensions:

- a) Height.
- b) Offset.
- c) LeverQ.
- d) LeverQ0.
- e) LeverR.
- f) Fingers.
- g) Thumb.
- h) Theta0.
- i) Theta1.
- j) Theta2.
- k) Theta3.

II. Length of the Spring (the initial force in the spring equation must also be changed). Go to step 4.

III. Fixation point of the spring. Go to step 4.

IV. Fixation point of the SMA actuator. Go to step 4.

V. Selection of a different spring. Go to step 3.

VI. Selection of a new configuration for the SMA actuator. Go to step 3.

The intermediate stages of the optimisation will not be shown here, since there were many. Figures 4.13, 4.14(a) and 4.14(b) show the outputs of the software for a satisfactory setup obtained as described above.

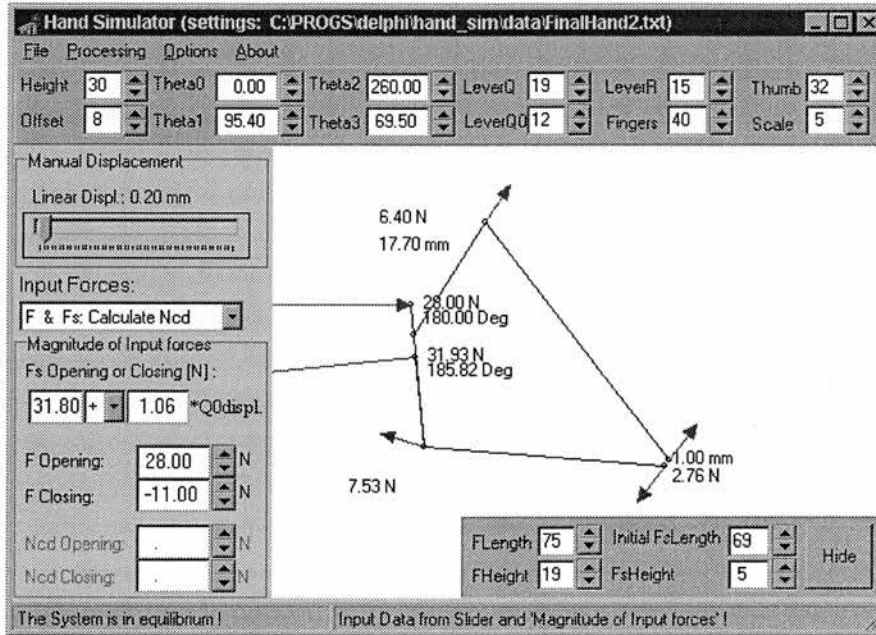
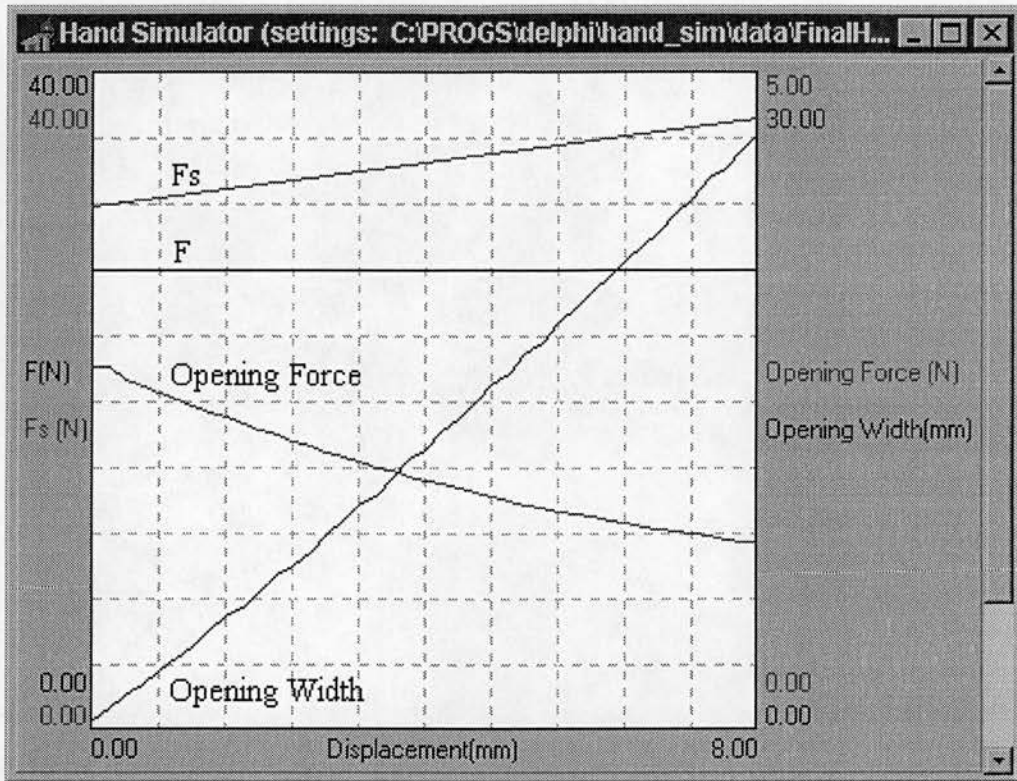
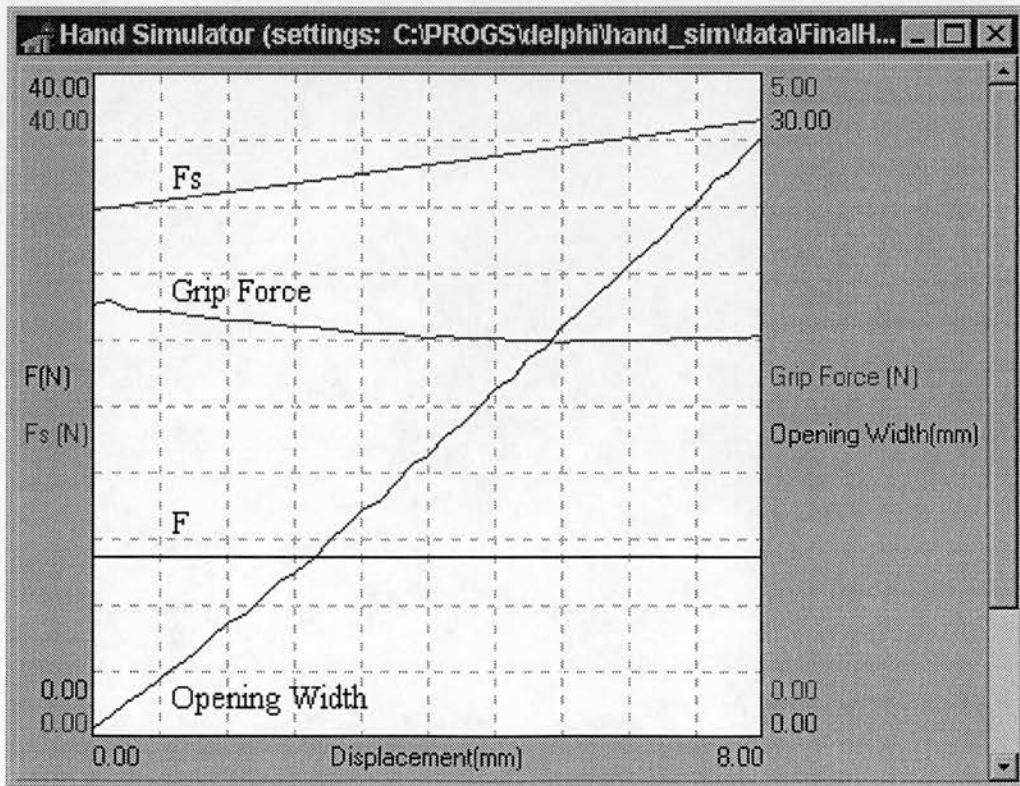


Figure 4.13: Snap shot of the main screen for the optimised hand mechanism.



(a)



(b)

Figure 4.14: Outputs for the optimised setup. (a) Hand opening; (b) Hand closing.

Note that since the inputs and outputs of the software represent the dimensions, forces and movements of the real system, those parameters can be used directly to specify the components of the hand, as follows:

Dimensions of the Hand Mechanism

Table 4.1 shows the correspondence between the simulation parameters and the real system (figure 4.4).

Simulation	Real System	Value
Height	a	30 mm
Offset	b	8 mm
Theta0	θ_0	0 °
Theta1	θ_1	96 °
Theta2	θ_2	260 °
Theta3	θ_3	69.5 °
ThetaF	θ_F	180 °
ThetaFs	θ_{FS}	186 °
LeverQ	c	19 mm
LeverQ0	c0	12 mm
LeverR	cR	15 mm
Fingers	e	40 mm
Thumb	f	32 mm

Table 4.1: Correspondence between the simulation parameters and the real system.

Using those data as the starting point, the basic hand mechanism was designed as shown in figure 4.15.

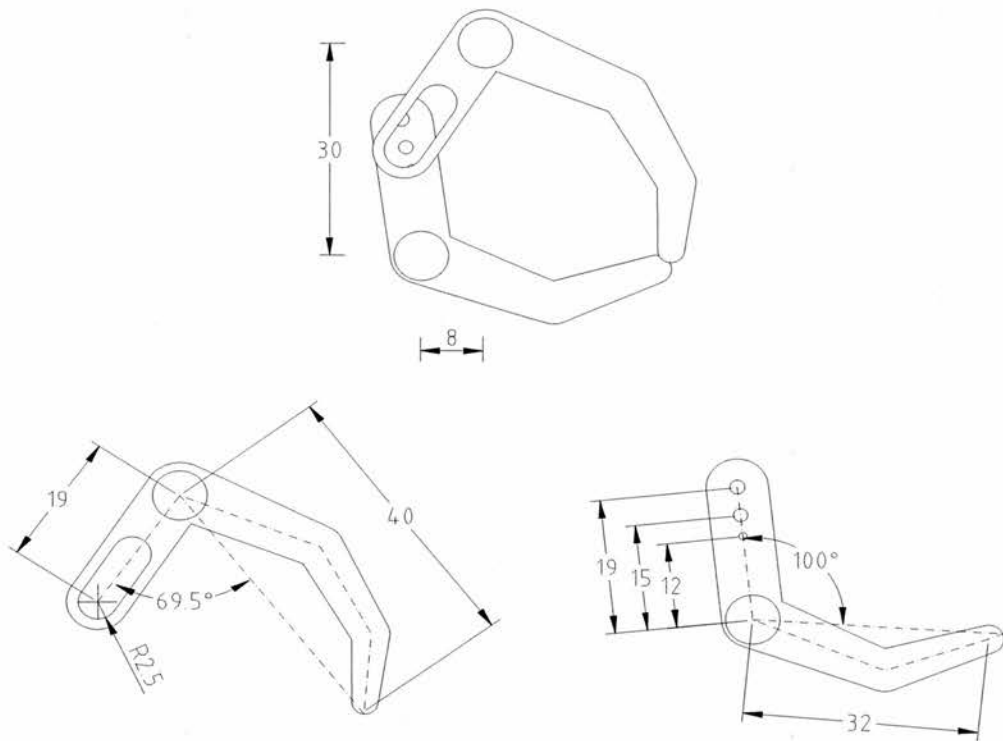


Figure 4.15: Dimensions of the hand mechanism (dimensions in mm).

Spring

The fields related to “Fs Opening or Closing (N)” (figure 4.13) were filled based on the specifications of the following spring:

- Supplier: SPEC[®] Associated Springs (UK)
- Specifications:
 - Part #: T31480
 - External diameter (D₀): 6.3 mm
 - Wire diameter (d): 0.9 mm
 - Initial length (L₀): 44.1 mm
 - Initial tension (I_T): 5.58 N
 - Recommended max. extension (L₁): 73.8 mm
 - Tension at L₁ (P₁): 37.1 N

- Spring Rate (P/f): 1.06 N/mm

Based on the above spring specification, the spring equation was set to:

$$F_s = 31.8 + 1.06 * Q0Displ.$$

where:

- Q0Displ.: Displacement of point Q0 (where the spring is connected to the thumb lever) calculated by the software.
- 1.06: Spring rate in N/mm
- 31.8: Force that the spring must be applying when the hand is fully closed. Since the initial tension of the spring (I_T) is 5.58 N with initial length (L_0) of 44.1 mm, it must be installed in the mechanism with the hand fully closed and its length must be adjusted to 68.8 mm. This force must be applied to point Q0 at an angle of 186° (θ_{FS}).

SMA actuator

The basic specifications for the SMA actuator are defined by the input fields “F Opening” and “F Closing” (figure 4.13) and by the necessary displacement of point Q. Therefore, the SMA actuator must be designed to provide 28 N (applied to point Q at an angle of 180° (θ_F)) to open the hand. This can be achieved by using 9 SMA wires Flexinol 150HT requiring a total of 11 N for deformation (see chapter 5 for details). The results also show that at least 7.2 mm of linear displacement must be provided by the SMA actuator to open the hand by 24 mm.

4.4 - Conclusion

This chapter described some fundamental problems involving the design and manufacture of small prostheses. A mathematical model of the hand mechanism was developed and, based on that, a computer program was written to simulate the movements and forces within the mechanism. The software was used to design the hand mechanism, to specify the main spring and to defined the basic specifications of the SMA actuator. The design and construction of the actuator will be explained in the next chapter.

Chapter 5

The Design and Construction of the SMA Actuator

5.1 - Introduction

Shape Memory Alloys can be used to create small, light and yet very powerful actuators. However, to achieve such characteristics the design and manufacturing must be done very carefully. This chapter discusses the design and manufacture of a SMA actuator according to the specifications defined in chapter 4. For a description of practical aspects of working with SMA see appendix D.

5.2 - Specifications of the Actuator

The required specifications for the SMA actuator were first defined in chapter 4 and are repeated here:

- It must fit into a volume of 30 mm x 30 mm x 100 mm.
- It must weigh less than 50 grams.
- The actuator must be able to stand high levels of vibration and work in any position.
- Time to open the hand: 1.5 seconds.
- Time to close the hand: 2 seconds.

- Lifetime better than 72000 cycles.
- Working temperature: 0 - 35 °C.
- Must provide at least 1.5 N at the tip of the fingers when opening the hand against a cosmetic glove. This can be achieved by applying 28 N to the linking barrel of the hand mechanism.
- Must generate at least 7.2 mm of linear displacement to achieve the necessary opening width of the hand.

5.3 - Selecting the Actuator Configuration

One of the first parameters to be considered when designing a SMA actuator is the method of heating the SMA elements. The most common approaches involve changing the ambient temperature and circulating electric current through the elements. It was decided that the use of electric current provided by a battery pack is the most suitable option for the application in question. Electrically driven SMA actuators are normally divided into two groups: Differential and bias actuators. Figure 5.1(a) shows the differential actuator where the central load is driven left by heating SMA “A” and cooling SMA “B”. The overall force that drives the load is given by $F = F_a(\text{recovery}) - F_b(\text{deformation})$. By heating “B” and cooling “A”, motion to the right is obtained with an overall force of $F = F_b(\text{recovery}) - F_a(\text{deformation})$. If both sets of SMA are matched, the forces in both directions are symmetrical. This is not the case if the load is driven by the bias actuator shown in figure 5.1(b). In this arrangement, motion to the left is obtained by heating SMA “A”, resulting in an overall force equal to $F = F_a(\text{recovery}) - F_s$. Motion in the opposite direction is obtained by letting SMA “A” cool down, resulting in an overall force given by $F = F_s - F_a(\text{deformation})$. Although the forces produced at high and low temperatures can be arbitrarily set on the bias actuator by adjusting the size of the bias force, the forces involved are lower than those possible for the differential actuator (Duerig *et al.* (1990)). Large operational strokes can not be easily obtained with the bias actuator, since the shape recovery force gradually diminishes as the

SMA approaches its original shape, while the bias force grows stronger (Suzuki (1987)). However this effect can be reduced by using a bias spring with very low rate (N/mm).

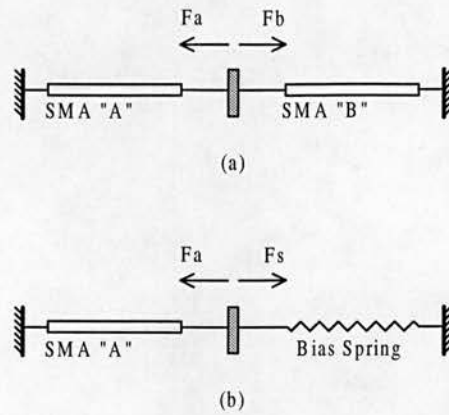


Figure 5.1: Two types of SMA actuators.
 (a) Differential actuator; (b) Bias actuator.

Since the actuator must be powered by a battery pack, power consumption is a major concern throughout the design. Taking into consideration that the hand will be closed or grasping an object most of the time, it is desirable that, when in this situation, the power consumption is set to a minimum or even zero. This can be achieved easily using the bias actuator. The force to open the hand can be provided by the recovery force of the SMA “A” and the bias spring would provide the necessary force to deform SMA “A”, close the hand and grasp objects. The disadvantage of this approach is that the grasping force can not be precisely controlled. However, as discussed later in chapter 6, precise control is not a requirement of this design and the bias actuator can fulfil the specifications. Finally, because the bias actuator has only one set of SMAs, it is usually simpler and easier to assemble than the differential actuator.

Therefore, according to the discussion above, the *bias actuator* will be used in this design as an attempt to produce a simple device, easy to manufacture and using as little power as possible.

5.4 - Selecting the SMA Elements

5.4.1 - Material Selection

Although many different alloys exhibit the shape memory effect, to date there are only two viable commercial options: NiTi and copper based alloys. Table 5.1 compares some basic features of those alloys.

	NiTi based alloys	Cu-based alloys
TTR (°C)	up to +110	up to +200
Resistivity ($\mu\Omega\text{cm}$)	70 - 100	18
Cost	more expensive	cheaper
Fabrication and machinery	difficult	easy
Max. strain (%)	8	4
Max. stress (MPa)	600	200
Corrosion resistance	excellent	problematic
Lifetime (strain @ 2%)	better than 100000	around 100

Table 5.1: Comparison between NiTi and copper based alloys.

Cu-based alloys have much higher transformation temperatures (TTR), are easier to manufacture and cost less than NiTi alloys. In this particular design, differences in costs are a minor worry since small quantities of SMA will be used. Higher transformation temperatures may be required to allow higher operational temperatures, or even a faster cooling rate when using convection in still air. However, since the operational temperature of the required system will be between 0 and 35 °C, either the NiTi or the Cu-based system can provide a large “gap” between the ambient temperature and the martensite finish (Mf) temperature. Nevertheless, the higher resistivity of NiTi alloys favours them in this design since the SMA elements will be heated electrically. Also, the higher levels of stress and strain and the longer lifetime of NiTi systems are highly desired features for this application.

Based on the specifications of the actuator and according to the analyses above, it was decided to use the NiTi alloy as the basic material for the SMA elements. The general properties of NiTi shape memory alloys are presented in table 5.2.

NiTi Properties		
Transformation properties	Transformation temperature	-200 to 110 °C
	Latent heat of transformation	5.78 cal/g
	Transformation strain	8% (single cycle)
		6% (for 100 cycles)
4% (for 100,000 cycles)		
	Hysteresis	30 to 50 °C
Physical properties	Melting point	1300 °C
	Density	6.45 g/cu.cm
	Thermal conductivity	0.18 W/cm°C (austenite)
		0.086 W/cm°C (martensite)
	Specific heat	0.2 cal/g°C
	Corrosion performance	excellent
Electrical and magnetic properties	Resistivity	~100 μΩcm (austenite)
		~80 μΩcm (martensite)
	Magnetic permeability	< 1.002
	Magnetic susceptibility	3.06E6 emu/g
Mechanical properties	Young's modulus (highly non-linear with temperature)	~83 GPa (austenite)
		~28 to 41 GPa (martensite)
	Yield strength	195 to 690 MPa (austenite)
		70 to 140 MPa (martensite)
	Ultimate tensile strength	895 MPa (fully annealed)
		1900 MPa (work hardened)
	Poisson's ratio	0.33
	Elongation at failure	25 to 50% (fully annealed)
		5 to 10% (work hardened)
	Hot workability	good
Cold workability	difficult	
Machinability	difficult	

Table 5.2: Properties of a typical NiTi alloy (Shape Memory Applications, Inc. - USA)

5.4.2 - Choice of the Shape and Dimensions of the SMA Elements

In order to develop a SMA actuator to satisfy the specifications, one has normally to choose from two basic shapes for the SMA elements: coil springs and wires. The use of SMA coil springs has the advantage of providing a large macroscopic

displacement out of a small microscopic strain. However, the stress distribution over the cross section of the wire is uneven, which contributes to the degradation of the shape memory effect and requires springs of very large cross sections to produce high forces. The use of SMA wires under tensile load has the advantage of optimum use of the material. This means that, with careful design, the energy efficiency of SMA wires is much higher than the efficiency of other types of SMA elements (Reynaerts & Van Brussel (1994)). Therefore, it was decided to use SMA wires under tensile load in the design of the actuator.

5.4.2.1 - Transformation Temperature

According to the specifications, the SMA actuator must work under temperatures that range from 0 to 35 °C. Since the initial design will rely upon convection in still air for cooling the SMA elements, it is important that the M_f temperature is well above the maximum ambient temperature. Therefore, the SMA elements will be selected taking into consideration that the martensite phase can be fully achieved at the highest ambient temperature. It is also desirable that M_f is as high as possible so that the “gap” between the maximum ambient temperature and M_f is as large as possible, which will increase the rate of heat exchange in still air.

5.4.2.2 - Choice of the SMA Wires

After studying various types of SMA wires, their characteristics and possible suppliers, it was decided to use the NiTi *Flexinol*^(tm) wires manufactured by Dynalloy Inc. (USA). The choice was based on the manufacturing process used by the company to produce SMA wires of small deformation stress and long lifetime, specially designed for use as actuator elements (the wires are also supplied heat treated).

Table 5.3 shows the typical properties of two types of Flexinol actuator wires (NiTi wires which are not processed by the Flexinol process will have different properties). Although there are other types of Flexinol wires, only those two were chosen as possible alternatives for this design.

		Flexinol 150HT	Flexinol 250HT
Physical	Wire diameter (μm)	150	250
	Wire cross-sectional area (μm^2)	17,671	49,087
Electrical	Linear resistance (Ω/m)	50	20
	Recommended current (mA)*	400	1000
	Recommended power (W/m)	8	20
Force	Max. recovery force @ 600 MPa (g)	1,056	2,933
	Rec. recovery force @ 190 MPa (g)	330	930
	Rec. def. force @ 35 MPa (g)	62	172
Response Time	Min. contraction time (sec)**	0.1	0.1
	Relaxation time (sec)**	1.2	3.5
	Typical cycle rate (cyc/min)**	46	17
Thermal	As ($^{\circ}\text{C}$)	90	90
	Af ($^{\circ}\text{C}$)	98	98
	Ms ($^{\circ}\text{C}$)	72	72
	Mf ($^{\circ}\text{C}$)	62	62
	Annealing temp. ($^{\circ}\text{C}$)	300	300
	Melting temp. ($^{\circ}\text{C}$)	1300	1300
Material Properties		Martensite	Austenite
(For all Flexinol wires)	Resistivity ($\mu\Omega\text{cm}$)	76	82
	Young's modulus	28	75
	Magnetic susceptibility ($\mu\text{emu/g}$)	2.5	3.8
	Density (g/cc)	6.45	
	Thermal conductivity (W/cm $^{\circ}\text{C}$)	0.1	
	Spec. heat or heat capacity (cal/g $^{\circ}\text{C}$)	0.077	
	Latent heat (joule/g)	24.2	
	Breaking strength (MPa)	1,000	
	Work output (joule/g)	1	
	Energy conversion efficiency (%)	5	
	Max. deformation ratio (%)	8	
	Rec. deformation ratio (%)	3-5	

Table 5.3: Properties of the NiTi Flexinol(tm) wires (Dynalloy Inc. - USA)

* For shape recovery in 1 second.

** In still air at 20 $^{\circ}\text{C}$.

Further analysis shows that, although the wires 250HT have a higher recovery force, the frequency response is considerably lower compared to 150HT. Since the use of active cooling systems is not intended at the present stage of this project, it was decided to design the actuator using the SMA wires Flexinol 150HT. Note that

although the basic properties of that wire are shown in the table above, the manufacturer states that those figures are only guidelines and strongly recommends that specific tests must be performed to evaluate those features with the specific application in mind. Therefore, an initial set of experiments was executed to analyse the basic properties of the SMA wire Flexinol 150HT. The tests were performed for wires 210 mm long strained at 3% and under a constant tensile stress of 176 MPa (those are the basic levels of strain and stress at which the SMA actuator is intended to work). Since the speed of actuation is also an important factor in this application, it would be desirable to use heating currents as high as possible. However, SMA elements are notorious for their strong history dependency, meaning that how they are used will affect their future performance. To evaluate this problem, three identical samples were tested under the conditions defined before but using different heating currents.

Sample 1: Flexinol 150HT

- Length: 210 mm
- Maximum strain: 3%
- Maximum stress: 176 MPa (3.1 N for this wire)
- Electrical resistance: 11.2 Ω in the martensite phase
- Heating voltage: 3.2 VDC

Sample 2: Flexinol 150HT

- Length: 210 mm
- Maximum strain: 3%
- Maximum stress: 176 MPa (3.1 N for this wire)
- Electrical resistance: 11.2 Ω in the martensite phase
- Heating voltage: 3.5 VDC

Sample 3: Flexinol 150HT

- Length: 210 mm
- Maximum strain: 3%
- Maximum stress: 176 MPa (3.1 N for this wire)
- Electrical resistance: 11.2 Ω in the martensite phase
- Heating voltage: 3.8 VDC

Note that although the heating of the SMA wires could be done by applying a DC current, the tests use a constant voltage. Since the resistivity of the SMA wires has a very non-linear behaviour (Miyazaki *et al.* (1992) and Airoidi *et al.* (1991)), no conclusions can be drawn about the exact current circulating through the wires during heating. However, the resistance of the elements in the martensite phase is given as a gross guideline for the initial heating current.

The training of each SMA wire and the experiments to investigate fatigue properties, response time and transformation temperatures were performed according to the conditions specified above and using the setup shown in figure 5.2. One end of the SMA wire was clamped (using screws with washers) to a fixed base and the other end was similarly clamped to a “free” base. A steel rod was used to attach the “free” base to the slider of a linear potentiometer (position sensor) and to the suspended load. A mechanical travel limit was adjusted so that, under load, the maximum deformation was limited to 3% of the “hot length” of the wire. A power driver and a PWM control system was used to control the heating rate of the SMA wire (see chapter 6 for details). A computer program generated the input (U) to the PWM and read the output value of the linear potentiometer.

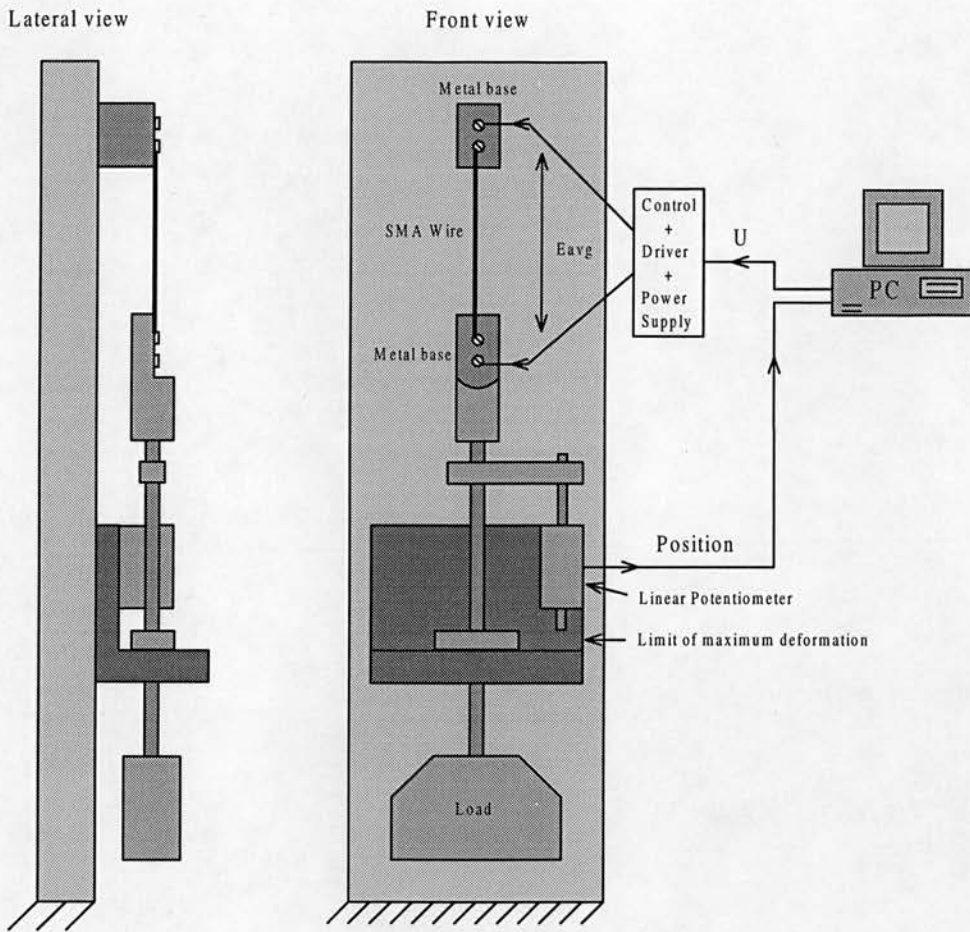


Figure 5.2: Experimental setup used for training, cycling and analysis of the time response and transformation temperature of the SMA wires.

TRAINING

The three samples of SMA wire were used under different heating conditions. Prior to the experiments each wire was cycled 200 times under a constant tensile stress of 176 MPa with the strain limited to 3%. Each cycle consisted of heating the SMA wire by applying a constant voltage (as specified for each sample) until full recovery was achieved and allowing it to cool to room temperature (22 °C) while deformed by the tensile load.

CYCLING

Each sample was cycled to evaluate fatigue properties. Each cycle was performed as defined in the training section. The experiments were terminated after 10000 cycles and the results are shown in figure 5.3.

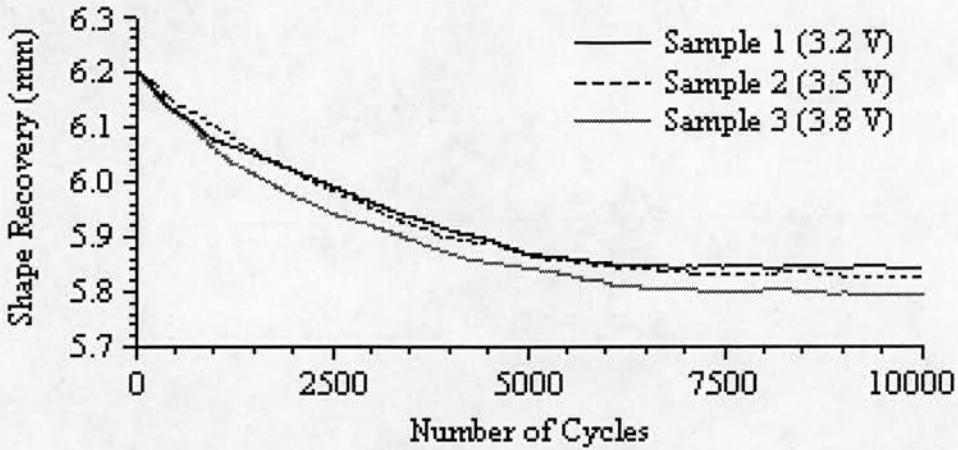


Figure 5.3: Cycling tests of Flexinol 150HT at given heating voltages.

The results show that different heating voltages within the range of 3.2 and 3.8 VDC do not have a significant effect on the long term cycling as far as the shape recovery is concerned. However, although the differences are not critical for the application in question, the experiment also shows that the use of higher heating currents tend to contribute to the degradation of the Shape Memory Effect as the number of cycles increases. Furthermore, although the wires were initially strained to 3% (6.3 mm for the samples under test), the maximum shape recovery observed at the beginning of the experiment was around 6.15 to 6.2 mm. This is because full shape recovery is only possible under zero stress. The effect of that partial recovery is that after each cycle the wire will train to a partial stroke, thus moving less and less with each stroke. This tends to stabilise as the number of cycles is increased. This effect is known and predicted by the manufacturer of the Flexinol SMA wires.

Once the cycling was completed the samples were tested to evaluate the response time, transformation temperature and the stress versus strain characteristics.

RESPONSE TIME

To evaluate the response time a single cycle, as described in the training section, was performed for each sample and the times for shape recovery and relaxation were measured. Figure 5.4 shows the results of the experiment.

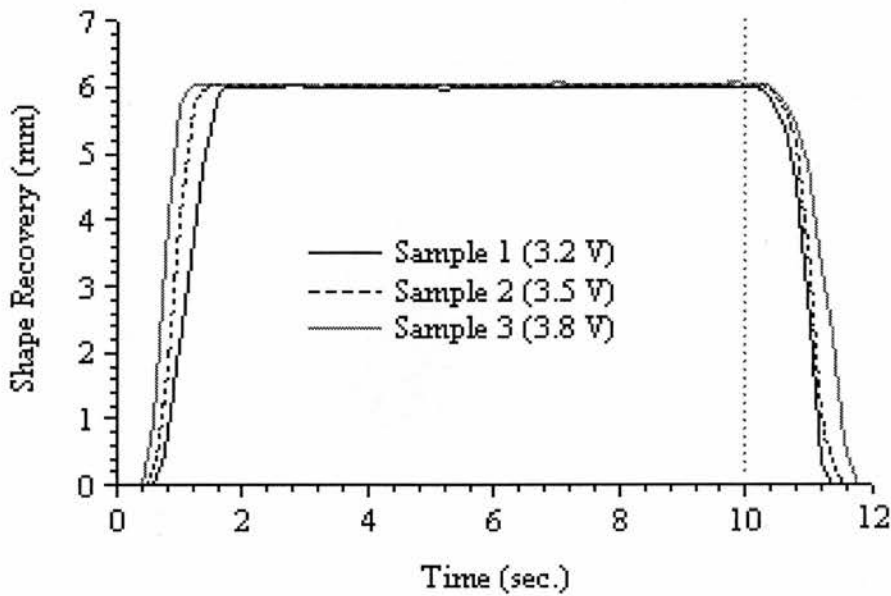


Figure 5.4: Time response for Flexinol 150 HT at given heating voltages. Heating started at 0 sec. Cooling started at 10 sec. Amb. temp. = 22 °C.

Time responses:

- Sample 1:
 - TRecovery: 1.6 sec.
 - TRelaxation: 1.4 sec.
- Sample 2:
 - TRecovery: 1.4 sec.
 - TRelaxation: 1.6 sec.

- Sample 3:
 - TRecovery: 1.2 sec.
 - TRelaxation: 1.7 sec.

As expected the results show very similar responses with the fastest shape recovery and slowest relaxation time being achieved with the highest heating voltage.

TRANSFORMATION TEMPERATURES

To evaluate the hysteresis of the samples, displacement was plotted while the voltage was slowly increased and decreased at constant load. This approach, as opposed to plotting displacement against temperature, is more appropriate to electrically driven devices and permits accurate analysis. Figure 5.5 shows the hysteresis cycles for the samples under test.

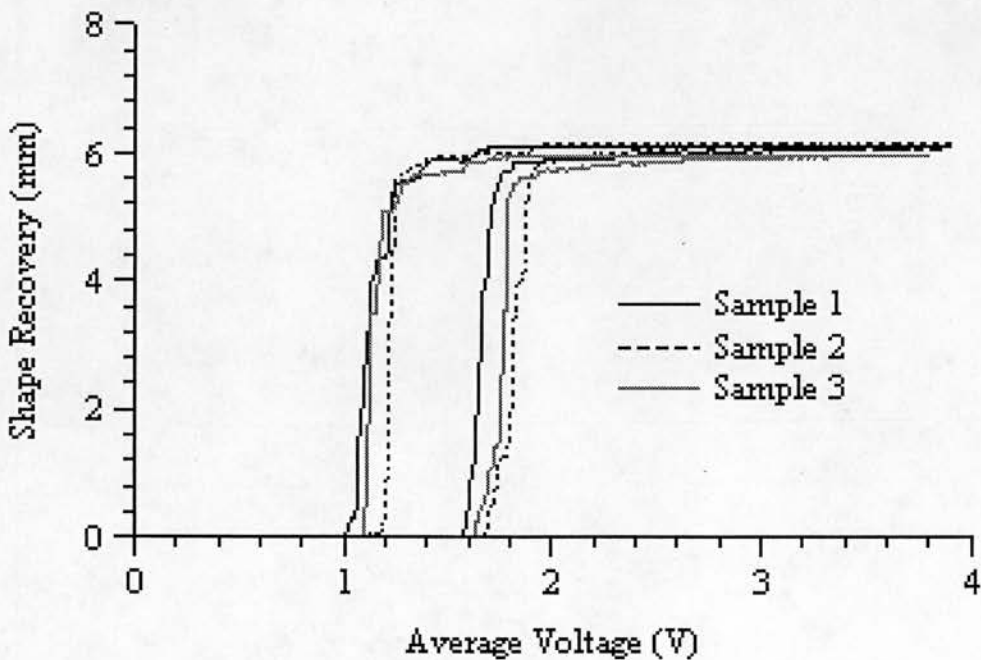


Figure 5.5: Hysteresis cycles for Flexinol 150 HT 210 mm long. Amb. temp. = 22 °C.

Transformation values (as explained in chapter 3):

- Sample 1:
 - Mf: 1.1 V
 - Ms: 1.2 V
 - As: 1.6 V
 - Af: 1.75 V
- Sample 2:
 - Mf: 1.2 V
 - Ms: 1.3 V
 - As: 1.7 V
 - Af: 1.95 V
- Sample 3:
 - Mf: 1.1 V
 - Ms: 1.2 V
 - As: 1.7 V
 - Af: 1.8 V

The results show small differences in the hysteresis cycles of the samples caused by the different working conditions but, in general steady voltages below 1 V are low enough for the samples to be in full martensite state and voltages above 2 V should be enough to make sure that the samples will reach the austenite state. However, those values can only express the voltages necessary to provide a full hysteresis cycle by maintaining the applied voltage for as long as it takes for the samples to recover/deform. In other words, if, for instance, one applies 5 V to the same samples for a shorter period of time, the shape recovery will proceed a lot faster than by using only 2 V.

STRESS VERSUS STRAIN

Figures 5.7 shows the stress versus strain curves for the samples under test. The curves were obtained in the martensite and austenite phases so that the deformation

and recovery stresses can be evaluated. Note that when applying high levels of stress and strain during the austenite phase the wires are damaged by overload. Figure 5.6 shows the setup used in this experiment.

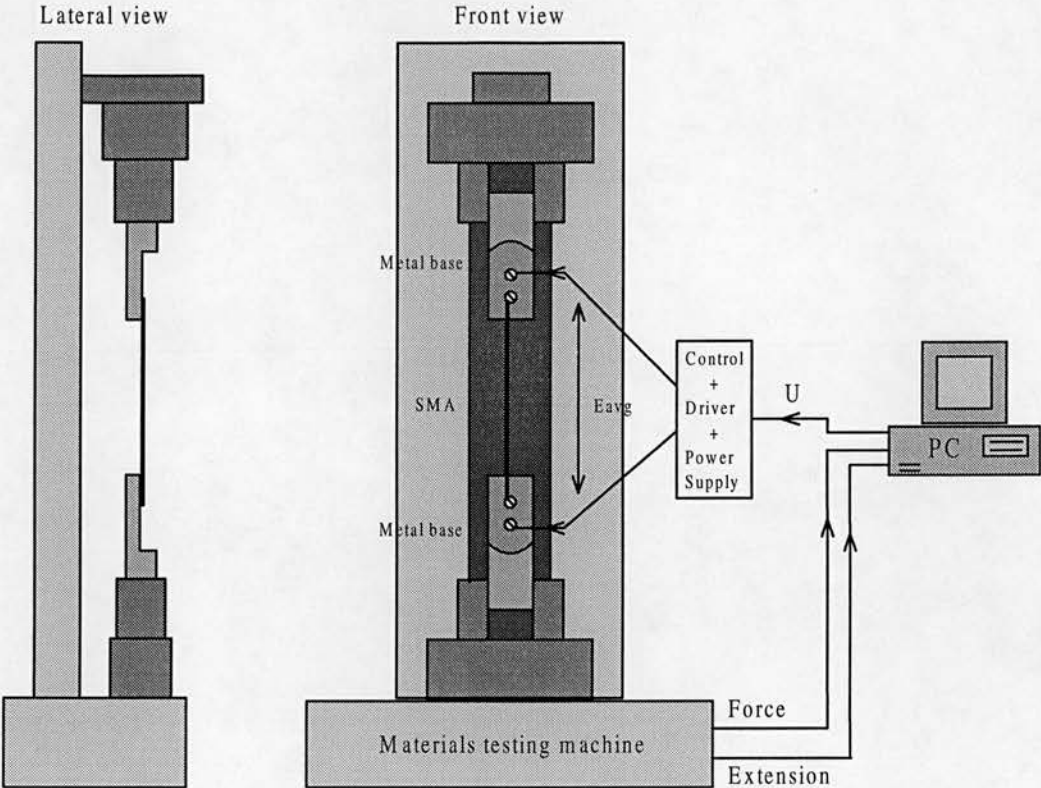


Figure 5.6: Setup used to acquire the stress against strain curves for Flexinol 150HT.

To set the point of zero stress and zero strain the wires were heated above A_f (heating voltage as defined for each sample) and the distance between the grips of the testing machine was adjusted so that the wires were under no tension. The martensite curves were obtained at ambient temperature (no current circulating through the wires: $E_{avg} = 0$ V). The austenite curves were obtained at temperatures above A_f by applying the heating voltage specified for each sample, as shown in figure 5.7.

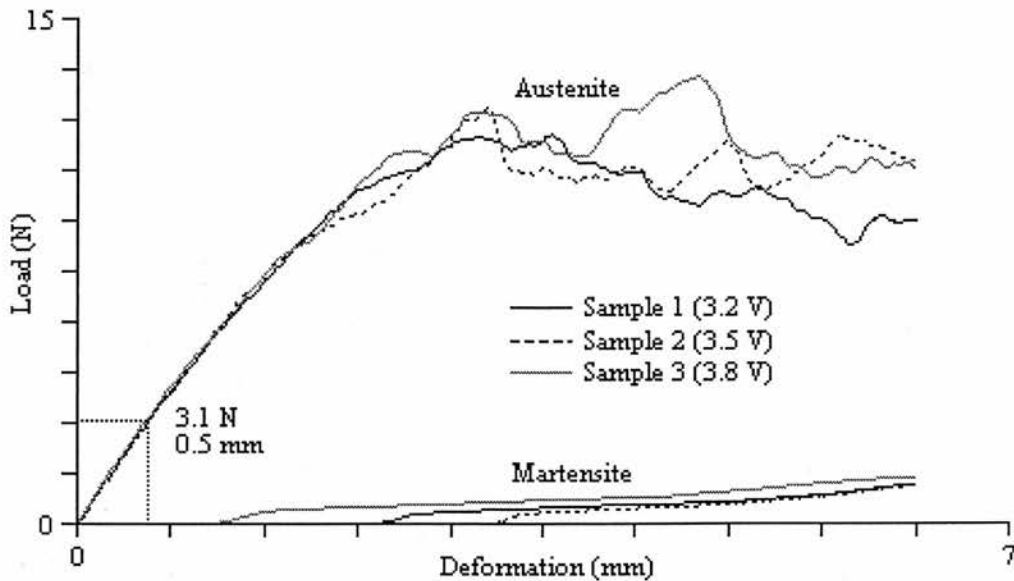


Figure 5.7: Stress versus strain curves for Flexinol 150 HT. Amb. temp. = 22 °C.

The most important data that can be extracted from this test are:

- The curves for shape recovery reach the yield point (austenite phase) at about 10 N for the heating voltages used.
- The deformation forces required for 3% strain (6.3 mm deformation) in the martensite phase are:
 - Samples 1 and 2: 1.15 N
 - Sample 3: 1.39 N
- In the austenite phase a deformation of 0.5 mm is observed when the samples are under a tensile force of 3.1 N (i.e., full recovery is not possible).

Figure 5.7 also shows that no deformation force was required until the samples were extended by some amount. On investigation it was found that the samples show a “two-way” effect that affects the required deformation forces. Figure 5.8 shows a schematic diagram of how this takes place. Before starting the deformation process, the samples were heated above A_f at 0% strain (a). The heat was then removed and, once the temperature dropped below M_f , the shape changed spontaneously to a deformed level which depended on the operational conditions (b). When the

extension process began, the deformation force remained zero until the resulting “slack” was removed (c). The force then increased until the full deformation was reached (d). The manufacture of the Flexinol wires explained that this effect was due to the manufacturing process and the fact that the wires were pre-trained at 5 % strain before delivery. The effect tends to be more pronounced if the operational strain is significantly different from the pre-trained one. However, this “two-way” effect tends to stabilise after about 1000 cycles. Since the experiment was performed after the samples were cycled 10000 times, it was assumed that the levels of deformation and recovery stress were stable and may safely be used as the worst case scenario (regarding the required deformation forces) in the design of the actuator.

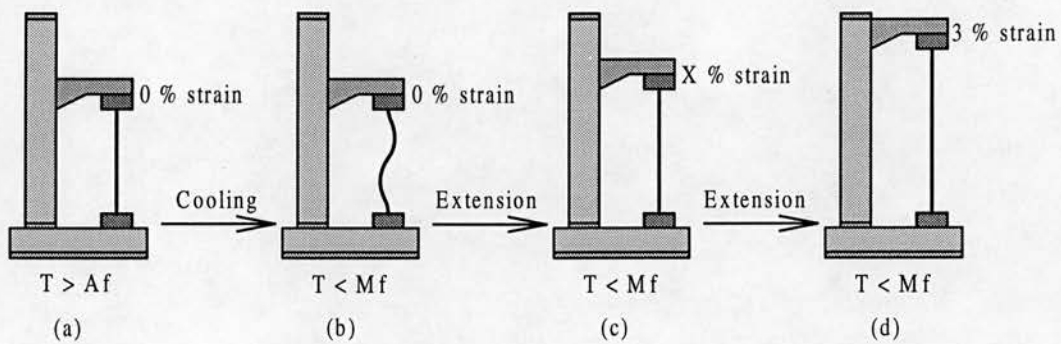


Figure 5.8: The influence of the two-way effect on the required deformation forces.

DISCUSSION

The results of the experiments do not show remarkable differences when using 3.2, 3.5 or 3.8 V for heating 210 mm of SMA wire Flexinol 150HT. The main differences can be observed in the time responses and in the deformation forces required for 3 % strain. Sample 3 had the fastest response time for shape recovery, however the use of high heating currents made it more difficult to be strained (required higher deformation forces). Sample 1 showed good overall results but the time response needed to be improved. Therefore, it seems that the use of heating voltages in the region of 3.5 V (as for sample 2) results in a good compromise for this application.

Table 5.4 shows a summary of the responses for sample 2. Those are thought to be good design parameters for the actuator in question.

	Flexinol 150HT
Heating voltage (for recovery in 1.4 sec.)	3.5 VDC
Deformation force at 3% strain	1.15 N
Contraction time @ 3.5 VDC, 176 MPa and 3 % strain	1.4 sec.
Relaxation time @ 176 MPa and 3% strain	1.6 sec.
As	1.7 VDC
Af	1.95 VDC
Mf	1.2 VDC
Ms	1.3 VDC

Table 5.4: Results of testing a SMA wire Flexinol 150HT 210 mm long strained at 3% under constant stress of 176 MPa and constant heating voltage of 3.5 VDC. (Ambient temperature = 22°C)

5.4.2.3 - Length and Maximum Strain of the SMA Wires

In order to achieve a lifetime better than 72000 cycles, the strain must be limited to 3% when using the martensitic transformation (Gilbertson (1992)). Another possibility is to use the R-Phase by working with levels of strain smaller than 0.5%. This has the advantage of better fatigue properties (Van Humbeeck (1991)). However, although 0.5% is quite a lot of strain for coil springs (in terms of macroscopic displacement), it is very low for wires. For instance, a wire 1440 mm long would be needed to provide 7.2 mm displacement at 0.5% strain. The specifications of the system are such that the accommodation of this long wire is not possible within the dimensions of the actuator. Therefore the martensite phase will be used in favour of the R-Phase and the strain will be limited to 3%.

The required strain and length of the SMA wires must be calculated based on the data provided by the experiments. According to the specifications the actuator must provide 7.2 mm of linear displacement. That value corresponds to the deformation to be applied to the SMA elements. However, the experiments show that during the austenite phase (shape recovery), when the recovery stress reaches 176 MPa (level to

be used in this design), a strain of 0.24% is still observed. Therefore, the length of the SMA wires must be calculated by using 3% strain and discounting 0.24% of non recoverable strain so that the useful displacement is 7.2 mm under 176 MPa stress. Simple calculations show that a SMA wire 261 mm long will be necessary to fulfil the requirements. However, as it will be shown later, the final actuator will use wires slightly longer (263.5 mm).

5.5 - Mechanical and Electrical Arrangement of the SMA Elements

Although table 5.3 shows that the recommended recovery stress for Flexinol 150HT is 190 MPa, this design will use 176 MPa (3.1 N for that wire) for better fatigue properties. Since 28 N are required to open the hand, at least 9 wires must be used in parallel to increase the total recovery force (the minimum deformation force for 3% strain will be 10.35 N).

Those nine lengths of wire can be electrically connected in series or parallel or by a combination of both. However, the parallel connection will be used. This is purely because it is the easiest approach and will meet the requirements at this stage of the research.

5.6 - Position Feedback

In order to control the movements of the actuator, one must carefully monitor the deformation and recovery of the SMA wires. This is normally done by feeding the position of the actuator back to an electronic control system. The following paragraphs describe some of the most common methods used to monitor the state of SMA devices.

a) Resistive Feedback:

This technique consists in monitoring the changes in the resistance of the SMA as it goes through the transformations. It has the advantage of using the SMA element to both produce work and act as the feedback device. Unfortunately, the electrical resistance of SMA elements has a very non-linear behaviour and changes dramatically depending on the stress, strain and temperature of the element (Miyazaki *et al.* (1992) and Airoidi *et al.* (1991)). However, if the design can use the R-Phase, the resistive feedback may be used under certain conditions (Ikuta *et al.* (1994)).

b) External Devices:

The use of devices such as encoders and potentiometers is the most common form of position feedback for SMA actuators. Compared with the resistive feedback this approach has the disadvantage of adding extra weight, extra wiring and sometimes bulky devices to the actuator.

c) Simulation (Open Loop Control):

By simulating the behaviour of the SMA elements, it may be possible to predict the current position of the device and use it as the feedback signal to the control system. This method, named open loop control, does not make use of any external device. However, although there are a number of mathematical descriptions of various aspects of the shape memory phenomenon (Berveiller *et al.* (1991), Colli & Sprechels (1993), Graesser & Cozzarelli (1994) and Colli (1995)), precise modelling of SMAs has never been achieved. The imprecision in current simulations mean that the open loop control would need regular calibrations to ensure that the model is in the same state as the real actuator.

Other methods such as magnetic susceptibility and thermal radiation have also been used to follow the hysteresis cycle of the SMA materials (Honma (1987)). However, these methods are difficult to implement and demand very accurate circuitry, which exclude them from most practical applications.

In this design a linear potentiometer will be used to provide position feedback. The slider of the potentiometer will be attached to the moveable part of the actuator, as shown in figure 5.9.

5.7 - Required Protections

In order to provide satisfactory performance and good lifetime, it is important to avoid overloading, overstraining and overheating the SMA elements.

5.7.1 - Protection Against Overstrain

This is usually easy to achieve and normally consists on limiting the deformation of the SMA elements by means of some mechanical limit, as shown in figure 5.9(a).

5.7.2 - Protection Against Overload

Protection against overload can be achieved in many different ways. In this design the power to the SMA wires is removed if the stress exceeds a certain safety limit. The overload signal is provided by the combined action of an overload spring and a snap action switch. As show in figure 5.9, both ends of the SMA wires are attached to moveable “anchors”. The overload springs hold one of the anchors with a force just above the maximum recommended loading for the wires Flexinol 150HT (9 *

3.234 = 29.1 N). While F_{LOAD} is below the overload limit, only the main anchor will move and the overload switch will stay “on” (figure 5.9(b)). However, if F_{LOAD} exceeds the specified limit, the SMA wires will try to recover by compressing the overload springs and the switch will be released (figure 5.9(c)). This indicates to the control system that the recovery process must be interrupted by removing the power from the SMA wires until the stress is again below the safety limit.

An ultra-miniature snap-action switch was chosen as overload sensor:

- Type: FP switch ABP8111P (Matsushita Automation Controls)
- Operational force: 0.3 N (max.)
- Dimensions: 3.4 x 3.4 x 3.7 mm
- Lifetime: 100,000 operations @ 20 cpm, 0.1 mA, 5 VDC
- Total stroke: 1.2 mm (ON/OFF stroke ~ 0.7 mm)

The overload protection will be provided by two identical compression springs, with half of the required force being provided by each one (figure 5.9). To activate the overload switch the springs must be compressed about 0.7 mm from the normal position. The specifications of the chosen springs are:

- Type: C0120 024 1250S from SPEC[®] Associated Spring - UK
- External diameter (D0): 3.05 mm
- Wire diameter (d): 0.61 mm
- Free length (L0): 31.75 mm
- Recommended max. loaded length (L1): 23.7 mm
- Load at L1 (P1): 20.87 N
- Spring rate (P/f): 2.61 N/mm

It was decided that the overload protection should be activated if the load exceeds 30 N. Therefore, the springs must be fitted with a initial length of 26 mm (total initial force of 30 N). Since the overload switch needs a stroke of about 0.7 mm for

activation, in an overload situation the springs will be compressed to a minimum length of 25.3 mm (total force of 33.7 N).

5.7.3 - Protection Against Overheating

Overheating can happen when excessive power is supplied to the SMA elements and the temperature raises above 200 °C (for the Flexinol wires). Kuribayashi (1991) proposed the attachment of a tiny temperature sensor to the SMA wires to monitor the temperature changes. Unfortunately, because of the small diameter of the wires used in this design, the same strategy cannot be applied. Therefore, to provide overheating protection, it was decided to limit the maximum power supplied to the SMA elements. As described earlier, the manufacture states that, for the Flexinol 150HT, heating currents of up to 400 mA can be applied continuously (at ambient temperatures of 20 °C) without any risk of damaging the wires. Since this design uses a maximum of 350 mA to heat each wire for no more than 2 seconds, no overheating should occurs in normal operation.

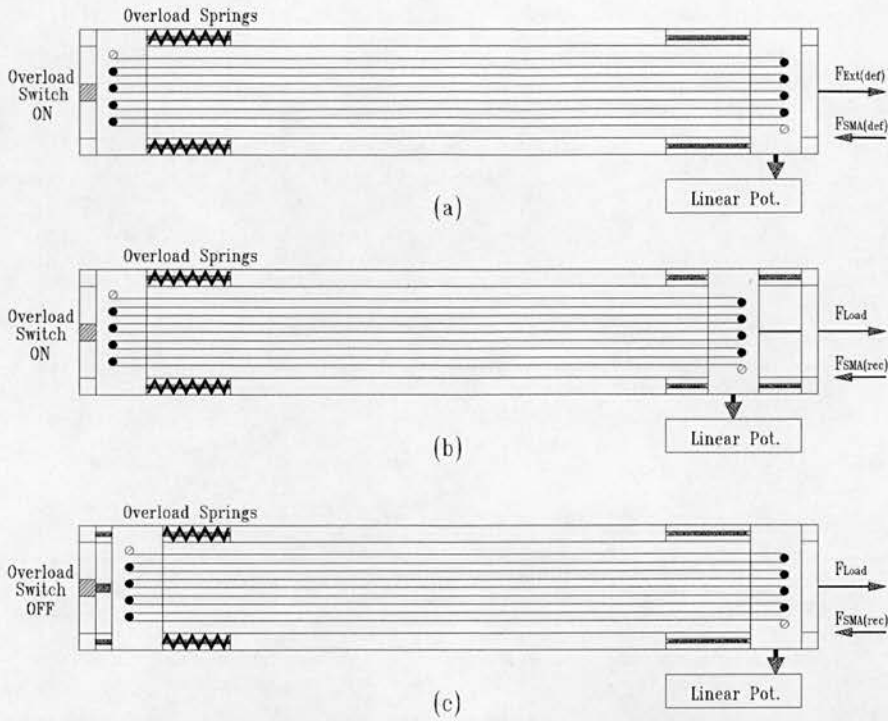


Figure 5.9. Diagram showing the arrangement of the SMA wires, springs, overload switch and position feedback. (a) Deformation of the SMA wires; (b) Shape recovery; (c) Overload situation.

5.8 - Development of the Final Actuator

5.8.1 - The First Prototype

As described earlier, the actuator will be built with nine SMA wires Flexinol 150HT mechanically and electrically in parallel. When joining those wires to the mountings it is very important that all wires have the same length and are under the same temperature, stress and strain. It was initially decided that a simple way to fulfil those requirements is to use one continuous length of wire equal to nine times the length of one single wire, loop it around pins fixed to the anchors and secure only the ends of that long wire, as shown in figure 5.9. To provide the required parallel electrical

connection a metallic plate was placed on the top of each “anchor” (figure 5.10(a)). If the plate also provides a solid grip, those parts of the wire on the anchors will not be “active” since they cannot be strained or heated (there will be no current circulating through them). Note that the mounting of the wires to the anchors has to be done at high temperature (austenite phase) to ensure that they all have exactly the same “hot length”.

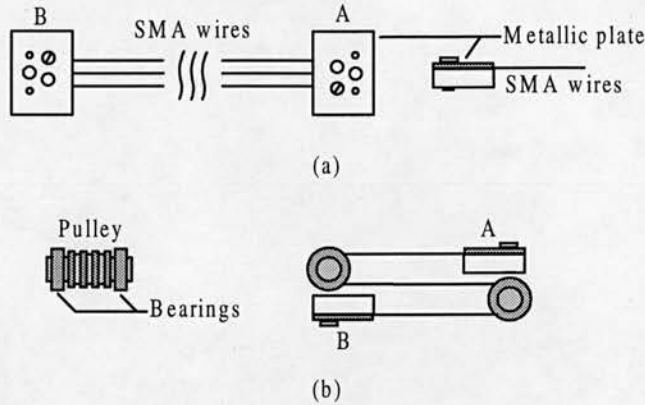


Figure 5.10: Arrangement of the SMA wires.

Since the actuator shown in figure 5.9 is at least 261 mm long, it will not fit into the specifications of the desired actuator (30 mm x 30 mm x 100 mm). The solution is to use two pulleys and loop the wires around them, as shown in figure 5.10(b).

The first prototype was built as shown in figure 5.11. The external dimensions of that device were 22 x 16 x 95 mm. For design reasons, the final length of the wires was increased to 263.5, which allow 7.27 mm of useful displacement when the actuator is under a load of 28 N (assuming maximum strain of 3%).

However, this initial attempt to combine wires was not successful. In particular the frequency response and the shape recovery forces of the device were poor. On investigation the following problems were identified:

- It was difficult to make sure that all the sub-lengths of the wire were exactly under the same stress and strain. The reason for this is thought to be because at temperatures higher than A_f (required for clamping) the wire tries to recover its original shape (a straight wire) making it difficult to hold it in position around the pins on the anchors. Different strategies were tried in an attempt to solve this problem but none of them was entirely successful.
- The electrical connection provided by the metallic plates was not satisfactory leading to the increase of the electrical contact resistance.
- The metallic plates (supposed to clamp the wires in place) were not rigid enough, resulting in uneven clamping of the wires. Therefore, some wires could slip when recovering under load.

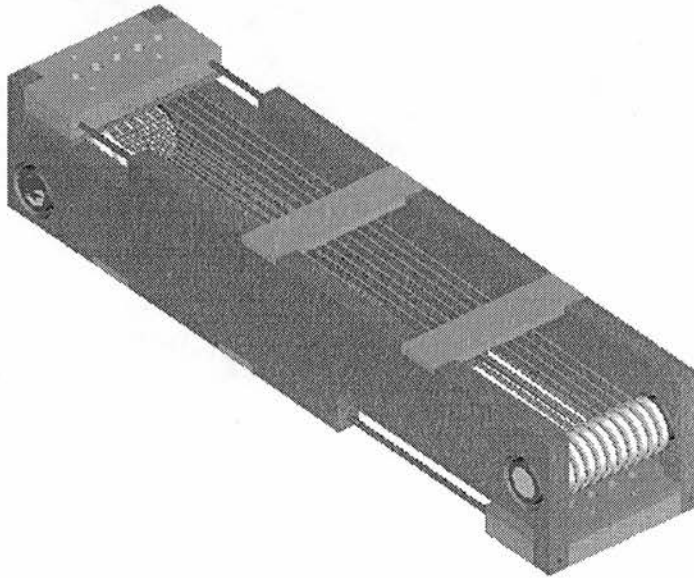


Figure 5.11: 3D view of the first prototype.

Therefore, the process of preparing and mounting the wires had to be re-evaluated. Each step was analysed and different solutions were examined.

5.8.2 - The Second Prototype

The “re-design phase” led to a detailed strategy aiming to achieve a reliable actuator.

It was decided that nine lengths of wire 263.5 mm long each were to be used instead of one single length as before. This avoids the problems of looping the wires around pins at high temperatures. Two metallic plates were used to clamp the wires. Those plates and the anchors were made of “ground flat stock” steel to ensure that the surfaces are perfectly flat, smooth and parallel to each other. Thin copper sheets were placed between the wires and the plates/anchors to reduce the electrical contact resistance (figure 5.12). In the same way as before, it is necessary to loop the wires around pulleys so that the dimensions of the device are within the specifications.

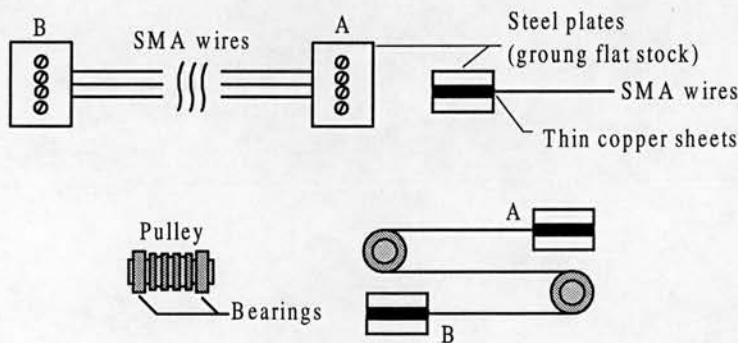


Figure 5.12: An improved clamping system.

The secondary anchor (associated with the overload protections) travels along two rods as shown in figure 5.9. The main anchor was assembled on a ball bearing slide to improve the smoothness of the movements (figure 5.13). Note that the position sensor (linear potentiometer) is mounted on the same platform as the slide and its cursor is attached to the main anchor.

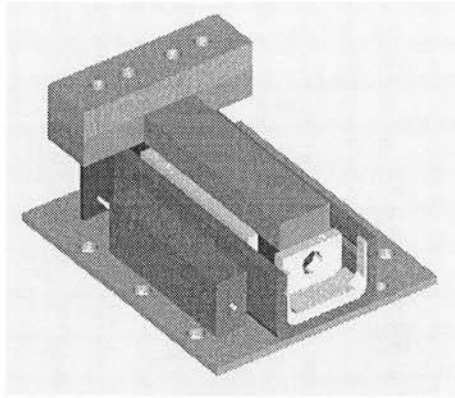


Figure 5.13: The arrangement of the main anchor, slide and position sensor.

To achieve the precision required, the clamping of the wires to the anchors must be done with the assistance of a jig. The anchors must be mounted on that jig exactly 263.5 mm apart (“face to face”). However, before clamping, each one of those nine lengths of wire was pre-trained under the intended working conditions. The training consisted of 200 cycles under constant tensile stress of 176 MPa (3.1 N for Flexinol 150HT) with the strain limited to 3%. In the same way as described earlier in this chapter, each cycle was performed by electrically heating the wires until full recovery was reached and letting them cool to room temperature (22 °C) while deformed by the tensile load.

To ensure that the SMA wires were parallel to each other and under the same stress and strain, the following strategy was adopted (refer to figure 5.14):

- Two auxiliary bases were built and fixed to a chamber. The top base was used to fix and guide one end of the wires, while the bottom base was used only as a guide.
- The jig (with the main anchors mounted on it) was placed in the chamber so that, with the jig hold vertical, the wires are parallel to each other and perpendicular to the anchors.
- The wires were mounted so that one end was fixed to the top base, passed “through” the anchors and through the guiding holes of the bottom base. A

load of 1N was crimped to each wire to keep them straight and under the same stress during the clamping process.

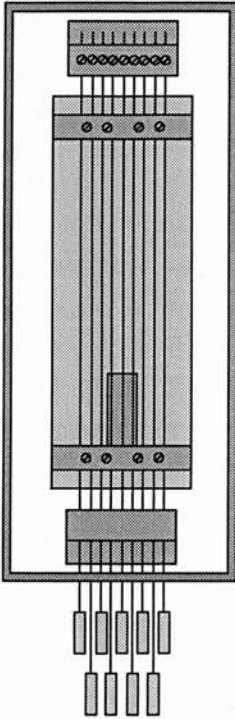


Figure 5.14: Diagram showing the mounting setup.

Once the wires were in place, a single thermal cycle was performed by circulating hot air through the chamber until the temperature was above $110\text{ }^{\circ}\text{C}$ ($A_f = 98\text{ }^{\circ}\text{C}$ for Flexinol 150HT) and then it was allowed to cool to room temperature. This ensured that the wires would move freely. To clamp the wires in their final position, the temperature was again raised above A_f . The top anchor (on the jig) was tightened first. Finally, the bottom anchor was tightened, the heating removed and the wires cut between the auxiliary bases and the anchors.

The performance of the nine wire arrangement was then assessed to establish how its performance differed from that of a single wire.

Some modifications were made to the mounting jig to allow the main anchor to move as the SMA wires contracted and deformed and the following tests were carried out (using the same setup as defined in figure 5.2 but substituting the single wire by the jig):

Training

Prior to the experiments the parallel arrangement was cycled 200 times under the desired operational conditions, as follows:

- Maximum stress: 176 MPa (per wire - provided by a hanging load of 28 N)
- Maximum strain: 3% (7.9 mm)
- Heating voltage: 4.4 VDC (for SMA wires 263.5 mm long)

Each cycle consisted of heating the wires until maximum recovery was reached and then letting them cool to room temperature (22 °C) while being deformed by the tensile load.

Response Time

A single cycle, as describe for training, was performed and the times of shape recovery and deformation were measured (figure 5.15).

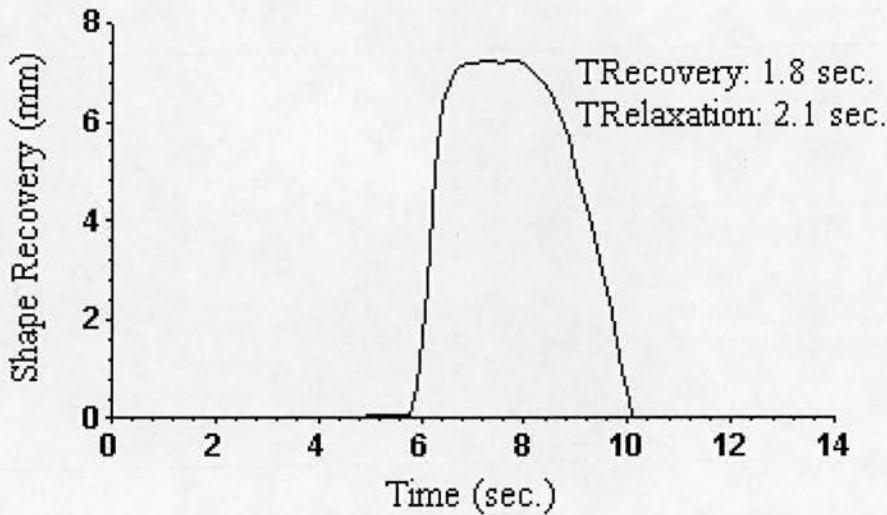


Figure 5.15: Response time for the parallel arrangement of 9 SMA wires Flexinol 150HT. Heating started at 5 sec. Cooling started at 8 sec. Amb. temp. = 22 °C. (responses measured from zero to 100% movement).

Transformation Temperature

To evaluate the hysteresis of the system, displacement was plotted while the voltage was slowly increased and decreased (figure 5.16). The wires were kept under a constant load of 28 N throughout the experiment.

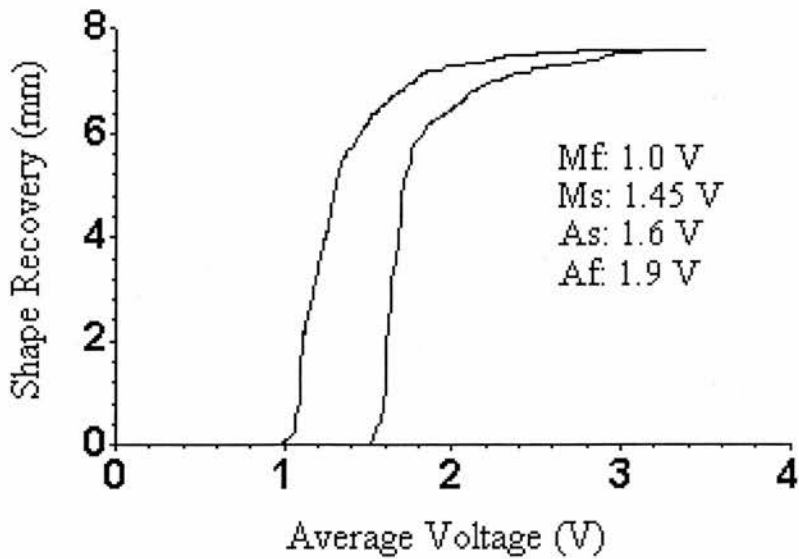


Figure 5.16: Hysteresis cycle for the parallel arrangement of 9 SMA wires Flexinol 150HT 263.5 mm long. Amb. temp. = 22 °C.

The experiments show that the parallel arrangement performs as expected. However, although the transformation values did not differ much from those obtained for a single wire, the time response of the parallel arrangement was slower. The main cause of this appears to be heat retention in the “anchors”.

To accommodate the new set of wires within the required dimensions, a second prototype actuator was built as shown in figure 5.17. A picture of the second prototype is shown in figure 5.18 (actual size). Note that the other components of the actuator, such as springs and overload switch, were assembled in the same way as explained for the first prototype.

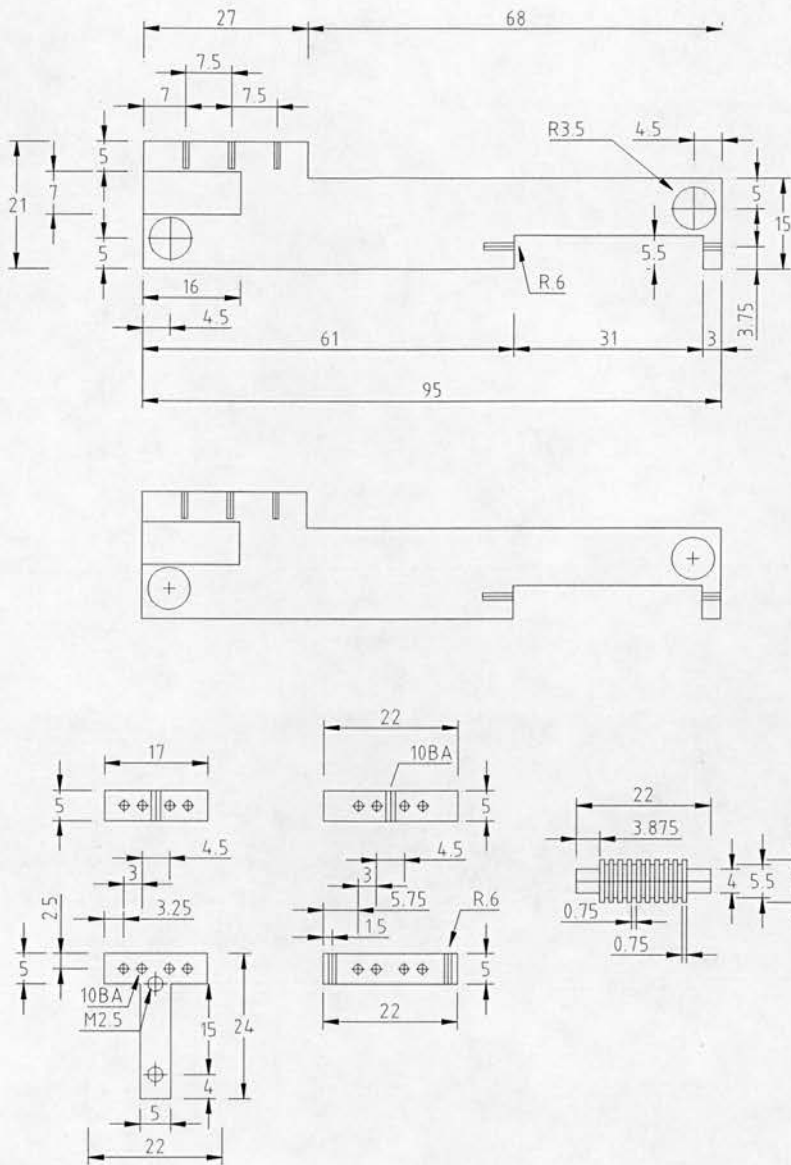


Figure 5.17: Dimensions of the main components of the SMA actuator (dimensions in millimetres).

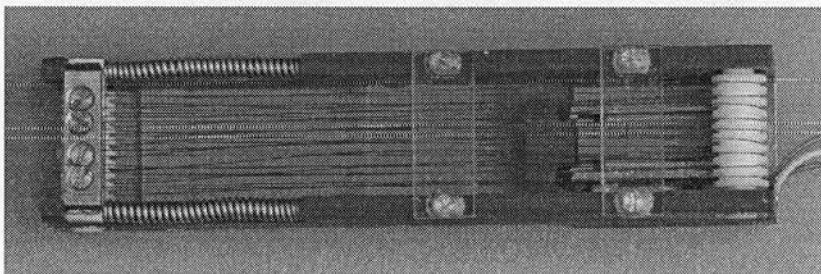


Figure 5.18: The SMA actuator (scale 1:1).

The main parameters of the SMA actuator are:

- Dimensions (see figure 5.17):
 - Minimum: 15 mm x 22 mm x 95 mm
 - Maximum: 21 mm x 22 mm x 95 mm
- Weight: 35 grams
- Maximum recovery force: 30 N
- Required deformation force: 10.35 N
- Relaxation/Deformation time: 2.1 seconds
- Contraction/Recovery time: 1.8 seconds

Since the SMA elements were now working around pulleys, and not straight, as before, it was important to train them under the new arrangement. The training was performed using exactly the same parameters as defined earlier for the parallel arrangement.

5.9 - Conclusion

This chapter described the design and construction of a SMA actuator as specified in chapter 4. The final actuator was constructed using nine SMA wires Flexinol 150HT mechanically and electrically in parallel. The prototype actuator using multiple wires showed similar transformation values to those of a single wire, but slower time responses. It is important to stress the fact that great care must be taken when designing and constructing SMA actuators. This is specially important when the device uses multiple wires in parallel, where minimal differences in stress and/or strain among the wires or even imprecision in the manufacture of the components can contribute to poor responses. A description of an electronic control system and more elaborated tests of the prototype are shown in chapter 6.

Chapter 6

A Control System for the SMA Actuator

6.1 - Introduction

Since the SMA transformation occurs as a continuous change over a temperature range, it is possible, by controlling the temperature of the alloy, to control the rate of recovery and deformation in a continuous fashion. As mentioned before, this technique allows us to achieve good resolution and the motion of the SMA elements is silent and smooth.

However, the design of a control system for SMA actuators can be a very complex task if the device requires precise control. Many factors contribute to this problem. For instance, one may argue that because SMAs generally have a large range of motion over a narrow range of temperature (see figure 6.1 (a)), precise control would be difficult to achieve. Nevertheless, there are ways of achieving a gradual temperature change. A common approach is to design the actuator so that the SMA elements work against a spring which increases the opposition stress as the elements recover their shape. By choosing the correct bias spring it is possible to modify the shape of the hysteresis cycle to suit the application. Figure 6.1(a) shows a typical hysteresis cycle when using a very low bias force. In contrast, figure 6.1(b) shows a much more gradual response when a stronger bias spring is in place.

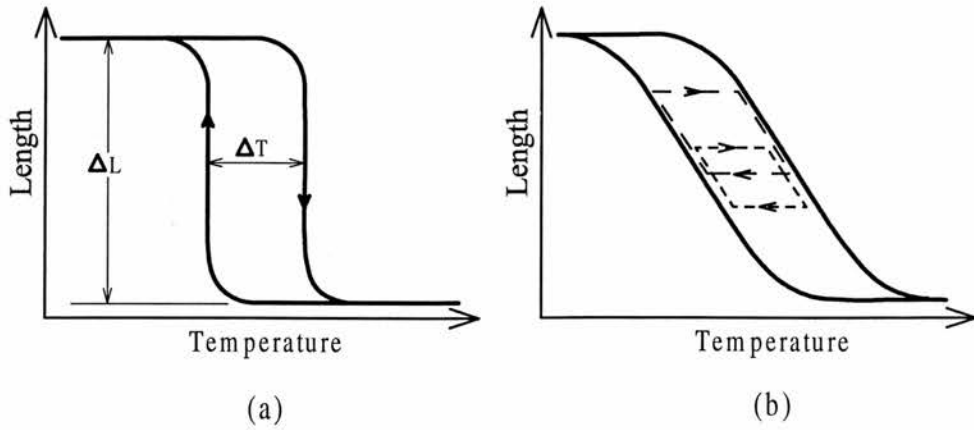


Figure 6.1: Changes in the shape of the hysteresis for different bias springs. (a) Very low bias force; (b) High bias force.

Another problem for the control system is the hysteresis gap. Suppose that one is moving the actuator by heating the SMA elements and then decides to change the direction of motion. As can be seen in figure 6.1(b), the SMA elements must cool down all the way through the hysteresis before any further cooling will cause any motion of the actuator. Although there are ways of handling this aspect of the control, they are normally not straightforward. As will be shown later, the actuator in question is to be used as an ON/OFF system, therefore the above problems will not have a serious effect on the performance of the device.

The problem of controlling SMA actuators was partially solved by Kuribayashi (1986a). However, his mathematical modelling resulted in a non-linear system. To simplify the problem he restricted the displacement to a range of a few tenths of a millimetre (he used a TiNi wire 100 mm long) so that a linear solution could be found. This linearization could only be applied to differential SMA actuators. The response of the system was later improved (Kuribayashi (1991)) by mounting a small temperature sensor on the SMA elements. Reynaerts and Brussel (1991) suggest a control system based on a Proportional-plus-Integral-plus-Derivative (PID) controller. The system used data acquired from experiments with the SMA actuator (hysteresis behaviour) to estimate the power needed to keep the actuator in a certain position. The PID control system was used to compensate for errors in the estimation.

Reynaerts and Brussel (1994) report position control accurate to 50 μm for their actuator by using such a technique.

The controllability of SMA actuators has already been established. However, the controller must be designed according to the specific needs of each application. The design of a control system for the actuator described in chapter 5 will be presented next.

6.2 The Requirements for the Operation of the Hand Mechanism

As explained in chapter 4, the operation of the hand is very simple, which should simplify the design of the control system. It was decided that, whatever the control system, it should be able to control the operation of the hand as follows:

- The hand is normally closed.
- An input signal (“open request”) will indicate that the hand must be fully opened.
- The SMA actuator must keep the hand open long enough for an object to be placed in between the fingers and the thumb. This can be achieved by heating the SMA wires until full recovery is reached, keeping them at temperatures above A_f for about 1 second and letting them cool to room temperature while being deformed by the bias spring. However, the wires will not be deformed immediately after the power is removed. They must cool down to M_s or through the hysteresis gap (figure 6.1 (b)). Preliminary experiments showed that this should keep the hand opened for about 2.5 seconds. If the user wants to keep the hand open for more than 2.5 seconds, he/she must continue sending “open requests”. One second after the last “open request” the wires in the actuator start cooling down (and therefore

will be deformed by the power spring, as explained in chapters 4 and 5), allowing the hand to close until an object is grasped or the hand is fully closed. Note that fine intermediate positioning is not necessary.

- The opening and closing time responses must be as defined in chapter 4.
- To release an object, the user should open the hand in the same way as explained above.
- If the SMA actuator is overloaded during the opening of the hand, the power to the SMA elements must be cut off.

6.3 - The Control System

A block diagram of the control system is shown in figure 6.2. The “open request” is sent to a timer circuit which generates the “desired output” signal (R), indicating that the hand must be fully opened for 2.5 seconds. The error (e) between R and the current position of the SMA actuator (V_{Sensor}) is adjusted by the compensator, resulting in the control variable U. A Pulse Width Modulator (PWM) is used to adjust the power sent to the SMA elements according to U. Since the current through the SMA elements is higher than the maximum output current of the PWM circuit, a power driver is used. The electronic diagrams and description of each block are given next.

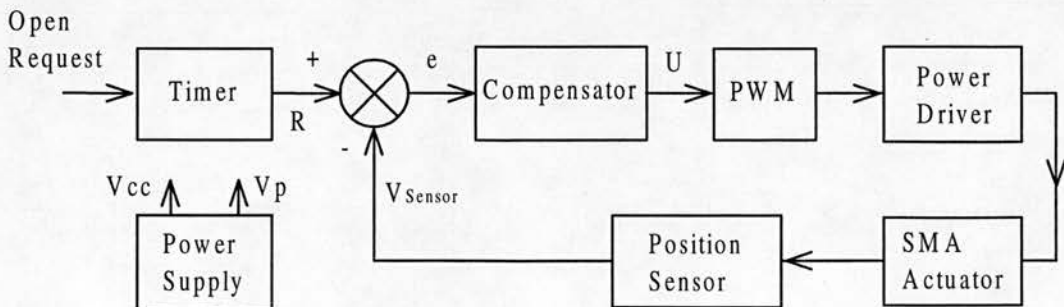


Figure 6.2: Block diagram of the control system.

6.3.1 - Timer

Figure 6.3 shows the electronic circuit of the timer unit. The “open request” (generated by a snap-action switch) is used to trigger a standard 555 timer operating as a monostable. The time constant was adjusted to produce a high output (+Vcc) for 3 seconds (1.8 seconds to heat the SMA elements and 1.2 seconds keeping them at temperatures above Af).

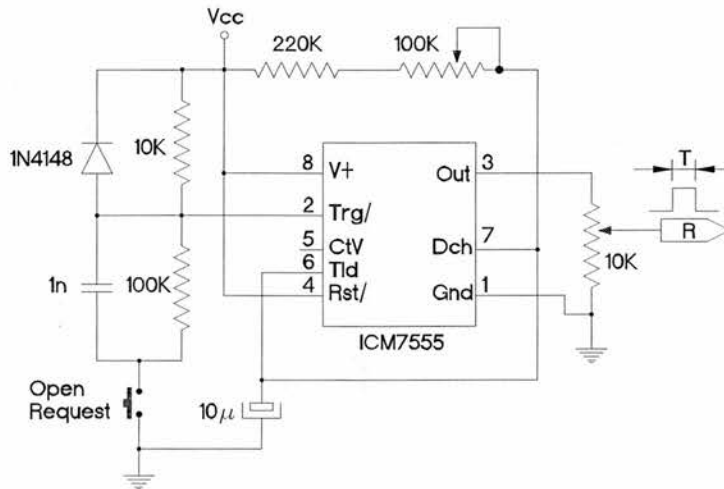


Figure 6.3: Timer circuit.

6.3.2 - Compensator

Since the specifications do not require fine control, it was decided to initiate the experiments using a simple proportional compensator as shown in figure 6.4. The circuit compensates the error (e) between the desired input (R) and the current position (V_{Sensor}), by adjusting the control variable U . The gain of the compensator (K_p) can be adjusted between 1 and 10 to provide full power to the SMA elements when the error is maximum.

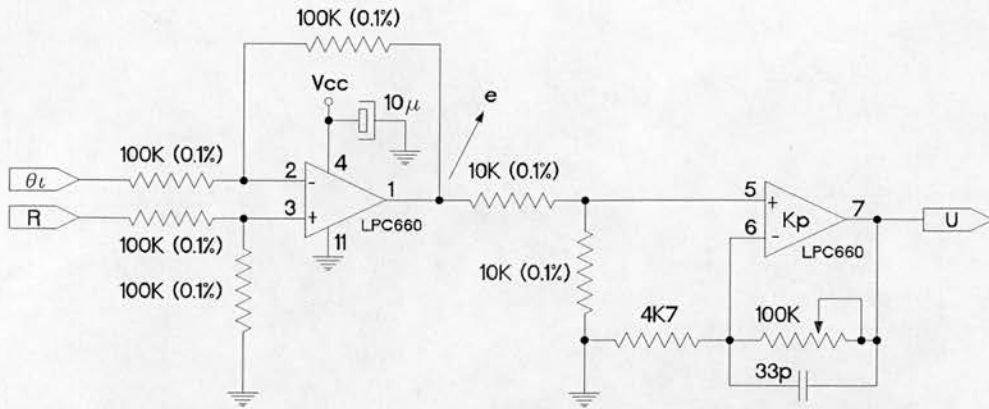


Figure 6.4: Electronic circuit of the proportional compensator.

6.3.3 - Pulse Width Modulator

In most designs of electrically activated SMA actuators, the operation is controlled by varying the pulse width (duty ratio) of the voltage supplied to the SMA elements. The compensator was designed to control the duty cycle of the PWM output wave as a function of the control voltage U . To predict the effects of such a strategy it is important to know the relationship between U and the average voltage applied to the SMA elements. Figure 6.5 shows a more detailed block diagram of the control system.

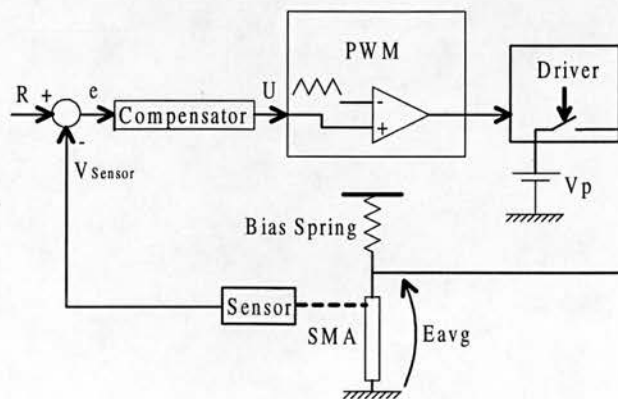


Figure 6.5: Block diagram of the SMA controller.

The output of the compensator is compared with a triangular wave resulting in a pulsed wave of constant amplitude but variable duty cycle. Figure 6.6 shows the time response of the control variable and other signals involved. The diagrams will be used to obtain theoretically the relationship between U and E_{avg} , as follows:

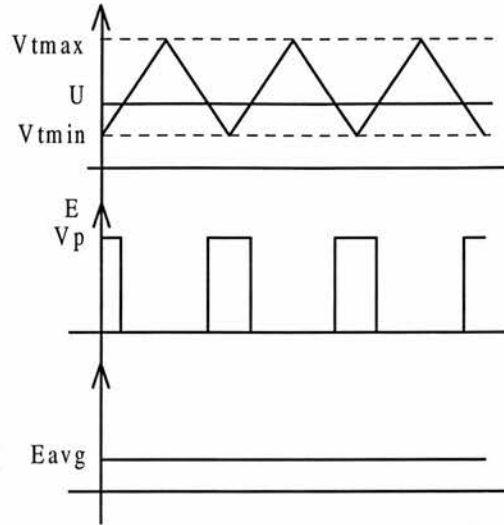


Figure 6.6: Time response of the PWM signals and the average voltage supplied to the SMA elements (E_{avg}).

The average voltage supplied to the SMA elements is given by:

$$E_{avg} = V_p * K \quad [1]$$

Where K represents the ratio between the time “E” is “on” (T_e) and the total period of the triangular wave (T).

From figure 6.7:

$$K = \frac{T_e'}{T'} \quad [2]$$

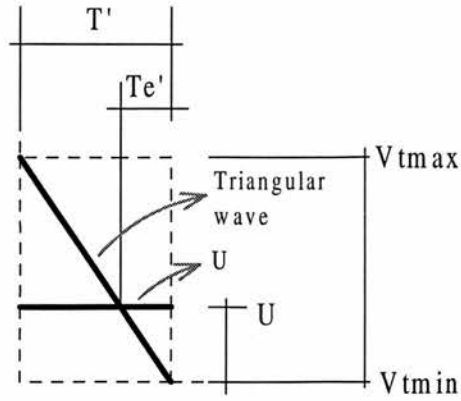


Figure 6.7: Zooming the inputs of the PWM showing only half of the triangular wave period.

Using the relationship between the triangles in figure 6.7:

$$K = \frac{Te'}{T} = \frac{U - V_{t \min}}{V_{t \max} - V_{t \min}} \quad [3]$$

Hence:

$$E_{avg} = V_p * \left(\frac{U - V_{t \min}}{V_{t \max} - V_{t \min}} \right) \quad [4]$$

Equation [4] is a linear relationship between E_{avg} and U , showing that by varying U from $V_{t \min}$ to $V_{t \max}$ the average voltage supplied to the SMA wires will vary from 0 to V_p . Since V_p , $V_{t \min}$ and $V_{t \max}$ are known and constant, by controlling U it is possible to control E_{avg} linearly. Figure 6.8 shows the electronic circuit of the PWM.

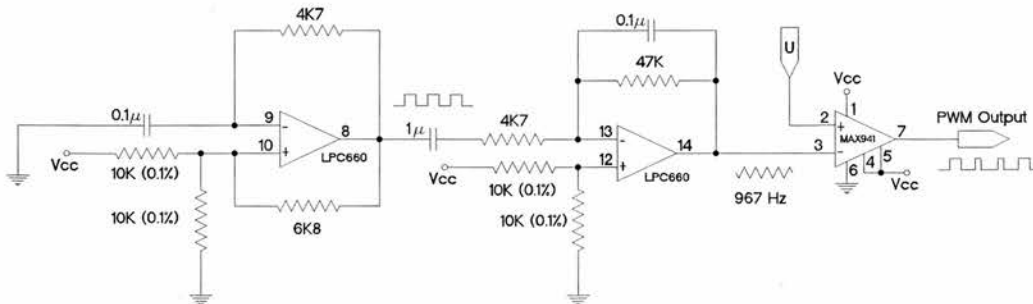


Figure 6.8: PWM circuit.

6.3.4 - Power Driver

A power driver (figure 6.9) based on a MOSFET is used to switch the current to the SMA elements. The specifications of the MOSFET are as follows:

- MOSFET Channel N: RFD1N14N05L with gate input optimised for low voltages (5 VDC)
- V_{DS} : 50 VDC
- $R_{DS(on)}$: 0.1Ω
- I_D : 14 A (@ 25 °C)
- t_r/t_f : 24/16 nSec.
- I_{DM} Pulsed: 35 A
- P_D : 40 W

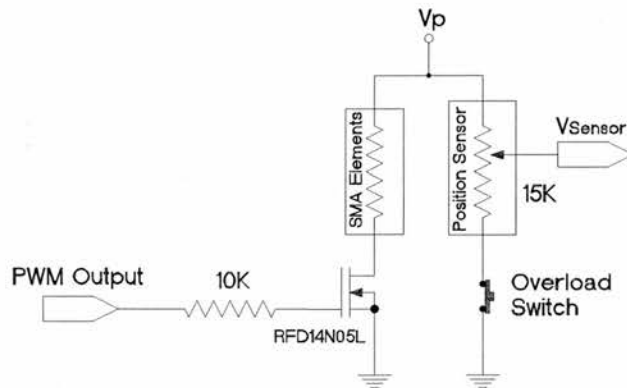


Figure 6.9: Power driver.

The diagram also shows the overload switch (normally closed) connected to the position sensor. For normal operation, the maximum value of R (refer to figure 6.3) must be adjusted to be the same as V_{Sensor} when the hand is fully open. Also, the maximum value of V_{Sensor} (with the hand fully opened) must be adjusted (during the mounting of the sensor) to be smaller than V_p . Therefore if the hand is closed and the user wants to open it (by sending an “open request”), a positive error signal is

generated and the compensator adjusts the power sent to the SMA elements proportionally to that error. However, if an overload occurs, the switch will open and V_{Sensor} will be equal to V_p . This would generate a negative error. Since, the electronic circuit is powered by a single supply voltage, the outputs are limited to 0 VDC and +Vcc, meaning that any error below or equal to zero, results in zero. Therefore, in an overload situation, the error is zero and no power is sent to the SMA elements. Also, by placing the overload switch in the control system, as shown, it was possible to use a very small, low current switch.

6.4 - Experiments

To evaluate the performance of the system a set of experiments was performed and the results are shown next.

The tests were performed according to the following settings:

- The timer was removed and the input R was provided by a signal generator
- Voltage supply to the electronic circuit (Vcc): 5 VDC
- Maximum voltage supplied to the SMA elements (V_p): 5 VDC
- PWM triangular wave oscillator settings:
 - $V_{\text{tmax}} = 4 \text{ V}$
 - $V_{\text{tmin}} = 1.22 \text{ V}$
 - Frequency = 967 Hz
- Proportional gain (K_p) = 8 (adjusted experimentally)
- The tests were performed at a constant tensile stress of 176 MPa per SMA wire (28 N total force) and a maximum strain of 3% (7.9 mm)
- Ambient temperature = 22 °C

Figure 6.10 shows the block diagram of the testing setup.

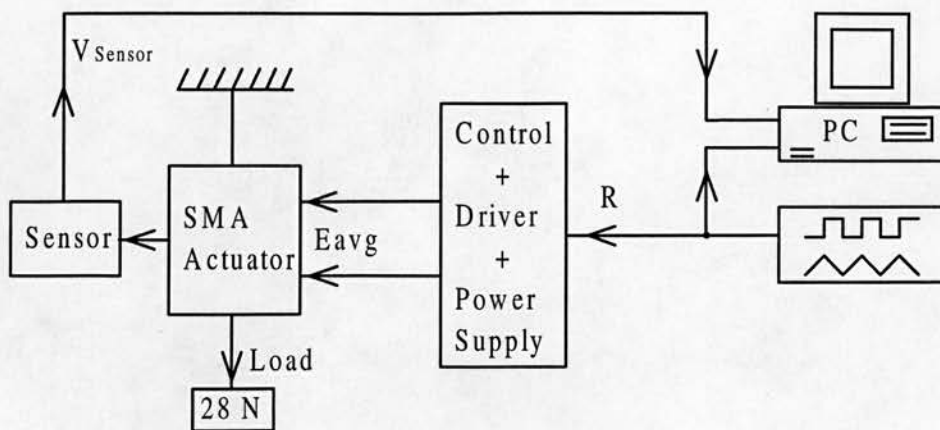


Figure 6.10: Testing setup used in the experiments with the control system.

6.4.1 - Follow-up Response for Triangular and Sine Wave Inputs

The experimental results for triangular and sine wave inputs of 0.1 Hz are shown in figures 6.11 and 6.12 respectively. The follow-up properties were shown to be satisfactory, indicating that position control of the actuator is possible.

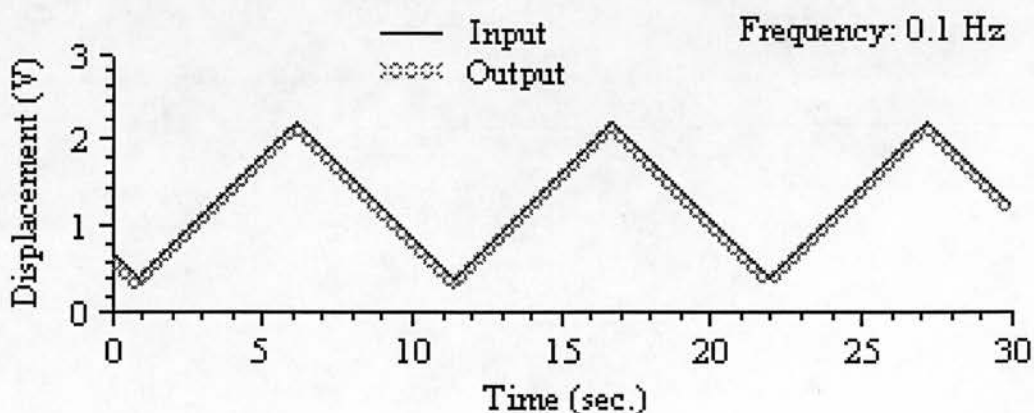


Figure 6.11: Follow-up response for a triangular wave.

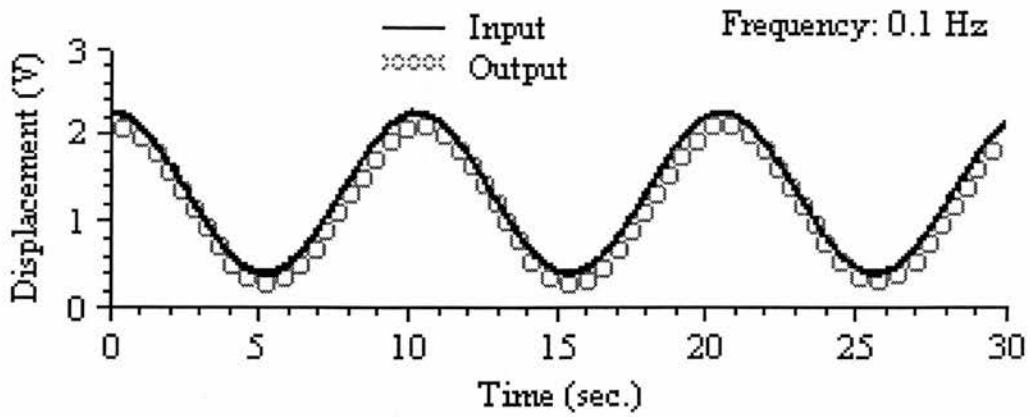


Figure 6.12: Follow-up response for a sine wave of 0.1 Hz.

6.4.2 - Step Response

To evaluate the properties for the ON-OFF control, a step input was used and the responses are shown in figure 6.13.

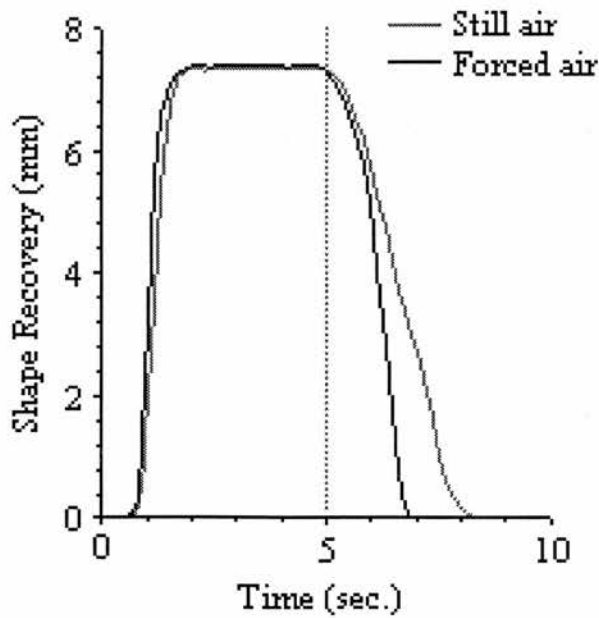


Figure 6.13: Step response. Heating started at 0 sec. and cooling started at 5 sec.

Response Time:

- Still air:
 - TRecovery: 1.7 sec.
 - TRelaxation: 3.2 sec.
- Forced air (approx. 2.5 m/s):
 - TRecovery: 1.7 sec.
 - TRelaxation: 1.7 sec.

As shown in the figure above, the relaxation time of the SMA elements was greatly increased when the elements were assembled in the actuator compared with the wires alone (see chapter 5). On investigation, it was found that the main cause is heat retention in the ceramic rollers which slows down the cooling of the SMA elements. To solve this problem and improve the response on cooling it was decided to use a small fan (15 mm diameter) powered by a mini-motor (10 mm diameter) to circulate air through the SMA elements and around the ceramic rollers (the fan operated only during the cooling phase). Figure 6.13 shows that the time response on cooling was considerably improved by using this approach.

6.5 - Conclusion

A control system was designed for the SMA actuator. Although the controller was designed to be as simple as possible, the experiments show that the performance is satisfactory for the intended application. However, to achieve the required time response the use of forced air was necessary for cooling the SMA elements.

During the tests described in chapters 5 and 6 the actuator was cycled 300 times. A life cycling test was not carried out on the completed actuator. However, it should be noted that the wires in the actuator are mostly under the same stress, strain and temperature variations as in the life cycling test for the wires alone (chapter 5). On

the bent sections around the ceramic rollers, the large diameter of the pulleys ensures that the strain due to bending is limited to around 3%.

Chapter 7 describes the construction of the hand prototype and other experiments aiming to investigate the performance of the final device.

Chapter 7

Construction and Evaluation of the Prototype

7.1 - Introduction

This chapter describes the construction of a hand mechanism according to the specifications defined in chapter 4. A support structure was built and the hand mechanism and the actuating system were attached to it. The performance of the prototype was investigated through laboratory experiments.

7.2 - The Hand Mechanism

The hand mechanism was constructed to the dimensions specified in chapter 4. The fingers and thumb were made of a metal “skeleton” surrounded by resin based filler to shape them as desired. Figure 7.1 shows 3D views of the various components of the hand mechanism and figure 7.2 shows a picture of the assembled mechanism (actual size).

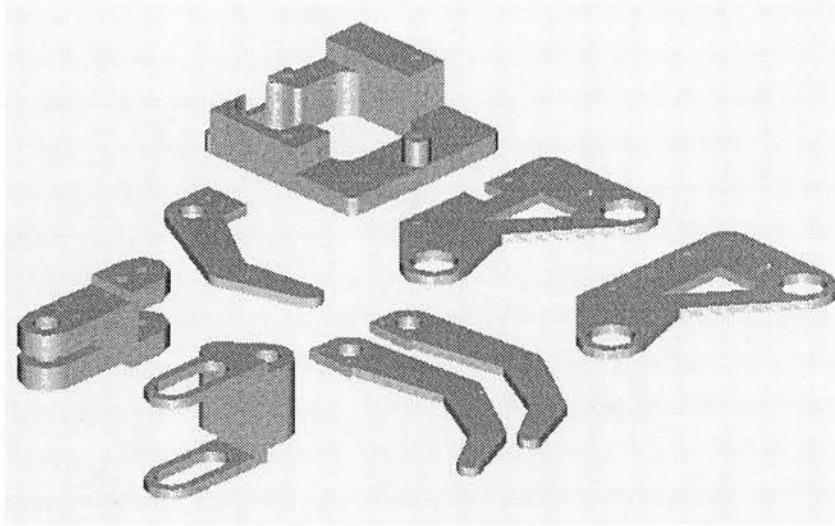


Figure 7.1: The components of the hand mechanism.

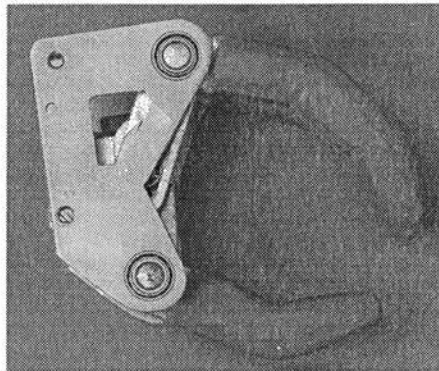


Figure 7.2: The hand mechanism (scale 1:1).

7.3 - Assembly of Prototype

A framework, representing the forearm of an upper limb prosthesis, was constructed, based on the dimensions defined in chapter 4, and the SMA actuator, “power spring” and hand mechanism were mounted as shown in figure 7.3 (actual size).

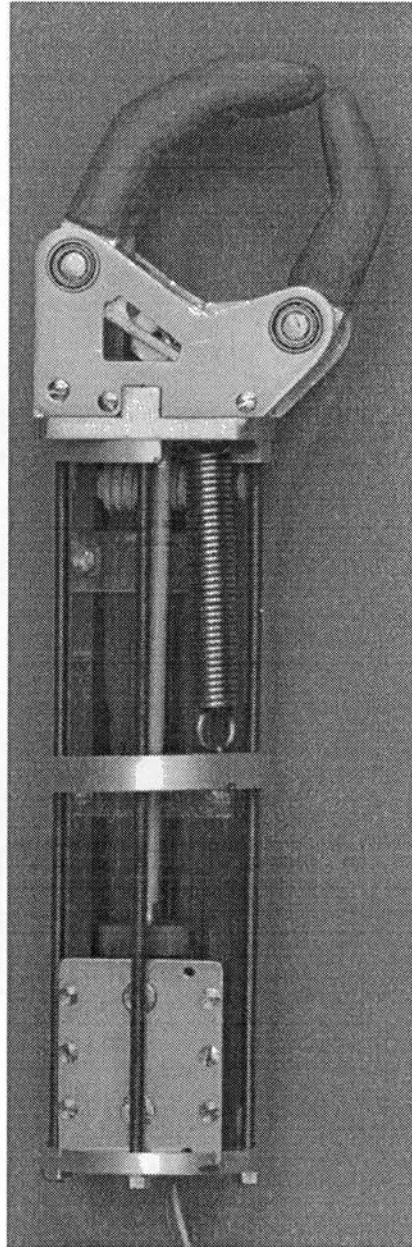


Figure 7.3: The hand prototype (scale 1:1).

The total weight of the device, as shown in figure 7.3, is 102 grams, compared with 148 grams for the Steeper Scamp Hand and 130 grams for the VV 0-3 electric hand produced by VASI (see appendix B). With the use of lighter materials, such as carbon fibre, the weight could be further reduced to about 60 grams comparing very favourably with standard commercial artificial hands for the age group in question.

7.4 - Laboratory Experiments

To investigate the performance of the prototype the following set of experiments was performed:

Time Response and Opening Width

In order to evaluate the time response, the movements of the hand were observed for a single open-close cycle at different ambient temperatures, as shown in figure 7.4.

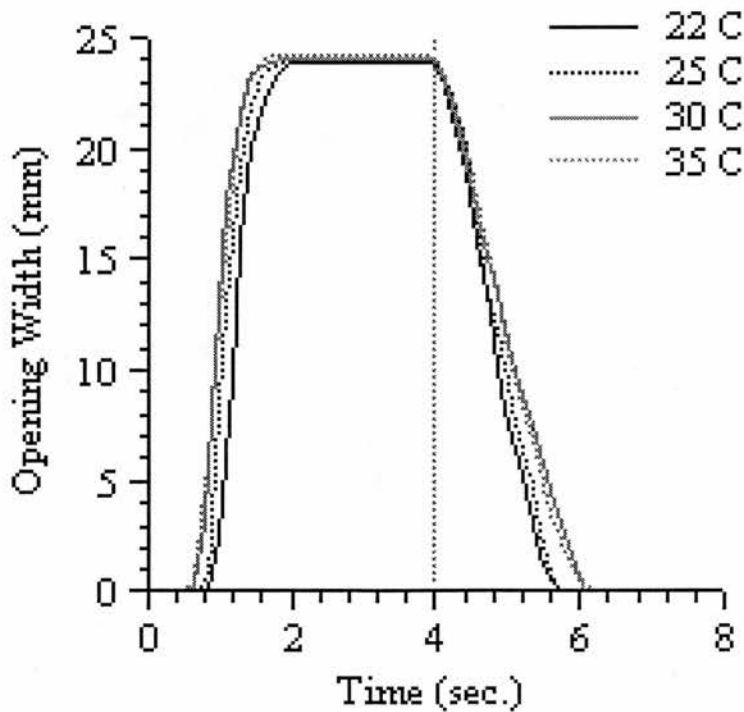


Figure 7.4: Response of the prototype for opening and closing the hand at various ambient temperatures using forced air during the cooling stage. Heating started at 0 sec. Cooling started at 4 sec.

Time Responses:

- 22 °C:
 - T(open): 1.7 sec.
 - T(close): 1.7 sec.
- 25 °C:
 - T(open): 1.7 sec.
 - T(close): 1.7 sec.
- 30 °C:
 - T(open): 1.6 sec.
 - T(close): 2.1 sec.
- 35 °C:
 - T(open): 1.6 sec.
 - T(close): 2.2 sec.

As expected, a small decrease is observed in the opening time and a small increase is seen in the closing time as the ambient temperature increases. Figure 7.4 also shows that the time responses for opening and closing are slightly higher than specified in chapter 4. If necessary, this can easily be improved by increasing the heating current of the SMA elements (for faster shape recovery) and by increasing the air flow during the deformation of the elements.

Forces

Figure 7.5 shows the grip force provided by the prototype along its range of motion.

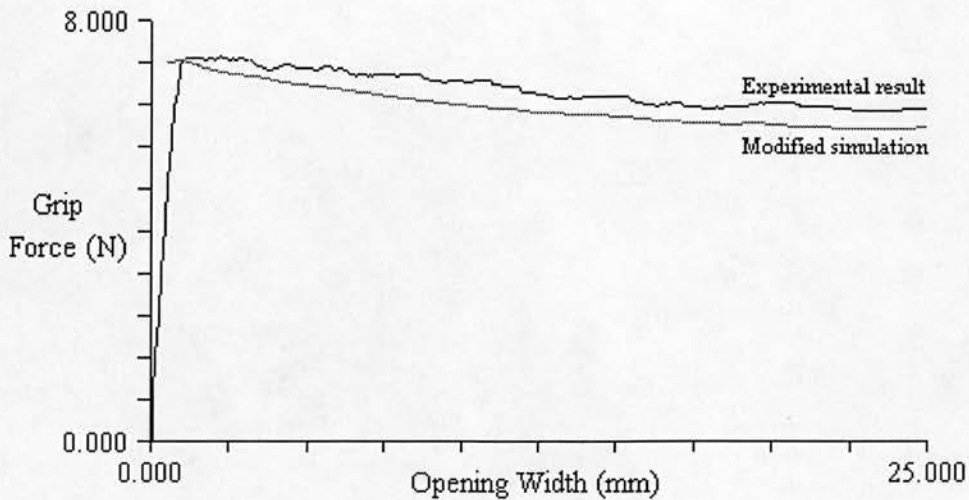


Figure 7.5: Grip forces of the prototype and the results obtained by the simulator program using “FClosing” = 0.

The experiment shows that the grip forces are much higher than those predicted by the simulation in chapter 4 (3 N). The reason for that is the two-way effect shown by the Flexinol SMA wires, as described in chapter 5. As explained earlier, those wires will revert spontaneously to some “deformed shape” as the temperature drops below M_f . For the hand mechanism in question, this means that during the closing of the hand the spring does not continue to act against the full deformation force (11 N) defined in the simulation. By running the simulator program, using the same parameters but setting “F Closing” to zero, a similar curve to the above is obtained (see figure 7.5). However, it is important to stress that this “gain” in grip force may vary as the number of cycles increases. The experiments in chapter 5 show that, in the worst case scenario, the deformation force would stabilise at about 1.15 N per wire (at 3% strain) while the grip forces shown in figure 7.5 would decrease and stabilise at a minimum of 3 N, in agreement with the simulation of the hand mechanism.

Power Consumption and Energy Efficiency of the Actuator

The power to the SMA actuator is provided by a power supply and is given by:

$$P = V * i \quad [W]$$

Where “V” (Volts) is the voltage and “i” (Amps) is the current applied to the SMA elements.

Note that, for a constant applied voltage, the current circulating through the SMA wires changes in a very non-linear fashion as they undergo changes in shape. A further complication in this particular project is that the current is pulsed (controlled by a PWM). To simplify the problem, it was decided to measure the maximum and minimum average currents supplied to the SMA actuator and use their mean to calculate the average power sent to the actuator during the shape recovery of the SMA elements.

It was found that during the actuation of the device the average current varies from 2.9 A and 3.2 A. Hence, the total input power during shape recovery can be calculated as follows:

$$P_{SMA(Input)} = 5 * 3.05 = 15.25 [W]$$

Since the actuator delivers 28 N over a distance of 7.24 mm during 1.7 seconds (recovery time) the output power of the device is:

$$P_{SMA(Output)} = \frac{28 * 7.24 * 10^{-3}}{1.7} = 0.12 [W]$$

Therefore, the efficiency of the SMA actuator during the shape recovery phase is about 0.8 %.

7.5 - Evaluation of the Prototype

The construction of the prototype followed a simple path since the aim of this work is not to generate a commercial device, but to investigate if it is possible to apply “SMA technology” to design the joint actuator. With this in mind, some major conclusions can be drawn from the evaluation of the characteristics of the prototype, as follows:

- The use of a SMA actuator requires great care regarding the design and construction of the hand mechanism, so that the forces generated by the actuator can be used as efficiently as possible. In general, it is important to find the best “geometry” for the components of the “prosthesis” and to build them as precisely as possible.
- The prototype weighs 102 grams without a cosmetic glove, which compares favourably with similar commercial prostheses such as the Steeper Scamp Hand (148 grams) and the VV 0-3 electric hand produced by VASI (130 grams). Through minor changes in the design such as using better manufacturing processes and employing lighter materials, such as carbon fibre, it is expected that the final weight of the device can be reduced to about 60 grams.
- The experiments showed that, overall, the device fulfils the initial expectations. A major concern when analysing those results is the low efficiency of the system. However, in practical terms, the battery energy required for each opening and closing cycle of the hand is most significant as it determines how many cycles can be achieved for each charge of the battery. Since the prototype requires about 26 J of electrical energy to open the hand ($15.25 \text{ W} * 1.7 \text{ sec.} = 26 \text{ J}$), a 750 mAh 6 V battery would provide over 600 cycles for each charge.
- Finally, the most remarkable feature of the device is undoubtedly the smooth and silent operation of the SMA actuated hand.

7.6 - Conclusion

The construction of the prototype and an investigation of its features were given. The device performed within the expectations in spite of the low energy efficiency of the SMA actuator. The next chapter presents a general discussion of this work and the final conclusions are given along with suggestions of future extensions of this work.

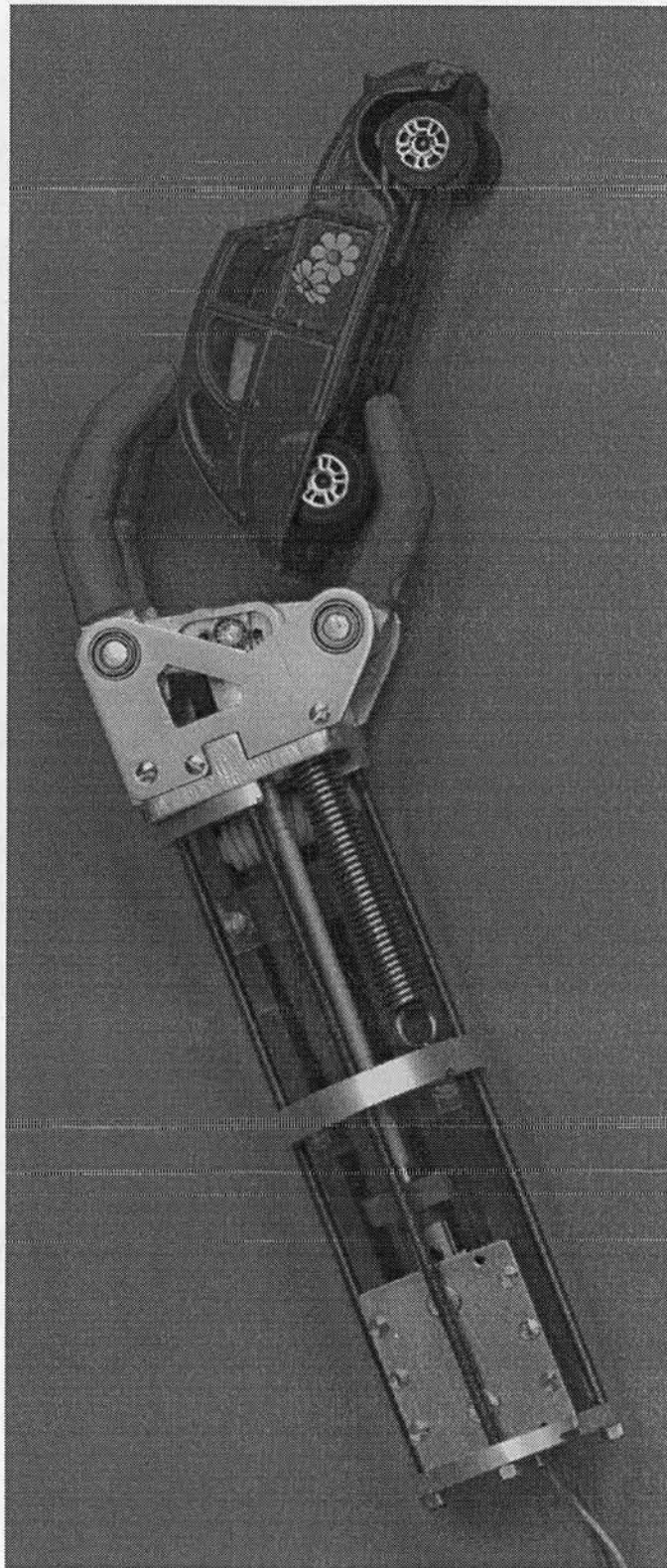


Figure 7.6: The basic profile assumed by the prototype when holding an object (scale 1:1).

Chapter 8

General Conclusions

and

The Way Ahead

8.1 - Introduction

The design of artificial limbs can be a very complex and sometimes frustrating task. Perfectly mimicking natural limbs is almost impossible with current technology. The obstacles to overcome are sometimes too great, which normally leaves the limb user with basically two options: either he/she accepts his/her disability as it is or uses an artificial device that very often looks unnatural and has a poor performance when compared to a sound limb.

This research did not aim to develop a perfect solution to the above problem, nor to seek for the best possible solution by using the current technology. The main aim was to investigate new possibilities to assist the development of future prostheses. The research was based on the use of shape memory alloys to develop joint actuators for small hand prostheses. A description of the requirements of such prostheses and of the SMA actuator was given. Methods for designing and building the hand mechanism and the SMA actuator were also described in detail.

This chapter presents the general conclusions that can be drawn from the research and suggests possible future works that can be undertaken to complement this project.

8.2 - Summary and General Conclusions

The aims outlined in chapter one of this thesis have been achieved and the results are summarised below.

A general introduction to the problems related to artificial limbs and the basic mechanism of how skeletal and “SMA” muscles work were described in chapter 1. A brief description of the similarities between the behaviour of SMA devices and skeletal muscles was also presented.

A review of the field of prosthetics, the “state of the art” and various aspects related to prosthetics usage was given in chapter 2. The important conclusion is that the current state of the art still does not allow the development of artificial limbs which are fully accepted by the majority of users. A number of variables must be considered, but it was found that aspects such as the lack of sensorial feedback, poor cosmetic appearance, unnatural and often noisy motion (particularly for externally powered upper limb prostheses), weight and uncomfortable fitting of the prosthesis are among the major reasons for low usage or even complete rejection of prostheses.

In chapter 3 the shape memory phenomenon was reviewed. The basic mechanism behind this effect was presented. The possibilities of using shape memory devices in various areas was described along with the main considerations involved when doing so. It was shown that, although SMA, at first, appears as a “magic material” with a

number of advantages, its use also introduces some problems¹ which can make SMAs very difficult or even impossible to use in many applications. It is therefore important to investigate in detail the intended application and consider all possible solutions.

The main features of SMA elements which are particularly interesting for the development of actuators for small joint mechanisms are:

- SMA can allow the development of very light, small and yet very powerful actuating devices.
- The motion of SMA devices is absolutely silent and can be controlled to look very much like the contraction of a skeletal muscle.

Chapter 4 described the aspects related to the design of an artificial hand to be used as part of an above elbow prosthesis for young children. To assist the design, a mathematical model of a chosen hand mechanism was developed and incorporated into a computer program to simulate the movements and forces within the hand. The program proved to be a very useful tool in the design of the hand mechanism and in the specification of the SMA actuator required for powering the joints of that hand. It was also shown that the use of the SMA actuator does not require any major modifications of a standard hand mechanism, provided that it can accommodate the linear motion provided by the SMA actuator.

Chapter 5 described the aspects involved in the design and construction of the SMA actuator. The first step was to choose, from among the various shape memory materials, which one is the most suitable for the application. A special NiTi SMA wire (Flexinol 150HT) produced by Dynalloy Inc. (USA) was chosen as the basic SMA element. The characteristics of the wire were assessed by a number of

¹ Most notably the low frequency response (if no active cooling system is used) and low energy efficiency.

experiments to ensure that it was suitable for the application. Because a single wire Flexinol 150HT cannot deliver the required force, it was necessary to use 9 wires mechanically in parallel. It was shown that many important variables must be carefully analysed when designing SMA actuators, specially when they involve the use of multiple wires in parallel. Particular problems were discussed along with the adopted solutions. A prototype was then designed and built and its performance was assessed by a set of experiments. The performance of the SMA actuator was considered satisfactory for the intended application.

The electronic system required to control the movements of the SMA actuator is described in chapter 6. After studying the operation of commercially available artificial hands for young children it was decided that the operation of the hand should be similar to that of an ON-OFF system. In other words, there are basically two static positions for the hand: fully opened or closed (including touching an object placed in between the fingers and thumb). A simple proportional control system was developed to adjust the heating rate of the SMA elements and a mechanism to avoid overloading of the SMA elements was incorporated in the design. Initial experiments showed that the time response of the actuator in still air was not satisfactory and that the use of forced air was necessary to reduce the time required for cooling the SMA elements.

Finally, the hand mechanism was built and mounted to a framework, as described in chapter 7. The SMA actuator and the main spring (for closing the hand and grasping objects) were mounted on the frame and attached to the hand mechanism as described in chapter 4. The performance of the prototype was then investigated through experiments. The results show that the movements and forces achieved by the prototype are satisfactory. As expected, the efficiency of the actuator during the shape recovery of the SMA elements was very low (0.8%). However, it was shown that even with this low efficiency it is possible to achieve a high number of open/close cycles per charge of a normal battery pack. The most remarkable feature

of the device was the absolutely silent and smooth motion provided by the SMA actuator.

The approach adopted in the design of the hand mechanism and construction of the prototype was relatively simple since it was not intended to produce a final commercial prosthesis. No consideration was given to the problems of cosmetic appearance, refinement of the actuator and other aspects such as the miniaturisation of the electronic system and a suitable power supply. However, the results of this work are encouraging. Given careful analysis of the problem and precise design and construction, it is possible to use SMA elements to solve particular problems in prosthetics such as those found when working with externally powered upper limb prostheses for young children. Other possibilities of using SMA, not mentioned in the main body of this work are described in a paper presented at "The Second International Conference on Shape Memory and Superelastic Technologies" (Appendix C).

Possibly the main achievement of this work was the complete elimination of noise during the operation of the hand mechanism. Silence is a highly desirable feature in prosthetic devices, usually difficult to achieve with other actuators. The grip forces and the weight of the prototype also compare favourably with some commercial artificial hands for young children. However, the device is, as yet, largely untested and some future work towards the improvement of the prototype followed by clinical tests would be required before any fair comparison may be made with other systems.

8.3 - Future Work

This thesis has been concerned with the use of SMA elements to provide alternative solutions to known problems in prosthetics. The approach adopted was to investigate what type of application could benefit most from the advantages of SMA devices. A SMA actuator was designed to provide power for the joint mechanism of an artificial

hand to be used as part of an above elbow prosthesis for young children. The use of different materials to construct the prototype could contribute to decreasing the overall weight of the device and a study of different electronic control systems might show possible ways of improving the performance and the efficiency of the prototype. No consideration was given on how the prototype can best be controlled by a child and a detailed investigation of possible mechanisms would be appropriate. Finally, although the device has proved robust in our limited laboratory tests, clinical tests (possibly after the improvements suggested above and a proper life time test) will certainly reveal new challenges.

Appendix A

Main Code of the Computer Program to Simulate the Operation of the Hand Mechanism

This appendix shows only the main part of the software. Secondary items such as procedures for file manipulation and control of the components of the user's interface are omitted.

```
{*****  
                                     Main unit  
***** }  
  
unit hand;  
  
{Paint form on the screen}  
procedure THandForm.FormPaint(Sender: TObject);  
begin  
  clearBMP(sender);  
  CurrentMode := pmNotXor;  
  drawhand(sender);  
  calculateForces(sender);  
  DrawForceVectors(Sender);  
end;
```

```

{Drawing the hand mechanism}
procedure THandForm.drawhand(Sender: TObject);
begin
  image.canvas.Pen.Mode := CurrentMode;
  ConnectPoints(HandColor);
  DrawPoint(PtA);           {Draw the main points of the hand mechanism}
  DrawPoint(PtB);
  DrawPoint(PtC);
  DrawPoint(PtQ);
  DrawPoint(PtQ0);
  DrawPoint(PtR);
  DrawPoint(PtD);
end;

```

```

{Draw a circle on canvas}
procedure THandForm.DrawPoint(MyPoint: TPoint);
begin
  image.canvas.pen.color := PointColor; {Set color}
  image.canvas.Ellipse(MyPoint.x - 2, MyPoint.y - 2,
                      MyPoint.x + 2, MyPoint.y + 2);
end;

```

```

{Draw lines connecting the main points of the hand mechanism}
Procedure THandForm.ConnectPoints(color:smallint);
begin
  with image.canvas do
  begin
    Pen.Color := HandColor; {Set color}
    moveto(PtC.X,PtC.Y);
    lineto(PtA.X,PtA.Y);
    lineto(PtQ0.X,PtQ0.Y);

```

```

moveto(ptA.X,PtA.Y);
pen.mode:= pmCopy;
lineto(PtQ.X,PtQ.Y);
lineto(ptR.X,PtR.Y);
lineto(PtB.X,PtB.Y);
lineto(PtD.X,PtD.Y);
end;
end;

```

```

{ ****
                                     MOTION
**** }

```

```

{ Calculate the coordinates of the main points of the hand mechanism }

```

```

Procedure THandForm.CalculateAllCoordinates(sender: TObject);

```

```

begin

```

```

    CalculatePtB(sender);    //The sequency is important

```

```

    CalculatePtA(sender);

```

```

    CalculatePtC(sender);

```

```

    CalculatePtQ(sender);

```

```

    CalculatePtR(sender);

```

```

    CalculatePtQ0(Sender);

```

```

    CalculatePtD(sender);

```

```

    CalculateHandOpening(sender);

```

```

end;

```

```

Procedure THandForm.CalculatePtA(sender: TObject);

```

```

begin

```

```

    PtA := Point(PtB.X - JointsOffset, PtB.Y + HandHeight);

```

```

end;

```



```
Procedure THandForm.CalculatePtB(sender: TObject);
```

```
begin
```

```
    PtB := Point(100 + JointsOffset, 50);
```

```
end;
```

```
Procedure THandForm.CalculatePtC(sender: TObject);
```

```
begin
```

```
    PtC := Point(round(PtA.x + ThumbLength*cos(DegtoRad(theta1+theta2))),  
                round(PtA.y - ThumbLength*sin(DegtoRad(theta1+theta2))));
```

```
end;
```

```
Procedure THandForm.CalculatePtQ(sender: TObject);
```

```
begin
```

```
    PtQ := Point(round(PtA.x + QLever*cos(DegtoRad(theta1))),  
                round(PtA.y - QLever*sin(DegtoRad(theta1))));
```

```
end;
```

```
Procedure THandForm.CalculatePtR(sender: TObject);
```

```
begin
```

```
    PtR_float[1] := PtA.x + RLever*cos(DegtoRad(theta1));
```

```
    PtR_float[2] := PtA.y - RLever*sin(DegtoRad(theta1));
```

```
    PtR := Point(round(PtR_float[1]), round(PtR_float[2]));
```

```
end;
```

```
Procedure THandForm.CalculatePtQ0(sender: TObject);
```

```
begin
```

```
    PtQ0 := Point(round(PtA.x + Q0Lever*cos(DegtoRad(theta1+theta0))),  
                round(PtA.y - Q0Lever*sin(DegtoRad(theta1+theta0))));
```

```
end;
```

```
Procedure THandForm.CalculatePtD(sender: TObject);
```

```

begin
Alpharad := MyArcTan(PtR_float[2]-PtB.Y, PtB.X-PtR_float[1]);
PtD := Point(round(PtB.x + FingerLength*cos(DegtoRad(theta3+180)+Alpharad)),
              round(PtB.y - FingerLength*sin(DegtoRad(theta3+180)+Alpharad)));
end;

Procedure THandForm.CalculateHandOpening(sender: TObject);
begin
//hand_opening = distance between points C and D
Hand_opening := sqrt(sqrt((PtD.X - PtC.X)/ScreenScale)+
                    sqrt((PtD.Y - PtC.Y)/ScreenScale));
end;

procedure THandForm.CalculatePtF(Sender: TObject);
begin {The Line PtFQ defines the direction of the force applied to point Q.}
calculateThetaF(sender);
PtF := point(PtQ.X + round(Flength*Cos(ThetaFRad)),
             PtA.Y - Fheight);
end;

procedure THandForm.CalculatePtFs(Sender: TObject);
begin {The Line PtFsQ0 defines the direction of the force applied to point Q0.}
calculateThetaFs(sender);
PtFs := point(PtQ0.X + round(Fslength*Cos(ThetaFsRad)),
             PtA.Y - Fsheight);
end;

{ *****
                                     TrackBar Control
***** }

```

```

procedure THandForm.TrackBarDSChange(Sender: TObject);
var
  newpos: Smallint;
  CanMove: Boolean;
begin
  newpos := trackbarDS.position;
  old_theta1 := theta1;
  {Every tick of the trackbar is equal to "Delta_trackBar_mm" mm of displacement at
  point Q}
  //Calculate new Theta1
  theta1 := theta1 - RadToDeg((Delta_trackBar_mm*ScreenScale*
                               (trackbarDS.position-trackbarpos_old)) / QLever);

  //check if it is consistent
  if theta1 < 0 then
    begin
      {if not restore theta1 and the position of the track bar}
      theta1 := old_theta1;
      trackBarDS.position := trackbarpos_old
    end
  else {theta1 is acceptable}
    begin
      calculateAllCoordinates(sender);
      { |(Fheight-(PtA.Y-PtQ.Y)| must be <= Flength. }
      if (abs(Fheight-(PtA.Y-PtQ.Y)) >= Flength) or
         (abs(Fsheight-(PtA.Y-PtQ0.Y)) >= Fslength) then
        begin      {revert values}
          theta1 := old_theta1;
          trackbarDS.position := trackbarpos_old;
        end
      else
        begin

```

```

calculateThetaF(sender);
CalculatePtF(sender);
calculateFixedPtFsThetaFs(sender);
{The tip of the fingers cannot cross the tip of the thumb and vice versa}
if PtD.Y >= PtC.Y then
begin          //revert values
  theta1 := old_theta1;
  trackbarDS.position := trackbarpos_old;
end
else
begin
  {Only move hand if the forces are in the desired direction and greater than 0}
  {Check who controls the track bar and what action has been performed}
  if ManualTrackBar then          {Users control:}
    if trackbarpos_old > trackbarDS.Position then
      {User wants to close the hand}
      HandOpening := False
    else
      if trackbarpos_old < trackbarDS.Position then
        {User wants to open hand}
        HandOpening := True;

```

{If the control is done by software (automatic control used for generating graphs, etc), the action is already defined and is stored in "HandOpening"}

```

  {Now calculated the forces for the new situation}
  calculateForces(sender);
{Check if the resulting force NCD is enough to move the hand: |NCD| > 0}
  CanMove := False;
  if HandOpening and (Ncd < 0) then
    CanMove := True;

```

```

if (Not HandOpening) and (Ncd > 0) then
  CanMove := True;
if CanMove then                                     //OK
  Begin {redraw the hand}
  MaskEditTheta1.text := format('%f',[theta1]);
  trackbarpos_old := trackbarDS.position;
  LabelLinearDispl.caption := 'Linear Displ.: ' +
                                format('%f',[TrackbarDS.Position *
                                Delta_trackBar_mm]) + ' mm';
  clearBMP(sender);                                //erase old draw
  currentMode := pmNotXor;
  drawhand(sender);                                //new draw
  DrawForceVectors(Sender); //redraw force vectors
  end
else
{The force was not enough to move the hand: restore theta1 and trackbar. A status
message was sent by CalculateForces informing that motion was not possible}
  begin
  theta1 := old_theta1;
  trackbarDS.position := trackbarpos_old;
  end;
end;
end;
end;
end;

{ *****
FORCES
***** }

{Calculate the forces within the hand mechanism}

```

```
procedure THandForm.CalculateForces(sender: TObject);
```

```
var
```

```
    SumFx,SumFy,Ax,Ay,Bx,By,Rx,Ry,NR: Extended;
```

```
begin
```

```
{First find out the correct values for the forces to be used in the equations.
```

```
The equations were developed for:
```

```
    . F: always trying to open the hand (FOpen is the positive direction)
```

```
    . Fs: always trying to close the hand
```

```
    . Ncd: indicates grip forces (closing hand).
```

Therefore, since those forces are entered only with the magnitude and the angle is calculated based on the relative position of the related points (Q, Qo, R, C, C0 and D), the signal must be adjusted according to the operation performed. }

```
{Find the input forces and the required output }
```

```
case ComboBoxInputForces.ItemIndex of
```

```
0: begin {Input forces: F and Fs; Calculate Ncd }
```

```
    Fs := CalculateFsEquation(Sender);
```

```
    if HandOpening then
```

```
        F := -1*InputFOpen
```

```
    else
```

```
        F := InputFClose;
```

```
end;
```

```
1:begin
```

```
    if HandOpening then
```

```
        begin
```

```
            F := -1*InputFOpen;
```

```
            Ncd := -1*InputNcdOpen;
```

```
        end
```

```
    else
```

```
        begin
```

```
            F := InputFClose;
```

```

    Ncd := InputNcdClose;
end;
end;
2: begin
    Fs := CalculateFsEquation(Sender);
    if HandOpening then
        Ncd := -1*InputNcdOpen
    else
        Ncd := InputNcdClose;
    end;
end;
end;

{Start calculation:}
{Find the main angles}
CalculateThetaBD(sender);
CalculateThetaCD(sender);
CalculateThetaAC(sender);
CalculateThetaF(sender);
CalculateThetaFs(sender);
{Calculate constant values}
K1 := sin(ThetaBDrad-ThetaCDrad)*(FingerLength / ScreenScale);
K2 := sin(ThetaFrad-degTorad(Theta1))*(QLever / ScreenScale);
K3 := sin(ThetaFsRad - DegToRad(Theta1+theta0)) * (Q0Lever / ScreenScale);
K4 := sin(ThetaACrad - ThetaCDrad) * (ThumbLength / ScreenScale);
K5:= (RLever/ScreenScale) * cos(alpharad-degTorad(Theta1));
{Calculate the distance between B and R (Current finger lever)}
calculateD(sender);
{Use the correct input according to user's choice and calculate the desired output}
case ComboBoxInputForces.ItemIndex of
    0:          {Input forces: F and Fs; Calculate Ncd}
        Ncd := ((K2/K5)*d*F + (K3/K5)*d*Fs) / ((K4/K5)*d + K1);

```

```

1:           {Input forces: F and Ncd; Calculate Fs}
Fs := (((K4/K5)*d + K1)*Ncd - (K2/K5)*d*F) / ((K3/K5)*d);
2:           {Input forces: Fs and Ncd; Calculate F}
F := (((K4/K5)*d + K1)*Ncd - (K3/K5)*d*Fs) / ((K2/K5)*d);
end;

{Now calculate the other forces within the hand}
NR := (K2*F + K3*Fs - K4*Ncd) / K5;
Rx := -1*NR*sin(alpharad);
Ry := -1*NR*cos(alpharad);
Ax := Ncd*cos(ThetaCDrad)-Fs*cos(ThetaFsRad)+Rx-F*cos(thetaFrad);
Ay := Ncd*sin(ThetaCDrad)-Fs*sin(ThetaFsRad)-Ry-F*sin(thetaFrad);
Bx := NR*sin(alpharad) - Ncd*cos(ThetaCDrad);
By := NR*cos(alpharad) + Ncd*sin(ThetaCDrad);
FA := sqrt(sqr(Ax) + sqr(Ay));
ThetaFaRad := MyArcTan(Ay,Ax);
FB := sqrt(sqr(Bx) + sqr(By));
ThetaFbRad := MyArcTan(By,BX);

//From the Free Body Diagram of the WHOLE structure:
//for equilibrium ==> SUM(Fx) = 0 and SUM(Fy) = 0
SumFx := Ax + Bx + F*cos(thetaFrad) + Fs*cos(thetaFsrad);
SumFY := Ay - By + F*sin(thetaFrad) + Fs*sin(thetaFsrad);
if (round(SumFx) <> 0) or (round(SumFy) <> 0) then
  StatusBar.Panels[0].Text := 'Error: The system is not in equilibrium !'
else
  StatusBar.Panels[0].Text := 'The System is in equilibrium !';
{Display an status message to indicate if the force is enough to open or close the
hand }
StatusBar.Panels[1].Text := 'Input Data from Slider and "' +
  GroupBoxInputForce.Caption + "' !";
if HandOpening and (Ncd >= 0) then

```



```

    StatusBar.Panels[1].Text := 'The resulting force is NOT ENOUGH to open the
                                hand!';
if (Not HandOpening) and (Ncd <= 0) then
    StatusBar.Panels[1].Text := 'The resulting force is NOT ENOUGH to close the
                                hand!';
end;

```

{ Calculate the current spring force by solving the equation:

$$F_s = F_{s0} \pm K \cdot Q_0 \text{Displac}$$

where:

$$Q_0 \text{displacement} = Q_0 \text{lever} / Q_{\text{lever}} * Dq(\text{displac. given by the track bar})$$

Function THandForm.CalculateFsEquation(Sender: TObject): Double;

begin

if ComboBoxInputFsSignal.ItemIndex = 0 then { + }

$$\text{CalculateFsEquation} := \text{InputFs0} + \text{InputFsK} * (Q_0 \text{lever} / Q_{\text{lever}}) * \\ (\text{TrackbarDS.Position} * \text{Delta_trackBar_mm})$$

else { - }

$$\text{CalculateFsEquation} := \text{InputFs0} - \text{InputFsK} * (Q_0 \text{lever} / Q_{\text{lever}}) * \\ (\text{TrackbarDS.Position} * \text{Delta_trackBar_mm});$$

end;

{ Angle between the line BD and the horizontal axis }

procedure THandForm.CalculateThetaBD(Sender: TObject);

begin

$$\text{ThetaBDrad} := \text{MyArcTan}(\text{PtD.y} - \text{PtB.y}, \text{PtB.X} - \text{PtD.X});$$

end;

{ Angle between the line CD and the horizontal axis }

procedure THandForm.CalculateThetaCD(Sender: TObject);

begin

$$\text{ThetaCDrad} := \text{MyArcTan}(\text{PtC.y} - \text{PtD.y}, \text{PtD.X} - \text{PtC.X});$$

end;

{ Angle between the line AC and the horizontal axis }

procedure THandForm.CalculateThetaAC(Sender: TObject);

begin

 ThetaACrad := MyArcTan(PtC.y - PtA.y, PtA.X - PtC.X);

end;

{ Angle at which the force F is applied to point Q }

procedure THandForm.CalculateThetaF(Sender: TObject);

begin

 ThetaFrad := Pi - Arcsin((Fheight-(PtA.Y-PtQ.Y))/Flength);

end;

{ Angle at which the force Fs is applied to point Q0 }

procedure THandForm.CalculateThetaFs(Sender: TObject);

begin

 ThetaFsrad := Pi - Arcsin((Fsheight-(PtA.Y-PtQ0.Y))/Fslength);

end;

{ Calculate the angle at which Fs is applied to Q0, if the coordinates of the fixed end of the spring are known. This subroutine can only be used if PtFs has been calculated at least once before }

procedure THandForm.CalculateFixedPtFsThetaFs(Sender: TObject);

begin

 ThetaFsrad := Pi - MyArcTan(PtFs.y - PtQ0.y, PtQ0.X - PtFs.X);

end;

{ Calculate the current finger lever }

procedure THandForm.CalculateD(sender: TObject);

begin

```
//The distance between R and B changes as the barrel moves along the slot
d := sqrt(sqrt((PtR.X - PtB.X)/ScreenScale) + sqrt((PtR.Y - PtB.Y)/ScreenScale) );
end;
```

```
{*****
                                     Graphic outputs
***** }
```

{This procedure creates a vector of displacement for point Q when OPENING the hand and calculates the output force for each point. After that, the “GraphicForm” is opened and the graphics are plotted. Other vectors are also created for Fa, Fb, levers and Fs }

```
procedure THandForm.ShowGraphicOutputOpeningClick(Sender: TObject);
```

```
var
```

```
  i,mysize: smallint;
```

```
begin
```

```
  Mysize := CreateMyVariantArrays(sender);
```

```
  if Mysize <= 0 then
```

```
    system.exit;
```

```
    HandOpening := True;      { automatic control of the track bar }
```

```
    ManualTrackBar := False;
```

```
    TrackBarDS.Position := 0; //set the track bar to zero
```

```
    TrackBarDSChange(sender);
```

```
    DisplVector[0] := TrackbarDS.Position*Delta_trackBar_mm;
```

```
    FVector[0] := abs(F);
```

```
    FsVector[0] := abs(Fs);
```

```
    NcdVector[0] := abs(Ncd);
```

```
    HandOpenVector[0] := Hand_opening;
```

```
    FingerLevers[0] := d;
```

```
    FaVector[0] := FA;
```

```

FbVector[0] := FB;
{Now open the hand using the track bar}
for i := 1 to mysize-1 do
begin
  TrackBarDS.Position := TrackBarDS.Position + TrackBarDS.Frequency;
  TrackBarDSChange(sender);
  displVector[i] := TrackbarDS.Position*Delta_trackBar_mm;
  FVector[i] := abs(F);
  FsVector[i] := abs(Fs);
  NcdVector[i] := abs(Ncd);
  HandOpenVector[i] := Hand_opening;
  FingerLevers[i] := d;
  FaVector[i] := FA;
  FbVector[i] := FB;
end;
//Return track bar to zero
TrackBarDS.Position := 0;
TrackBarDSChange(sender);
ManualTrackBar := True; //Restore manual control of the track bar
if TransferVectors(Sender, Displvector, FVector, FsVector, NcdVector, FaVector,
  FbVector, HandOpenVector, FingerLevers, 'Displacement(mm)',
  'F(N)', 'Fs (N)', 'Opening Force (N)', 'FA (N)', 'FB (N)',
  'Opening Width(mm)', 'Fingers Lever(mm)') then
  GraphicOutputForm.Show
else
  begin
    ShowMessage('Can"t process vectors. Aborting operation!');
    system.exit;
  end;
end;

```

{This procedure creates a vector of displacement for the point Q when CLOSING the hand and calculates the output force for each point. After that, the “GraphicForm” is opened and the graphics are plotted. Other vectors are also created for Fa, Fb, levers and Fs}

```

procedure THandForm.ShowGraphicOutputClosingClick(Sender: TObject);
var
  i,mysize: smallint;
begin
Mysize := CreateMyVariantArrays(sender);
if Mysize <= 0 then
  system.exit;
HandOpening := False;      {automatic control of the track bar}
ManualTrackBar := False;
//Set the Track bar to maximum
TrackBarDS.Position := TrackBarDS.Frequency * MySize;
TrackBarDS.Change(sender);
DisplVector[0] := TrackbarDS.Position*Delta_trackBar_mm;
FVector[0] := abs(F);
FsVector[0] := abs(Fs);
NcdVector[0] := abs(Ncd);
HandOpenVector[0] := Hand_opening;
FingerLevers[0] := d;
FaVector[0] := FA;
FbVector[0] := FB;
for i := 1 to mysize-1 do      {now close the hand using the track bar}
begin
  TrackBarDS.Position := TrackBarDS.Position - TrackBarDS.Frequency;
  TrackBarDS.Change(sender);
  displVector[i] := TrackbarDS.Position*Delta_trackBar_mm;
  FVector[i] := abs(F);
  FsVector[i] := abs(Fs);

```

```

NcdVector[i] := abs(Ncd);
HandOpenVector[i] := Hand_opening;
FingerLevers[i] := d;
FaVector[i] := FA;
FbVector[i] := FB;
end; //end of the loop
//Track bar is at zero. Restore manual control.
ManualTrackBar := True;
if TransferVectors(Sender, Displvector, FVector, FsVector, NcdVector, FaVector,
    FbVector, HandOpenVector, FingerLevers, 'Displacement(mm)',
    'F(N)', 'Fs (N)', 'Grip Force (N)', 'FA (N)', 'FB (N)', 'Opening
    Width(mm)', 'Fingers Lever(mm)') then
    GraphicOutputForm.Show
else
    begin
        ShowMessage('Can"t process vectors. Aborting operation!');
        system.exit;
    end;
end;

```

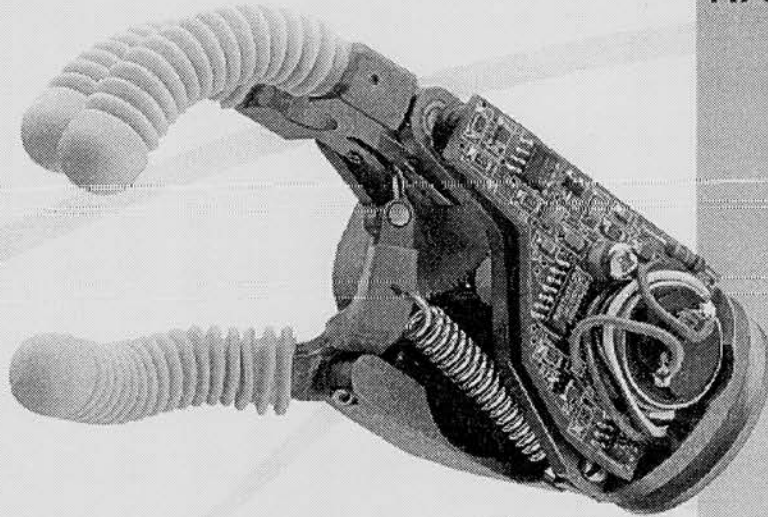
Appendix B

The Steeper Scamp Hand

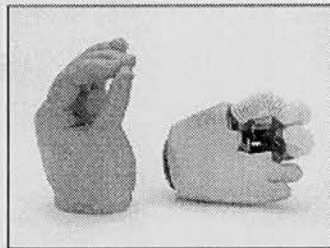
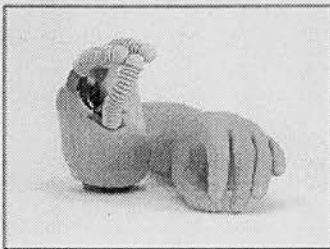
and

**The VV Series Electric Hands from
Variety Ability Systems Inc.**

THE STEEPER SCAMP HAND



A miniature electric hand designed for children between the ages of 6 months and 6 years. A single control sensor allows simple operation. The hand may also be opened manually if required, enabling simple



guidance and training. The foam cosmesis and ribbed finger covers provide a safe and reliable grip, and with a range of PVC and Silicone cosmetic gloves the "Scamp" hand presents a realistic children's prosthesis.

The Steeper Group of Companies



THE STEEPER SCAMP HAND

Any electric hand designed for children aged between 6 months and 6 years must be both lightweight and durable. The Steeper "Scamp" Hand meets these objectives, whilst also providing an efficient grasp.

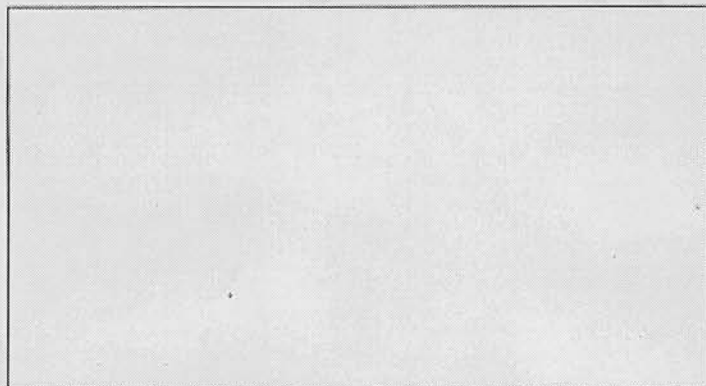
Its unique electro-mechanical drive system provides fast but controllable movement in response to a signal from the single control sensor. A range of additional sensors gives on/off switch or threshold myo control of the hand. The choice depends upon the application.

The drive system of the hand allows the child to release the grip mechanically without power should the battery be discharged. The geometry and finish provide a secure grip, whilst using low safe closing forces.

The hand is mounted onto the prosthesis with a small, lightweight friction wrist unit that provides 320° of rotation and has a variable friction facility. The whole assembly is protected by a foam cover, and either a PVC or Silicone Cosmetic Glove is fitted to complete the cosmesis.

TECHNICAL INFORMATION

WIDTH ACROSS KNUCKLES	1 1/4" - 2" (42 - 51mm)
OPERATING VOLTAGE	6V DC
OPENING/CLOSING TIME	0.5 seconds
MAXIMUM PINCH FORCE	10N
WEIGHT - MIN/MAX (INCLUDING COSMESIS)	143 - 140g
RUNNING CURRENT	Less than 150mA



Literature No. L20878 Issue 1 March 1995

HUGH STEEPER LIMITED

Queen Mary's University Hospital, Roehampton Rehabilitation Centre, Roehampton Lane, London SW15 5PL England.

Tel: 44-(0)181-788 8165 Fax: 44-(0)181-788 0137

STEEPER EUROPE BVBA

Kortrijksteenweg 1065, B-9051 Gent, Belgium.

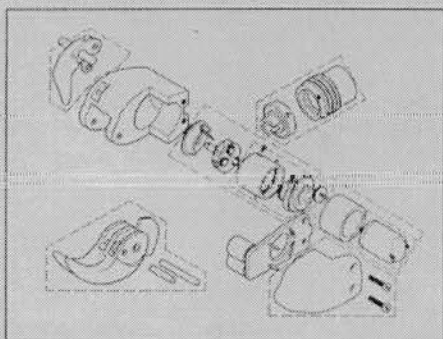
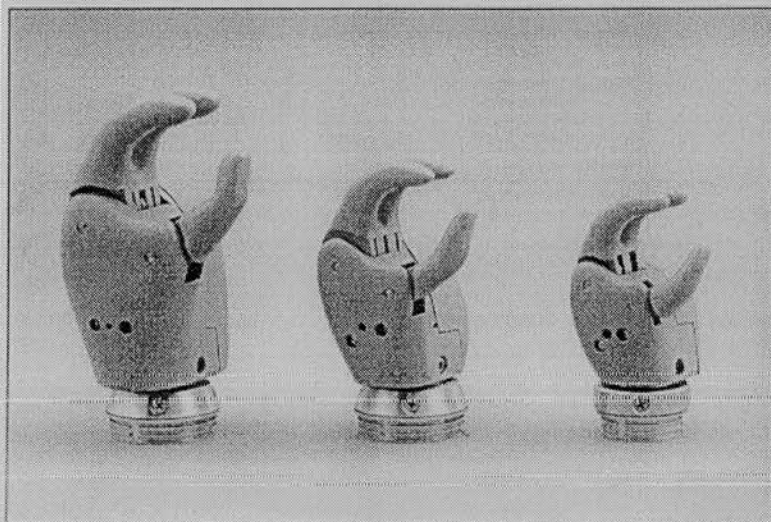
Tel: 32 (0) 9-2214622 Fax: 32 (0) 9-2202968

The Steeper Group of Companies





*The world's smallest
lightweight
electric hands
for children.*

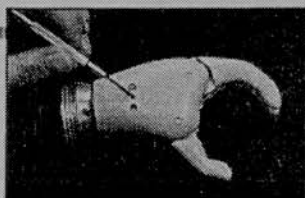


Variety Ability Systems Inc.

3701 Danforth Ave., Scarborough (Toronto) Ontario, Canada M1N 2G2 (416) 698-1415 Fax (416) 698-5860

Administered by THE HUGH MACMILLAN REHABILITATION CENTRE for VARIETY CLUB ONTARIO, TENT No. 28

VASI



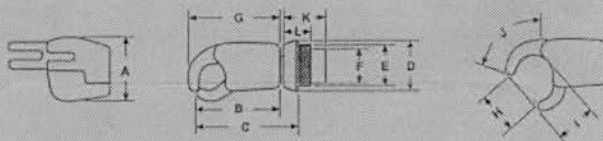
Easy screwdriver access through side of hand permits manual opening of hand, facilitating glove placement and removal.



Unique Energy Saver circuit extends the useful life of a single battery charge.

SPECIFICATIONS						
Model		VV 0-3		VV 2-6		VV 5-9
Age range (yrs)		0 - 3		2 - 6		5 - 9
Weight		130g (4.6 oz.)		166g (5.9 oz.)		247g (8.7 oz.)
Dimensions (closed position)	KEY	mm.	in.	mm.	in.	mm.
Max. width	(A)	48	1.90	53	2.10	64
Hand body / thumb tip	(B)	53	2.10	67	2.63	84
Lamination ring / thumb tip	(C)	65	2.55	78	3.08	95
Overall wrist diameter*	(D)	33	1.31	40	1.57	40
Lamination ring - outside diameter	(E)	23	1.12	37	1.46	37
Lamination ring - inside diameter	(F)	24	0.94	30	1.19	30
Max. length (excluding wrist)	(G)	62	2.43	75	2.93	91
Max. opening	(H)	38	1.50	50	1.95	62
Finger opening depth	(I)	28	1.10	33	1.30	36
Length of longest finger	(J)	33	1.43	48	1.89	54
Wrist unit	-long	20	1.10	28	1.10	-
	-short**	17	0.68	17	0.68	17
Power bridge with energy saver						
Quiescent current		0		0		0.3 mA
Before deactivation		<35 mA		<35 mA		5.0 mA
After deactivation		<5 mA		<5 mA		0.3 mA
Current sensing level		-		-		500 mA
Nominal operating voltage		6V DC		6V DC		6V DC
Maximum current (motor)		260 mA		340 mA		1.4 AMPS
Pinch force (glove on)		20 N (4.5 lbs.)		20 N (4.5 lbs.)		38 N (8.5 lbs.)
Maximum open or close time		1 sec.		1 sec.		1.2 sec.

*Two size options. Hands are interchangeable in existing forearm having VASI lamination ring.
 **Dexter adapters available to fit wrist disarticulation. Adaptor available for installation of VASI hands to Systemteknik Lamination rings in existing prosthesis.



The VV series electric hands, known for their quality and reliability, have been designed for child amputees in the one to nine year age range. The 'VV 0-3', 'VV 2-6' and the 'VV 5-9' are aesthetic and lightweight yet can withstand the rigors of child play because of injection molded construction techniques.

All three of VASI's hands are compatible with the most popular switch and myoelectric control systems from VASI, Otto Bock and University of New Brunswick and other manufacturers. Connection is made easy with the commonly used Otto Bock 4-pin type connectors. Friction wrists, standard with all hands, allow the hand to be passively positioned. Optional wrists are available to fit wrist disarticulation and to adapt Variety hands to Systemteknik lamination rings. Also, inquire about VASI's new children's powered wrist designed to improve prosthetic function.

The totally modular design simplifies maintenance. All electronic components are packaged to permit economical repair or replacement. Similarly, the integrated motor and gear housing can be easily removed and replaced in minutes.

An optional integrated power-bridge and energy-saver circuit allows the prosthetist to easily customize the hand to the child's needs for one or two-muscle operation. As well, VASI's switch controls include single-action, dual-action and pull-switch types. These facilitate prosthetic fabrication and service with VASI's exclusive 3-pin connector system. Contact your VASI representative for more details.

3701 Danforth Ave., Scarborough (Toronto) Ontario, Canada M1N 2G2 [416] 698-1415 Fax [416] 698-5860
 Administered by THE HUGH MACMILLAN REHABILITATION CENTRE for VARIETY CLUB ONTARIO, TENT No. 28

Appendix C

Publications

Soares, Alcimar B; Brash, Harry M & Gow, David (1997). "The Application of SMA in the Design of Prosthetic Devices". Proceedings of The Second International Conference on Shape Memory and Superelastic Technologies (SMST97), March 1997, Pacific Grove - CA - USA.

THE APPLICATION OF SMA IN THE DESIGN OF PROSTHETIC DEVICES

Alcimar B. Soares*, **Harry M. Brash**** and **David Gow*****

* Departamento de Engenharia Elétrica, Universidade Federal de Uberlândia, MG, BRAZIL

Department of Medical Physics and Medical Engineering, The University of Edinburgh, UK

** Department of Medicine, The University of Edinburgh, UK

Department of Medical Physics and Medical Engineering, The University of Edinburgh, UK

***Bioengineering Centre, Princess Margaret Rose Orthopaedic Hospital, Edinburgh, UK

ABSTRACT

Shape Memory Alloys (SMA) have already proved their usefulness in various applications. Although some researches using SMA in the development of prosthetic devices were reported in the past, they did not reach clinical application for reasons such as low frequency response and low efficiency. However, new developments have been reported since then. This paper describes how techniques using SMA can be used to complement and sometimes replace traditional methods or even provide a unique solution for prosthetic devices. The design and construction of a small artificial hand using an SMA actuator as joint motivator are presented.

INTRODUCTION

The idea that we could develop an artificial muscle is seductive to prosthetic engineers. After all, on a daily basis they are faced with the limits and frustrations presented by our existing technologies: noisy and heavy actuators; low battery energy density; limited function and sensation; poor feedback and control systems.

It is hardly surprising that SMA have been hailed as the answer to some of these seemingly impenetrable technical barriers. Here we have prosthetic contractile “tissue” which can turn electrical energy into mechanical motion and force, silently and with greater intensity per cross sectional area than the real thing. The trouble is, it's not that simple. The limitations of SMA are well understood and documented, so how can those of us who have remained faithful to its promise take our hopes forward? Here are some potential applications of SMA in prosthetics:

- SMA actuator used as a muscle replacement in prosthetic devices - more about this later.

- SMA actuator used to lock and unlock a prosthetic joint. This would allow relatively efficient actuators such as electric motors to be used for movement with steady positions being held by means of a lockable joint. For example, in wrist rotation mechanisms, SMA could be used to make a flexible, miniature braking actuator in a restricted space. Current technologies use small motors as shaft locks with the disadvantages of weight, size and noise of operation.
- SMA could be used as a shape changing mechanism. For example, a prosthetic hand could be switched from flat profile to a thumb/finger in opposition grasp mode for functional purposes.
- SMA could be used as an electronic counterbalance to offload some of the gravitational loading on the prostheses. In a complete arm prosthesis for example, if SMA were used to take the weight of the arm componentry, then the actuators could be designed to lift the payload only.
- SMA wires could be used as artificial tendons to give low movement/high force outputs at distal articulations such as the thumb. Used in conjunction with faster, lighter actuators in the prosthesis for positioning digits and giving light prehensile grips, the SMA would supply the larger forces required when increased grip is indicated.
- It may be possible to use SMA to give pressure/force feedback to patients. Mechanical feedback has always been an attractive idea but the very nature of bulky motors and gearboxes being located in patients' sockets has made implementation difficult. SMA could solve this problem in that it is flexible, lightweight and could be fitted into restricted or awkwardly shaped spaces.

USE OF PROSTHESES WITH VERY YOUNG CHILDREN

We have been working on the development of an SMA powered upper limb prosthesis for very young children - up to about 18 months old. This particular project was selected because SMA appeared to offer advantages in terms of size, noise and weight over conventional alternatives for young children in this age group.

In general, the first fitting of a prosthesis to a very young child occurs when he or she shows interest in standing, can sit and starts to use the hands to explore and manipulate objects. At six to eight months the child is too young to operate a terminal device such as an active artificial hand, although a passive device to hold objects inserted by an adult will certainly draw the child's attention to the idea of wearing a prosthesis. The subsequent introduction of an active prosthetic device to a very young child may be viewed as a training tool which prepares the child for more practical devices to be provided later.

Older children and adults often recognize the advantages which prostheses can offer and are therefore willing to tolerate the associated disadvantages. However, for very young children, the disadvantages will often be the overriding factor and the device may be rejected out of hand. In the case of an upper limb prosthesis, the common problems are the need for a harness and the weight of the device. Minimizing this discomfort and maximizing the interest or entertainment value of the device for the young child is our challenge.

THE DESIGN OF THE SMA POWERED HAND MECHANISM

We set out to design an SMA powered hand as part of an above elbow prosthesis for children under 18 months old. Current commercially available artificial hands for this age group weigh between 130 and 150 grams (excluding gloves, batteries and suspension devices). Some basic dimensions for our proposed prosthesis are shown in figure 1.

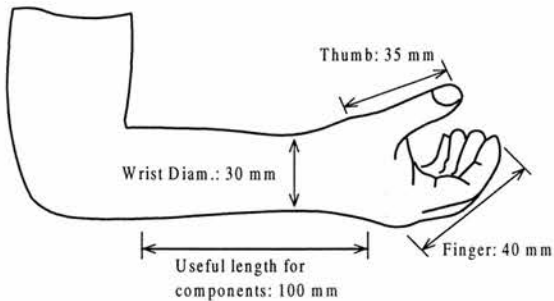


Figure 1: Basic dimensions of a small above elbow prosthesis.

The hand mechanism chosen for the purpose of this work is a very common design used in many prostheses. Two fingers (medium and index) are locked together to grasp or pinch an object against the thumb. The other two fingers are basically for cosmetic reasons and just follow the movements of the “active” fingers. Figure 2 shows a diagram of such a scheme.

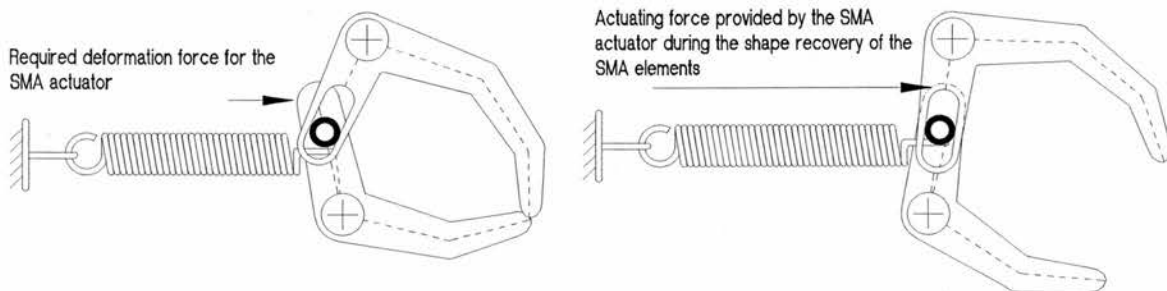


Figure 2: The chosen hand mechanism.

The fingers and thumb are linked so that moving the thumb results in motion of the fingers and vice-versa. An ordinary spring is used to provide the closing/grasping force and an actuator will be used to open the hand against the spring. Our system uses a *bias-type SMA actuator*, which requires an external force to deform the SMA elements. In this design the bias force is provided by the same spring responsible for the grip force. The necessary power for the SMA actuator is provided by a battery pack. The main advantage of this arrangement is that the SMA actuator is powered only while opening the hand. Since the device is closed or holding an object most of the time (grip force provided by the spring), this extends the operating time for each battery charge.

The actuator for the joint mechanism must be designed so that it is as light and compact as possible, leaving enough room for the other components of the prosthesis (such as mechanical parts and electronics). As mentioned previously, the main reason for fitting very young children with artificial limbs is to provide them with a “training device” and accustom them to wearing prostheses. With this in mind, it was decided that the actuator should provide a grip force of 3 N (without cosmetic glove) and 1.5 N for opening the hand against a cosmetic glove (both values measured at the tip of the fingers and thumb). A minimum lifetime of 72000 cycles was considered satisfactory for the actuator. This value is not necessarily related to the lifetime of the prosthesis itself, but was chosen to give approximately 4 months of continuous use at a rate of 600 cycles a day. Although 72000 cycles is a low value for conventional prostheses it would be adequate if the actuator is relatively

inexpensive and could be replaced (if necessary) when the prosthesis is returned to the prosthetic centre for review (which, for this range of prostheses, normally happens every three months).

Our main problem was to devise a hand mechanism well matched to the characteristics of a practical SMA actuator and a commercially available power spring. In comparison to electric motor/gearbox combinations, SMA actuators can function only within a very narrow 'window' of force and displacement. Efficient and reliable operation of an SMA powered device can be achieved only through great attention to detail. The common 'cut and try' approach of repeatedly refining and reconstructing an initial design looked like being very laborious and frustrating in the case of SMA. As an alternative, it was decided to optimize the design using a computer simulation of the movements and forces within the hand mechanism. The program allowed us to analyze the design and evaluate the consequences of modifying any parameter without actually building anything until we were satisfied with the overall performance and knew that it would match to a practical SMA actuator and available spring.

THE DESIGN OF THE SMA ACTUATOR

Since the actuator must be powered by a battery pack, power consumption was a major concern throughout the design. Taking into consideration that the hand will be closed or grasping an object most of the time, it is desirable that, when in this situation, the power consumption is set to a minimum or even zero. This can be achieved easily using a bias actuator. The force to open the hand can be provided by the recovery force of the SMA actuator and the bias spring provides the necessary force to deform the SMA elements, close the hand and grasp objects. The disadvantage of

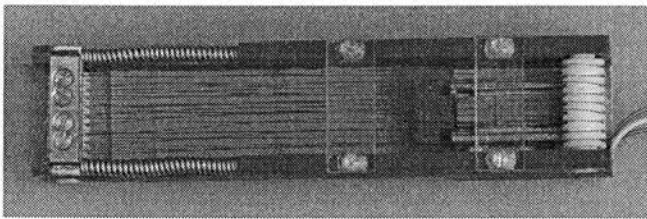


Figure 3: The SMA actuator.

this approach is that the grasping force cannot be controlled precisely. However, as a training tool for young children, precise control is not a requirement and the bias actuator can fulfill the specifications.

The simulation showed that the SMA actuator must provide 27 N over a displacement of 7.2 mm to open the hand by 24 mm. This was achieved by using 9 SMA wires Flexinol™ 150HT, mechanically and electrically in parallel, each 263.5 mm long. The prototype and its time response are shown in figures 3 and 4 respectively.

The wires were mounted in the actuator body around two grooved ceramic rollers as shown in figure 3. Two springs provide protection against overload. Movement against these pretensioned springs activates a micro-switch which removes all power from the wires.

Initial tests with the assembled actuator indicated a significant increase in deformation time compared with the wires alone. The main

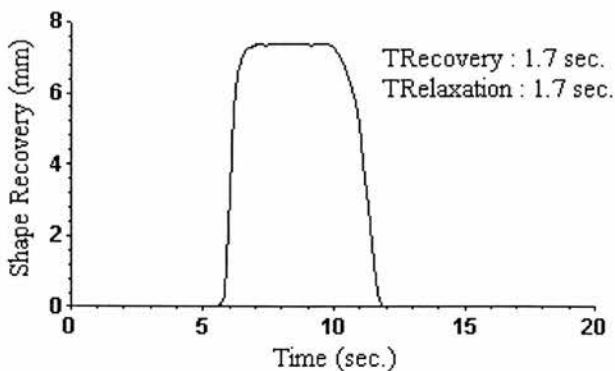


Figure 4: Response time of the actuator. Heating started at 5 sec. (350 mA per wire); Cooling started at 10 sec; Amb. temp. = 22 °C; Responses measured from zero to 100% movement under a load of 27 N.

cause of this appears to be heat retention in the rollers which keeps the wires hot after electrical power is removed. The use of a small electrical fan (15 mm diameter) during the deformation phase effectively restored the response times to the values shown in figure 4. All the results given for the assembled hand were taken with the fan in operation. The measured characteristics of the SMA actuator are:

- . Dimensions: 15 mm x 22 mm x 95 mm (min.) / 21 mm x 22 mm x 95 mm (max.)
- . Weight: 35 grams
- . Required deformation force: 10.35 N
- . Contraction/Recovery time: 1.7 seconds
- . Maximum recovery force: 30 N
- . Relaxation/Deformation time: 1.7 seconds
- . Displacement (zero stress): 7.9 mm

CONSTRUCTION AND MECHANICAL PERFORMANCE OF THE HAND PROTOTYPE

The hand mechanism was built to the dimensions from the computer simulation as discussed previously. The fingers and thumb were made of a metal “skeleton” surrounded by resin based filler to shape them as desired. A framework, representing the forearm of an upper limb prosthesis, was constructed, based on the dimensions of the artificial arm shown earlier, and the SMA actuator, “power spring” and the hand mechanism were mounted as shown in figure 5. The total weight of the device is 102 grams, comparing favourably with standard commercial hands for the age group in question.

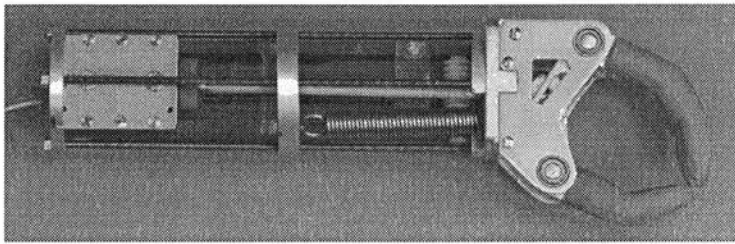


Figure 5: The hand prototype.

The movements of the hand were observed for a single open-close cycle at different ambient temperatures, as shown in figure 6.

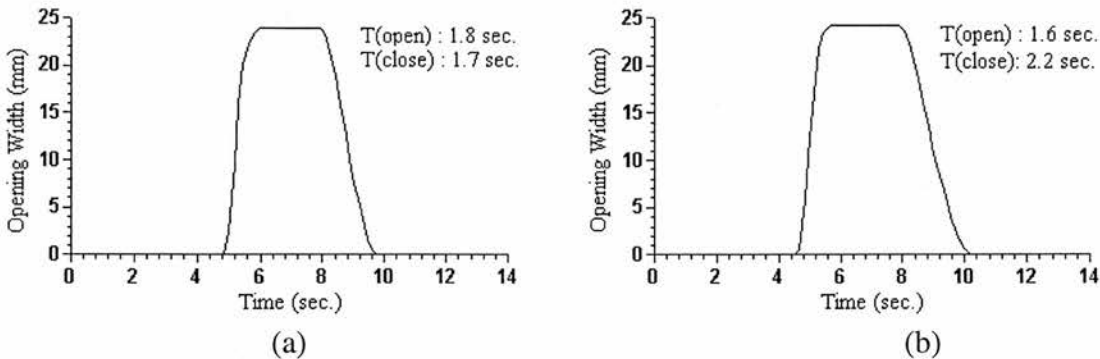


Figure 6: Response of the prototype for opening and closing at ambient temperatures of (a) 22 °C and (b) 35 °C.

The results show that the increase in the ambient temperature, within the range of 22 °C to 35 °C, has very little effect on the overall time response. As expected, we observed a small decrease in the opening time and a small increase in the closing time as the ambient temperature increases.

The measured grip force within the range of movement of the prototype was essentially as predicted by the simulation program and according to the specifications.

POWER CONSUMPTION AND EFFICIENCY OF THE DEVICE

In practical terms, the battery energy required for each opening and closing cycle of the hand is most significant as it determines how many cycles can be achieved for each charge of the battery.

The prototype hand requires about 27 J of electrical energy to open. A 750 mAh 6V battery would provide 600 cycles for each charge.

It is interesting to note that the mechanical work done by the actuator against the spring during the recovery phase is only about 0.22 J giving an actuator efficiency during the recovery phase of 0.8%.

CONCLUSIONS

The aim of this work was not to generate a commercial device, but rather to investigate if it is possible to apply “SMA technology” to construct a practical prosthesis. With this in mind, some conclusions can be drawn from our experience in the development and evaluation of this prototype hand mechanism:

- It is possible to construct a practical SMA powered hand prosthesis which is light, small and effectively **silent**.
- The use of an SMA actuator requires considerable care regarding the design of the hand mechanism, so that the forces and displacements generated by the actuator are used as efficiently as possible. In general, it is essential to determine the best “geometry” for the components of the “prosthesis” and to build them as precisely as possible.
- With a weight of 102 grams (without cosmetic glove or battery) our prototype compares favourably with commercial prostheses. Through minor changes to the design and the use of lighter materials, it is likely that the weight of the SMA powered prosthesis could be reduced to about 60 grams.
- The device has proved robust in the laboratory but the real test of clinical use is yet to come.

There is commercial interest in developing of the device, employing lighter materials such as carbon fibre.

ACKNOWLEDGMENTS

The authors would like to express their gratitude to Mr. Robert O’Donnell, Prof. W. N. McDicken, and CAPES (Brazilian government) for supporting this research.

Appendix D

Practical Aspects of Working with Shape Memory Alloys Based on Experience During the Development of the Hand Actuator

This appendix is an attempt to pass on the author's practical experience to help future workers in this field to avoid some of the more obvious pitfalls. For a more detailed description of the engineering aspects of SMA see Duerig *et al* (1990).

SMA and its Application

Although SMA is often viewed optimistically at the early stages of projects, it is very important to identify the disadvantages along with the benefits of using such alloy. A detailed analysis of the application is essential prior to the decision to use SMA. It may be that other alternatives will provide better solutions for the problem.

Choice of SMA Material

Unfortunately there are no universal standards for SMA, so it is not possible to read a handbook and select the required properties as one might do for other materials. Currently the best source for specific information is manufacturers whose data can often be used only as a gross guideline. Therefore, to choose the optimum material one must consider different manufacturers and alloys and test selected samples separately before a decision is made. Although the supplier may not be willing to provide information on the alloy chemistry, he can usually help the designer to choose the best alloy for the application.

Vendors can supply SMA elements in draw condition or already heat treated and pretrained. Acquiring the material in its draw state has the advantage that the designer may tailor the elements for the specific application. For instance, specific shapes and performance can be achieved with different heat treatment and training. However, this stage is normally very long and demands many trials before a satisfactory solution can be found. If the designer is fortunate enough to acquire SMA elements already heat treated, and possibly pretrained, the design phase can be greatly reduced. In this work, both alternatives were tried.

SMA wires were acquired in draw condition and different diameters. Various heat treatments (using a furnace) were tried and laboratory tests showed remarkable differences between them. Since the heat treatment is such an important part of the preparation of the SMA elements great care must be taken to guarantee that the samples are at the desired temperature for the required time. A vacuum furnace or salt water bath is preferred for the heat treatment but, if this is not possible, a standard furnace will suffice for less demanding applications. Rapid cooling (using water quench) is recommended.

Tests were also made with SMA wires which had already been heat treated. After a set of experiments it was decided that the Flexinol wires supplied by Dynalloy Incorporation would satisfy the specifications for the hand actuator. Although the manufacturer specified the various properties and expected performance for those wires, experiments were developed to evaluate those SMA elements with the specific application in mind. Many different results were obtained showing great variation between wires. Even sections of wires cut from the same original length showed different results. Since it is not possible for the manufacturer to produce a perfectly homogeneous alloy, differences such as observed will always be encountered. Therefore, it is advisable to test each sample before it is used in the final device.

Characterisation of SMA Properties

Once again, although the manufacturer can supply data sheets with the various properties of the material, there will be differences in the performance as explained above. An extensive process for characterisation of the material was developed during this work. The most important experiments are described in chapters 5 and 6 but these represent only the final stages. The characterisation tests were based on the experience of other researches described in the literature and thoroughly summarised in Duerig *et al* (1990).

Clamping of SMA Wires

Normally dismissed as a simple process, the clamping of the SMA elements to other parts of the device is critical. Clamping a single wire is generally straightforward. For the experiments developed during this work, single wires were clamped using crimps and screws with washers. These methods proved very reliable and simple. However,

care must be taken to avoid sharp edges and/or overtightening since these may later lead to fracture of the SMA element.

A much more complex problem is the clamping of multiple wires. In addition to the care required for a single wire, one must add the difficulties of ensuring that the wires will share the stress equally and will be strained to the same levels. Therefore, the designer must be extremely careful in the design and construction of the various components and when clamping the wires. The best technique for placing wires in parallel will depend on the application and may only be achieved after a number of trials. A description of the technique used in the design of the hand actuator can be found in chapter 5.

Electrical Heating

As the most common method of heating the elements of SMA actuators, electrical heating is very reliable when performed carefully. Some points worth considering are listed next:

- **Electrical contact:**
 - SMA elements will normally arrive in the designer's hands with a layer of oxide. Normally forgotten, this oxide layer must be removed in the areas of electrical contact.
 - It is very difficult to solder wires to SMA elements. Soldering will normally damage the SMA and can only be done by using very elaborate techniques. Most designers clamp the elements to provide electrical contact. This is generally satisfactory and can produce very reliable results.
- **Electrical Current and Power:** Careful control of the power supplied to the SMA elements is important. During the hysteresis cycle the resistivity of the alloy changes in a very non-linear way and cannot always be predicted. For this reason, the resistance of the SMA element at a specific phase may not be used to control

the current through the alloy - for example, to avoid overheating. The use of devices such as PWM controllers allows fine control of the power supplied to the device.

Further practical information such as the need for protection and the two way effect often observed in the SMA elements can be found in chapters 3, 5 and 6.

References

Aesthetic Concerns Inc. (1996). "Aesthetic Concerns' Living SkinTM - Prosthesis and Prosthetic Skin", Extracted from the Internet site: "<http://www.prosthetics.com/>".

Aghili F & Haghpanahi M (1995). "Use of a Pattern Recognition Technique to Control a Multifunctional Prosthesis", *Medical & Biological Eng. & Computing*, Vol. 33, pp. 504-508.

Airoldi G, Ranucci T & Riva G (1991). "Mechanical and Electrical Properties of a NiTi Shape Memory Alloy", *Journal de Physique IV*, Vol. 1, No. C4, pp. 439-444.

Banks R M (1981). "Nitinol Engines". *Metals Forum*, Vol. 4, No. 3, pp. 184-190.

Berveiller M, Patoor E & Buisson M (1991). "Thermomechanical Constitutive Equations for Shape Memory Alloys", *Journal de Physique IV*, Vol. 1, No. C4, pp. 387-396.

Besselink P A, Van Roermund A W J, Kurver P and Buys N W (1991). "Lamp Robot with Memory Metal Drives", *Journal de Physique IV*, Vol. 1, No. C4, pp. 117-121.

Boggs R N (1993). "How Memory Metals Shape Product Designs", *Design News*, June 21, 1993.

Borden T (1991). "Shape-Memory Alloys: Forming a Tight Fit", *Mechanical Engineering*, October 1991, pp. 67-72.

Carballo M, Pu Z J & Wu K H (1995). "Variation of Electrical Resistance and the Elastic Modulus of Shape Memory Alloys Under Different Loading and Temperature Conditions", *Journal of Intelligent Material Systems and Structures*, Vol. 6, No. 4, pp. 557-565.

Challis R E & Kitney R I (1990). "Biomedical Signal Processing. Part 1: Time-domain Methods", *Medical & Biological Eng. & Computing*, Vol. 28, November 1990, pp. 509-524.

Challis R E & Kitney R I (1991a). "Biomedical Signal Processing. Part 2: The Frequency Transforms and Their Inter-relationships", *Medical & Biological Eng. & Computing*, Vol. 29, January 1991, pp. 1-17.

Challis R E & Kitney R I (1991b). "Biomedical Signal Processing. Part 3: The Power Spectrum and Coherence Function", *Medical & Biological Eng. & Computing*, Vol. 29, May 1991, pp. 225-241.

Childress D S, Grahn E C, Heckathorne C W, Uellendahl J, Weir R F & Wu Y (1995). "Direct Muscle Attachment: Multifunctional Control of Hands and Arms", Technical Report of Researches at V A Lakeside Medical Center (VALMC) and Northwestern University Prosthetics Research Laboratory (NUPRL) - USA - August 1995, extracted from the internet site: "<http://www.repoc.nwu.edu/>".

Colli P & Sprekels J (1993). "Positivity of Temperature in the General Frémond Model for Shape Memory Alloys", *Continuum Mech. Thermodyn.*, Vol. 5, No. 4, pp. 255-264.

Colli P (1995). "Global Existence for the Three-Dimensional Frémond Model of Shape Memory Alloys", *Non-linear Analysis, Theory, Methods & Applications*, Vol. 24, No. 11, pp. 1565-1579.

De Luca C J (1978). "Control of Upper-Limb Prostheses: A Case for Neuroelectric Control", *J. Med. Eng. & Tech.*, Vol. 2, No. 2, pp. 57-62.

De Luca C J (1979). "Physiology and Mathematics of Myoelectric Signals", *IEEE Trans. Biom. Eng.*, Vol. BME-26, No. 6, pp. 313-324.

Doeringer J A & Hogan N (1995). "Performance of Above Elbow Body-Powered Prostheses in Visually Guided Unconstrained Motion Tasks", *IEEE Trans. Biom. Eng.*, Vol. 42, No. 6, pp. 621-631.

- Duerig T W, Melton K N, Stockel D & Wayman C M (1990). "Engineering Aspects of Shape Memory Alloys", Butterworth-Heinemann Ltd, UK.
- Edelstein J E & Berger N (1993). "Performance Comparison Among Children Fitted with Myoelectric and Body-Powered Hands", Arch. Phys. Med. Rehabil., Vol. 74, April 1993, pp. 376-380.
- Escher K, Hornbogen E & Mertmann M (1992). "The Two-Way Effect in Homogeneous Alloys and Composites for Robotic Applications", Proc. Int. Conf. on Martensitic Transformations, Monterey - CA - USA, pp. 1289-1294.
- Filip P & Mazanec K (1995). "The Influence of Thermal and Mechanical Treatment on the Reactive Stress in TiNi Shape Memory Alloys", Journal of Materials Processing Technology, Vol. 53, No. 1-2, pp. 139-146.
- Geake T H (1994). "Advanced Feedback System for Myoelectrically Controlled Prostheses", M. Phil. Thesis, School of Computer Science and Electronic Systems, Kingston University, UK.
- Gilbertson R G (1992). "Muscle Wires", Third Edition, Mondo-Tronics Inc., San Anselmo - CA - USA.
- Ginell W S, McNichols J L & Cory J S (1979). "Nitinol Heat Engines for Low-Grade Thermal Energy Conversion", Mechanical Engineering, May 1979, pp. 28-33.
- Goubaa K, Masse M & Bouquet G (1991). "Detection of the R-Phase in Ni-Ti Shape Memory Alloys", Journal de Physique IV, Vol. 1, No. C4, pp. 361-366.
- Graesser E J & Cozzarelli F A (1994). "A Proposed Three-dimensional Constitutive Model for Shape Memory Alloys", Journal of Intelligent Material Systems and Structures, Vol. 5, No. 1, pp. 78-89.
- Guyton A C (1991) "Basic Neuroscience: Anatomy & Physiology", Second Edition, W. B. Saunders Company, Philadelphia - PA - USA.

- Hashimoto M, Takeda M, Sagawa H, Chiba I & Sato K (1985). "Application of Shape Memory Alloy to Robotic Actuators", *Journal of Robotic Systems*, Vol. 2, No. 1, pp. 3-25.
- Hermansson L M (1991). "Structured Training of Children Fitted with Myoelectric Prostheses", *Prosthetics and Orthotics International*, Vol. 15, No. 2, pp. 88-92.
- Hesselbach J & Stork H (1994). "Electrically Controlled Shape Memory Actuators for Use in Handling Systems", *Proc. First Int. Conf. on Shape Memory and Superelastic Technologies*, Pacific Grove - CA - USA, pp. 277 - 282.
- Hodgson D (1990). "Using Shape Memory for Proportional Control", "Engineering Aspects of Shape Memory Alloys", (Duerig T W - Butterworth-Heinemann Ltd, UK), pp. 362-366.
- Hodgson D E & Krumme R C (1994). "Damping in Structural Applications", *Proc. First Int. Conf. on Shape Memory and Superelastic Technologies*, Pacific Grove - CA - USA, pp. 371-376.
- Hof At L (1991). "Errors in Frequency Parameters of EMG Power Spectra", *IEEE Trans. Biom. Eng.*, Vol. 38, No. 11, pp. 1077-1088
- Honma T (1987). "TiNi-Based Shape Memory Alloys", "Precision Machinery and Robotics, Vol. 1: Shape Memory Alloys", Edited by Hiroyasu Funakubo, Gordon and Breach Science Publishers, London - UK, pp. 61-115.
- Hudgins B, Parker P & Scott R N (1993). "A New Strategy for Multifunction Myoelectric Control", *IEEE Trans. Biom. Eng.*, Vol. 40, No. 1, pp. 82-94.
- Ikuta K, Tsukamoto M & Hirose S (1994). "A New Evaluation Method for a Shape Memory Alloy as an Actuator Material", *Proc. First Int. Conf. on Shape Memory and Superelastic Technologies*, Pacific Grove - CA - USA, pp. 289-298.

Ivshin Y & Pence T J (1992). "A Simple Mathematical Model of Two-Way Memory Effect", Proc. Int. Conf. on Martensitic Transformations, Monterey - CA - USA, pp. 389-394.

Jacobsen S C, Knutti D F, Johnson R T & Sears H H (1982). "Development of the Utah Artificial Arm"; IEEE Trans. Biomedical Eng., Vol. BME-29, No. 4, pp. 249-269.

Jordan L, Masse M, Collier J Y & Bouquet G (1994). "Effects of Thermal and Thermomechanical Cycling on Phase Transformations in NiTi and Ni-Ti-Co Shape-Memory Alloys", Journal of Alloys and Compounds, Vol. 212, pp. 204-207.

Jordan L, Masse M, Villafana A & Bouquet G (1992). "Effects of Thermal Treatments on the Respective Behaviour of "R" and Martensitic Phases in Ni-Ti-Co Shape Memory Alloys", Proc. Int. Conf. on Martensitic Transformations, Monterey - CA - USA, pp. 635-640.

Kejlaa G H (1993). "Consumer Concerns and the Functional Value of Prostheses to Upper Limb Amputees", Prosthetics and Orthotics International, Vol. 17, No. 3, pp. 157-163.

Kennon N F & Dunne D P (1981). "Shape Memory Behaviour". Metals Forum, Vol. 4, No. 3, pp. 130-134.

Krebs D E, Edelstein J E & Thornby M A (1991). "Prosthetic Management of Children with Limb Deficiencies", Physical Therapy, Vol. 71, No. 12, Dec. 1991, pp. 920-934.

Kruit J & Cool J C (1989). "Body-powered Hand Prosthesis with Low Operating Power for Children", Journal of Med. Eng. & Tech., Vol. 13, No. 1/2, pp. 129-133.

Kuribayashi K (1986a). "A New Actuator of a Joint Mechanism Using TiNi Alloy Wire", Int. Journal of Robotics Research, Vol. 4, No. 4, pp. 47-58.

- Kuribayashi K (1986b). "A New Compact Robot Hand Using TiNi Alloy Actuator and Stepping Motor Controlled by Micro-computer", IEEE, IECON'86, pp. 538-543.
- Kuribayashi K (1991). "Improvement of the Response of an SMA Actuator Using a Temperature Sensor", *Int. Journal of Robotics Research*, Vol. 10, No. 1, pp. 13-20.
- Kuruganti U, Hudgins B & Scott R N (1995) "Two-Channel Enhancement of a Multifunction Control System", *IEEE Trans. Biom. Eng.*, Vol. 42, No. 1, pp. 109-111.
- Kyberd P J & Chappell P H (1994). "The Southampton Hand: An Intelligent Myoelectric Prosthesis", *Journal of Rehabilitation Research and Development*, Vol. 31, No. 4, pp. 326-334.
- Kyberd P J (1990). "Algorithmic Control of a Multifunctional Hand Prosthesis", PhD Thesis, Southampton University, Southampton, UK.
- Kyberd P J, Holland O E, Chappell P H, Smith S, Tregidgo R, Bagwell P J & Snaith M (1995). "MARCUS: A Two Degree of Freedom Hand Prosthesis with Hierarchical Grip Control"; *IEEE Trans. Rehab. Eng.*, Vol. 3, No. 1, pp. 70-76.
- Kyberd P J, Mustapha N, Carnegie F & Chappell P H (1993). "A Clinical Experience with Hierarchical Controlled Myoelectric Hand Prosthesis with Vibro-tactile Feedback", *Prosthetics and Orthotics International*, Vol. 17, No. 1, 56-64.
- Lamb D W & Law H T (1987). "Upper-Limb Deficiencies in Children - Prosthetic, Orthotic and Surgical Management", Little, Brown and Company, Boston, USA.
- Lamb D W (1993). "State of the Art in Upper-limb Prosthetics", *Journal of Hand Therapy*, Vol. 6, No. 1, pp. 1-8.
- LeBlanc, M A (1991). "Current Evaluation of Hydraulics to Replace the Cable Force Transmission System for Body-Powered Upper-Limb Prostheses", *Assistive Technology*, Vol. 2, pp. 101-107.

- Lippmann R P (1987). "An Introduction to Computing with Neural Nets", IEEE ASSP Magazine, Vol. 4, No. 2, pp. 4-22.
- May I L, Cheung-Mak S K P & Jacobsen P (1992). "Thermal Fatigue of SME Alloys", Proc. Int. Conf. on Martensitic Transformations, Monterey - CA - USA, pp. 1301-1306.
- Melzer A & Stöckel D (1994). "Performance Improvement of Surgical Instrumentation Through the Use of Ni-Ti Materials", Proc. First Int. Conf. on Shape Memory and Superelastic Technologies, Pacific Grove - CA - USA, pp. 401-409.
- Meredith J M, Uellendahl J E & Keagy R D (1993). "Successful Voluntary Grasp and Release Using the Cookie Crusher Myoelectric Hand in 2-Year-Olds", American Journal of Occupational Therapy, Sept. 1993, Vol. 47, No. 9, pp. 825-829.
- Merletti R & Lo Conte L R (1995a). "Advances in Processing of Surface Myoelectric Signals: Part 1", Medical & Biological Eng. & Computing, Vol. 33, May 1995, pp. 362-372.
- Merletti R & Lo Conte L R (1995b). "Advances in Processing of Surface Myoelectric Signals: Part 2", Medical & Biological Eng. & Computing, Vol., 33, May 1995, pp. 373-384.
- Miyazaki S, Liu Y, Otsuka K & McCormick P G (1992). "Electrical Resistance Change in a Ti-Ni Alloy During a Thermal Cycle Under Constant Load", Proc. Int. Conf. on Martensitic Transformations, Monterey - CA - USA, pp. 929-934.
- Nakano Y (1984). "Hitachi's Robot Hand", Robotics Age, July 1984, pp. 18-20.
- Nishimura S, Tomita Y & Horiuchi T (1992). "Clinical Application of an Active Electrode Using an Operational Amplifier", IEEE Trans. Biom. Eng., Vol. 39, No. 10, pp. 1096-1099.

O'Neill P A, Morin E L & Scott R N (1994). "Myoelectric Signal Characteristics from Muscles in Residual Upper Limbs", IEEE Trans. Rehab. Eng., Vol. 2, No. 4, pp. 266-270.

Otsuka K & Shimizu K (1981). "Pseudoelasticity". Metals Forum, Vol. 4, No. 3, pp. 142-152.

Otsuka K (1990). "Introduction to the R-Phase Transition", "Engineering Aspects of Shape Memory Alloys", (Duerig T W - Butterworth-Heinemann Ltd, UK), pp. 36-45.

Patterson P E & Katz J A (1992). "Design and Evaluation of a Sensory Feedback Systems that Provides Grasping Pressure in a Myoelectric Hand", Journal of Rehabilitation Research and Development, Vol. 29, No. 1, pp. 1-8.

Perkins J & Hodgson D (1990). "The Two-Way Shape Memory Effect", "Engineering Aspects of Shape Memory Alloys", (Duerig T W - Butterworth-Heinemann Ltd, UK), pp. 195-206.

Plettenburg D H (1989). "Electric Versus Pneumatic Power in Hand Prostheses for Children", Journal of Med. Eng. & Tech., Vol. 13, No 1/2, pp. 124-128.

Poncet P P & Zadno R (1994). "Applications of Superelastic Ni-Ti in Laparoscopy", Proc. First Int. Conf. on Shape Memory and Superelastic Technologies, Pacific Grove - CA - USA, pp. 421-426.

Pronk G M (1989). "A kinematic Model of the Shoulder Girdle: A Résumé", Journal of Med. Eng. & Tech., Vol. 13, 1/2: 119-123.

Reynaerts D & Van Brussel H (1991). "A SMA High Performance Actuator for Robotic Hands", Journal de Physique IV, Vol. 1, No. C4, pp. 157-162.

Reynaerts D & Van Brussel H (1994). "Shape Memory Alloy Based Electrical Actuation for Robotic Applications", Proc. First Int. Conf. on Shape Memory and Superelastic Technologies, Pacific Grove - CA - USA, pp. 271 - 276.

- Sanders J E (1995). "Interface Mechanics in External Prosthetics: Review of Interface Stress Measurement Techniques", *Medical & Biological Eng. & Computing*, Vol. 33, July 1995, pp. 509-516.
- Saridis G N & Gootee T P (1982). "EMG Pattern Analysis and Classification for a Prosthetic Arm", *IEEE Trans. Biom. Eng.*, Vol. BME-29, No. 6, pp. 403-412.
- Schetky L M (1984). "Shape Memory Effect Alloys for Robotic Devices", *Robotics Age*, July 1984, pp. 13-17.
- Schetky L M (1994). "The Application of Constrained Recovery Shape Memory Devices for Connectors, Sealing and Clamping", *Proc. First Int. Conf. on Shape Memory and Superelastic Technologies*, Pacific Grove - CA - USA, pp. 239-243.
- Scott R N & Parker P A (1988). "Myoelectric Prosthesis: State of the Art", *Journal of Med. Eng. & Tech.*, Vol. 12, No. 4, pp. 143-151.
- Shimizu K & Tadaki T (1987). "Shape Memory Effect: Mechanism", "Precision Machinery and Robotics, Vol. 1: Shape Memory Alloys", Edited by Hiroyasu Funakubo, Gordon and Breach Science Publishers, London - UK, pp. 1-60.
- Silcox D H, Rooks M D, Vogel R R & Fleming L L (1993). "Myoelectric Prostheses - A Long Term Follow-Up and a Study of the Use of Alternate Prostheses", *Journal of Bone and Joint Surgery*, Vol. 75-A, No. 12, pp. 1781-1789.
- Simpson D C (1974). "The Choice of Control System for the Multimovement Prosthesis: Extended Physiological Proprioception (e.p.p.)", In: *The Control of Upper-Extremity Prostheses and Orthoses* (P. Herberts *et al.* eds) Springfield, Illinois, C. C. Thomas, pp. 146-150.
- Stoeckel D & Waram T (1991). "Thermo-Variable Rate Springs: A New Concept for Thermal Sensor-Actuators", *Springs*, Vol. 30, No 2, Oct. 1991.
- Stoeckel D (1990). "Shape-Memory Alloys Prompt New Actuator Designs", *Advanced Materials & Processes*, Vol. 138, Oct. 1990, pp. 33-38.

Strnadel B, Ohashi S, Ohtsuka H, Ishihara T & Miyazaki S (1995). "Cyclic Stress-Strain Characteristics of Ti-Ni and Ti-Ni-Cu Shape Memory Alloys", *Materials Science and Engineering A-Structural Materials Properties Microstructure and Processing*, Vol. 202, No. 1-2, pp. 148-156.

Suzuki Y (1987). "Methods for Using Shape Memory Alloys", *Precision Machinery and Robotics*, Vol. 1: *Shape Memory Alloys*", Edited by Hiroyasu Funakubo, Gordon and Breach Science Publishers, London - UK, pp. 176-202.

Tanaka K (1990). "A Phenomenological Description on Thermomechanical Behaviour of Shape Memory Alloys", *Journal of Pressure Vessel Technology*, Trans. of the ASME, Vol. 112, May 1990, pp. 158-163.

Van Humbeeck J (1991). "Cycling Effects, Fatigue and Degradation of Shape Memory Alloys", *Journal de Physique IV*, Vol. 1, No. C4, pp. 189-197.

Watanabe Y, Mori Y & Sato A (1993). "Training Effect in Fe-Mn-Si Shape Memory Alloys", *Journal of Materials Science*, Vol. 28, pp. 1509-1514.

Wayman C M & Duerig T W (1990). "An Introduction to Martensite and Shape Memory", "Engineering Aspects of Shape Memory Alloys", (Duerig T W - Butterworth-Heinemann Ltd, UK), pp. 3-20.

Wayman C M (1993). "Shape Memory Alloys", *MSR Bulletin*, Vol. 18, No 4, pp. 49-56.